1.

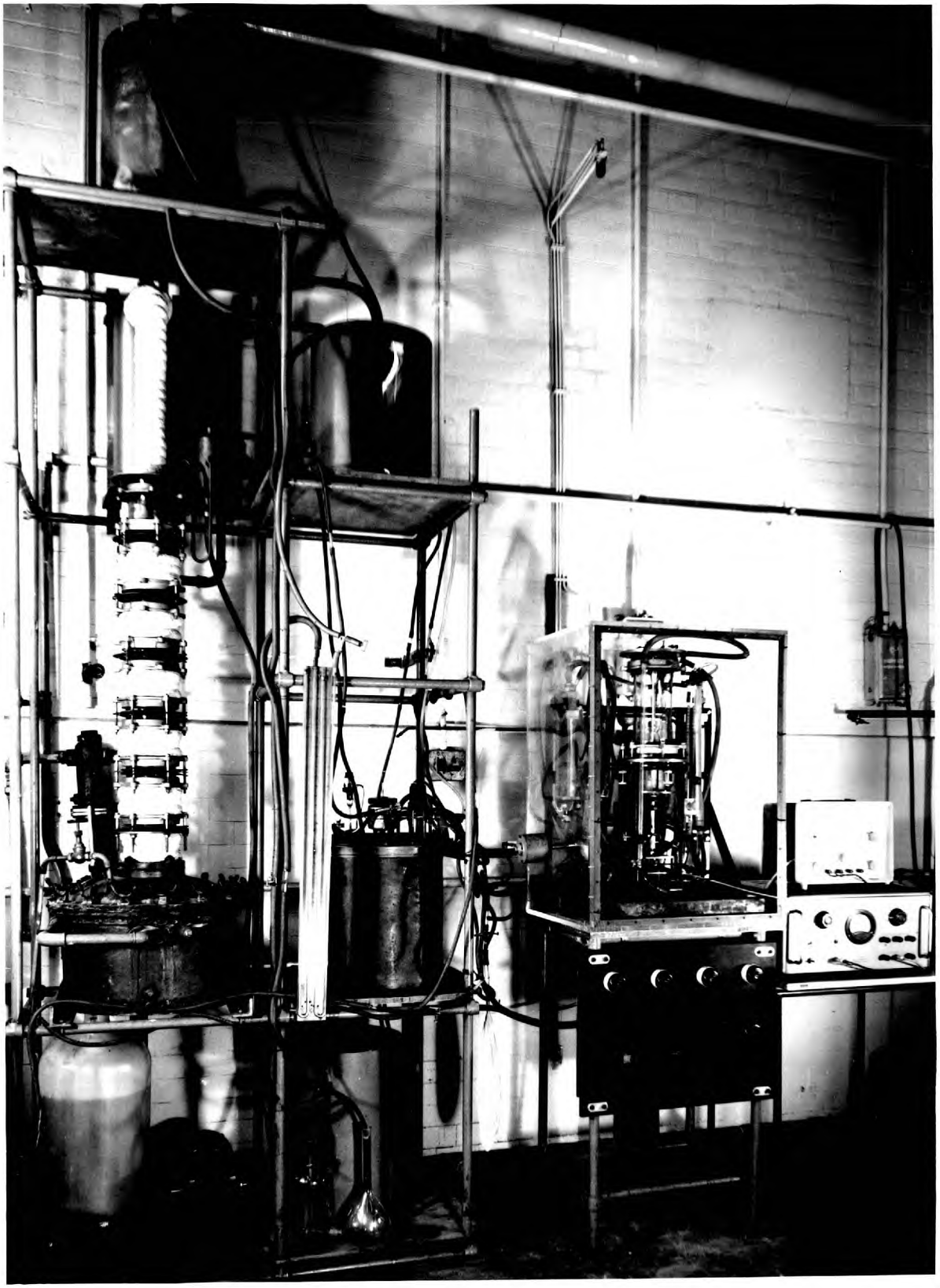

GAS ABSORPTION INTO LIQUID FILMS FALLING OVER ROUGHENED AND VIBRATING SURFACES

A THESIS SUBMITTED FOR THE DEGREE OF

DOCTOR OF PHILOSOPHY

IN THE FACULTY OF ENGINEERING OF THE

UNIVERSITY OF LONDON

BY

HASEEB AKHTAR ZAIDI

DEPARTMENT OF CHEMICAL ENGINEERING,

IMPERIAL COLLEGE OF SCIENCE AND TECHNOLOGY,

LONDON, S.W.7.

JULY, 1964.

ABSTRACT

Investigations were carried out on an itensification of transfer coefficients in gas absorption with a view to improving the performance of film-type equipment.

Short cylindrical wetted wall absorbers (height < 18.0 cm.), with the liquid film falling on the outside surface, were used to study the absorption kinetics of CO_2 into water. The importance of a short wetted wall column arises from the fact that it appears to provide a model in which liquid flow conditions are very similar to those existing when liquid flows over packing elements in a packed tower, and yet the results are amenable to theoretical analysis and easily reproducible.

(1) The first investigations dealt with the behaviour of absorption into a falling film in the absence of an intensifying agent. It was found that when the liquid flow was in the laminar region (Re < 1200) and pure water was used, the absorption results could not be related to theory because of excess absorption due to rippling on the film. The presence of a surface active agent in water (Lissapol NX, 0.01% by volume) eliminated rippling and the results were then successfully related to the penetration theory provided that a small interfacial resistance to absorption was assumed. Interfacial resistance was not introduced by the surface active agent but was found to exist even in the case of pure water.

Absorption rates were obtained at various heights of wetted wall, temperatures, and liquid flow rates. A general equation for predicting the absorption rate by a falling film, in the laminar region of liquid flow, was derived.

For the turbulent region of liquid flow, the thickness was determined photographically and related to a semi-theoretical equation. This equation for film thickness, along with the assumption of a flat velocity profile, was used to derive an expression for predicting the absorption coefficient. Another empirical equation was also obtained from the experimental absorption rates for purposes of comparison with the results of itensification. The addition of a surface active material to water did not affect absorption in this region.

(2) The intensification of absorption on artificially roughened walls of the absorber was studied next. Various magnitudes and shapes of roughness, surfaces with grooves and protrusions, were used. The heights of the roughness elements were increased to become comparable with the thickness of the liquid film. Studies were carried out both in the laminar and the turbulent regions of flow, and with/without the addition of surface active agent.

In the laminar region, absorption was intensified only with rippling films and to a maximum of 6%. When surface active agent was present in water, the absorption rate was not affected.

When the liquid flow was turbulent ($Re > 1200$), absorption was intensified, only at surfaces in which the roughness was in the form of protrustions, to as much as 130%. The presence of surface active material did not affect the intensification ratio. An optimum intensification was reached at a concentration of $2.005/cm.^2$ of the protrustions.

(3) Another method of intensification used, was the mechanical vibration of the absorption column at sonic frequencies and small amplitudes ($Am. \leq 0.15$ cm.). Absorption results were obtained for rippling and non-rippling films and liquid flow rates as high as $Re = 4820$, were used. The influence of both the vibration parameters, amplitude and frequency, was studied.

With rippling films in the laminar region, the increase in absorption was found to be as much as 73%. Peaks in absorption rate occurred at certain frequencies and were independent of the peaks in the amplitude of vibration. The intensification ratio at various liquid flow rates ($\Gamma_v > 1.00$) was nearly constant and equal to 1.730. When surface active agent was introduced into the water in order to suppress rippling, the intensification was found to be very small ($\approx 4\%$). The absorption results with the surface active material were related to the theory by assuming arbitrary values of an interfacial resistance, $\frac{1}{k_i}$.

The increase in absorption at turbulent liquid flows was as much as ~~99%~~ 100%. The degree of intensification of absorption was higher here as compared to the laminar region. The presence of surface active material was found to depress the intensification.

ACKNOWLEDGEMENTS.

The author wishes to thank Professor K.G. Denbigh, whose advice and encouragement has been invaluable in the conduct of the research described in this thesis. He is greatly indebted to him and Professor A. Salam for their help in obtaining a Colombo Plan Fellowship for the author, without which this work could not be completed.

Thanks are also expressed to Mr. J. Oakley for his help in the design and construction of the apparatus.

Finally, the author wishes to thank all the workshop staff members and Mr. A. Dey for his assistance in photography.

CONTENTS.

SECTION 1.

GAS ABSORPTION INTO LIQUID FILMS FALLING OVER SMOOTH SURFACES.

CHAPTER I

THEORY OF WETTED WALL COLUMN

Art. 1.1. Velocity Distribution and Thickness of a Falling Liquid Film

An understanding of the mechanics of film flow is important because such films are encountered in a large number of mass and heat transfer equipment. In spite of extensive work done in the field, very few of the theories put forth are conclusive.

Most of the earlier work done was in connection with heat transfer (1, 2, 3, 4, 5). Attempts were made to measure the mean film thickness with the liquid flowing down an inclined plane or a vertical wetted wall. The accuracy of the measurements was complicated by the fact that waves appeared on the interface and the height of the waves was sometimes several times the average film thickness.

Later work was directed towards understanding the nature of the velocity distribution and the thickness of the film, because the interfacial velocity affects the rate of a diffusional transfer process across the interface. Various techniques have been employed for measuring these parameters. Hold-up methods were used for measuring the film thickness by several authors (6, 7, 8). This was carried out by stopping the flow, weighing the drainage and adding to this the weight of the liquid adhering to the wall. Kirkbride (9) used a micrometer arrangement to measure the thickness directly.

Duckler and Bergelin (10) developed a capacitance technique which also gave the pattern of wave structure at the interface. Grimley(11) used a conductivity method as well as an optical shadow method. Jackson (12) employed a radio-active tracer. All these authors have tried to compare their results with the classical mathematical theory of Claassen (3) for liquids of low viscosity, and which was later elaborated by W. Nusselt (2). The experimental evidence strongly upholds this theory as far as average film thickness is concerned, up to a certain region of flow (Re, 1080-1500, and one author extending the range up to Re, 2300).

Friedman and Miller (8) measured the velocity of the liquid at the interface by timing the passage of a drop of dye, injected at the interface between two fixed points. They found that, due to the presence of ripples which started at Reynolds number of 20-30, the velocity at the interface was very irregular and considerably higher than that predicted from theory. They concluded that there was a pseudo-critical flow point at Re, 20-30, at which the flow pattern changed to a pseudo-streamline state.

Grimley (11) repeated their work using the same method but substituting potassium permanganate for their organic dye. He determined both the interfacial velocity and the velocity profile by an ultramicroscopic technique using a suspension of magnetically charged lead iodide. He came to the same general conclusions as Friedman and Miller (8) as regards the velocity at the interface. As regards the

distribution of velocity, he found that near the wall the velocity was less than the theoretical. Further away the velocity was greater than the theoretical, the maximum being a very short distance from the interface. Elimination of rippling by the introduction of 'Teepol' caused a modification of the velocity distribution but it was still quite different from the theoretical. Although the particular experimental technique of his work is not very reliable or reproducible, his data as well as that of Friedman and Miller suggest that the mathematical theory is in error in its estimation of the interfacial velocity and probably in its prediction of the velocity gradient. This is only to be expected from the fact that the theory ignores the existence of ripples. What is more surprising is the fact that the mean film thickness is the same whether or not ripples occur, and is in close agreement with the theory. Grimley suggested that the faster outer layers compensated the slower inner ones. It is difficult to imagine why this should be so, and how the compensation can be so exact. Grimley thought that there was some sort of discontinuity with a very thin outermost layer moving very much faster than the bulk. As this layer is very thin, its effect on the total flow rate is not detected. A point that raises doubt in his estimation of velocity distribution is that even when ripples were suppressed, the theoretical distribution was not obeyed, although the assumptions of the mathematical theory are seen to be valid.

Furthermore, with viscous liquids, when rippling occurs, the volume of the ripples is rather more appreciable, and therefore it is to be expected that the deviation in the film thickness will be greater. Indeed, this was shown to be the case by Jackson (12). The evidence thus points to the existence of a very thin outermost layer moving faster than the adjacent liquid film.

Duckler and Bergelin (10) presented their own velocity distribution based on Von Karman's (13) universal velocity profiles, with constants experimentally determined by Nikuradse (14) for pipe flow. When the film thickness is much smaller than the pipe radius, and when there is no tractive force being exerted on the gas-liquid interface, they gave the following equations for the estimation of film thickness 'δ' for any flow rate (both laminar and turbulent regions);

$$\frac{\Gamma_v}{\mu} + 64 = 3.0\eta + 2.5\eta \ln \eta \qquad \ldots (1.11)$$

$$\delta = \left[\frac{\eta \nu}{g^{1/2}}\right]^{2/3} \qquad \ldots (1.12)$$

here Γ_v = volumetric flow rate/periphery, $cm.^3/cm.sec.$

μ = viscosity, g m/cm.sec.(poises)

g = acceleration due to gravity, 981 $cm/sec.^2$.

For any flow rate the value of η is frist calculated from Eqn.(1.11) and then substituted in Eqn.(1.12). Their data upheld

their theory as far as film thickness was concerned, no attempt having been made to measure the local velocities in the film. However, the theory did not take into account the effect of ripples and degenerated to the classical theory (2) below Reynolds number of 1080.

An important criticism, that may be made of much of the experimental work, is that proof is not given that steady flow conditions are reached when a liquid flows down a wetted wall, and that the film does not accelerate for any appreciable distance. This criticism was made by Duckler (23) about all the hold-up methods for measuring mean film thickness. Recently, however, Kramers (15), in connection with his work on absorption in short wetted wall columns, made a large scale experimental model to determine the distance taken by the film in accelerating to a steady velocity. He found that the distance required to accelerate to 90% of the equilibrium velocity was only 12 times the film thickness. The error which is thus introduced, is negligible for all but a very short column, less than 1 cm. long.

Although no very definite advances have been made in recent years in our knowledge of the falling film parameters, the results of a few recent papers are of great interest. H. Brauer (16) measured the average film thickness photographically. He used long wetted wall columns and observed that there were two broad regions

of flow. At very low Reynolds numbers the surface of the film was smooth while at higher Reynolds numbers it was wavy. In the region below Reynolds number 1600 (laminar region) the experimental values gave the relation already postulated by W. Nusselt (2), that is,

$$\delta_l = \left(\frac{3\nu^2}{4g}\right)^{1/3} \mathrm{Re}^{1/3} \qquad \ldots (1.13)$$

and for Re $>$ 1600 (turbulent region), the empirical formula was given as,

$$\delta_t = \mathrm{Re}_c^{-1/5} \left(\frac{3\nu^2}{4g}\right)^{1/3} \mathrm{Re}^{8/15} \qquad \ldots (1.14)$$

Here δ_l and δ_t are film thicknesses in the laminar and turbulent regions respectively. Re_c is the critical Reynolds number at which the flow becomes turbulent. Its true value was defined by three independent measuring methods as, $\mathrm{Re}_c = 1600$.

As has been said, the formula for the sub-critical region of flow agrees with that given by W. Nusselt. It should, however, by no means be concluded from this coincidence that the Nusselt theory for flow is valid, and therefore, that the mass and heat transfer numbers calculated by its use are correct up to the critical Reynolds number. The data of mass and heat transfer numbers, in fact, shows extensive divergence. The agreement between the theoretical and the experimentally determined values of film thicknesses must be regarded primarily as a purely

experimental coincidence. Brauer measured the surface velocities also. From the Nusselt theory, the extremely important quantity for mass transfer, the surface velocity 'v_i' stands in the following relationship to the mean film velocity '$v_{av.}$', as,

$$v_i/v_{av.} = 3/2 \qquad \ldots (1.15)$$

Even at Re $=32$, the measured values of this ratio began to deviate from $3/2$. From Re $=$ 20 to Re $\sim$ 100, the values of $v_i/v_{av.}$ were found to be equal to 2.0 and for Re $> Re_c$ (i.e. in the turbulent region) it was $3/2$. Thus in both the sub-critical and the super-critical regions of the rippling flow, the value of the ratio '$v_i/v_{av.}$' is greater than it should be according to theory.

Thomas and Portalski (17) studied the hydrodynamics of wetted wall columns and reported the mean film thicknesses of the liquid films for both still air and a countercurrent flow of air. They used the hold-up method claiming that their technique was superior to hold-up methods used previously. Their results predict the value of Re_c as 1160, compared to Duckler and Bergelin's 1080, and Brauer's 1600.

The distribution of residence times of a tracer injected into a falling water film on the outside of a cylind rical tube was measured by Asbjornsen (18) using frequency response method. The mean residence time of the tracer was found to be from 2-7% greater than the mean residence time derived from Nusselt's theory.

This is only to be expected when both eddy (due to rippling) and molecular diffusion effects are present. It was found that the deviation from laminar theory in the distribution function for the residence times of a tracer in pure water is caused mainly by the ripples on the gas-liquid interface. When a surface active agent was used in sufficient concentration, the ripples practically disappeared and the distribution coefficient approached closely to a pure laminar-film distribution, even up to Reynolds number of 1600.

Wilkes and Nedderman (19) carried out measurements of velocity profiles in thin falling films of liquid (small Reynolds numbers), both in the wavy and wave-free regions of flow, and also in the entry region. It was done by stereoscopic photography of small air bubbles moving with the fluid. They found that, in almost all cases, the velocity profile was nearly parabolic. This means that the predictions of film thickness and the surface velocity from Nusselt theory were valid for the flow regimes studied. This observation seems to contradict all the previous ones for the wavy flow. However, they reported that in the latter region there were fluctuations in the velocities and that the addition of surface active agents suppressed both the waves and the velocity fluctuations.

Very little work has been reported on film flow in the turbulent region. Isolated data are available up to Re of 5,000 from the work of Brauer (16, 20). An equation was developed by the latter for the film thickness in the turbulent region (Eqn. 1.14), but the scatter of experimental points was large.

Zhivaikin (21) measured the thickness of liquid films on the walls of vertical pipes with zero gas flow, and with gas flows both co-current and countercurrent to the liquid flow. His results for zero gas flow show that even for rippling films in the laminar region, the measurements of average film thickness agree fairly well with the Nusselt theory. For the turbulent region he proposed the following equation :

$$f = \frac{0.090}{Re^{0.25}} \qquad \ldots (1.16)$$

from which the equation for film thickness is,

$$\delta = 0.141 \left(\frac{\nu^2}{g}\right)^{1/3} Re^{7/12} \qquad \ldots (1.17)$$

here, f = fanning friction factor.

All the work done on the liquid film characteristics consists of studies on long wetted wall columns and mostly on wavy films with countercurrent or co-current gas traction at the interface. For short wetted wall columns ($\approx$1-20 cm.) with wave-free surface (15, 22), it has generally been assumed that the film thickness and the interfacial velocity are given by the Nusselt theory.

The importance of a short wetted wall column arises from the fact that this appears to provide a model, in which liquid flow conditions are considerably similar to those existing when liquid flows over packing elements in a packed tower, and yet is amenable to analytical treatment and reproducible results. If the view that complete mixing takes place at the discontinuities is accepted, then each packing element acts as a short wetted wall column, and the performance of the whole column can be obtained by the integration of the performances of individual elements. The long wetted wall column represents the flow dynamics of a packed column only when the view of 'no-mixing' at the discontinuities is assumed. The experimental work on discontinuities stands more in favour of 'complete-mixing' (or 'partial mixing') than 'no-mixing'. Therefore a better understanding of the flow mechanics of short wetted wall columns is necessary. The photographic work, described in this thesis later, was carried out mainly for the following two reasons:

1. To interpret the parameters of the liquid film falling on surfaces with protrusions and notches as well as on vibrating surfaces.
2. To obtain data for liquid films' thickness in the turbulent region of flow. This is non-existent in the literature for short length smooth films and for which not even a reliable theoretical equation is available (except Duckler's (23) semi-theoretical analogy from pipe flow).

Art. 1.2. Interfacial Area

For a liquid-film controlled absorption in a wetted wall column or a packed column, the driving force is fixed by the equilibrium concentration and the initial concentration of the solute in the solvent. The remaining factors affecting the transfer rate are the transfer coefficient and the interfacial area. The transfer area depends on the wave motion at the gas-liquid interface, and for flow over a non-plane surface, depends in addition, on the liquid film thickness. This area enters into the mass transfer equations for cases of either gas or liquid film controlling. The mass transfer coefficient is independent of the liquid properties where gas-phase resistance is controlling. When only the liquid resistance is significant, the coefficient is a function of liquid properties and internal turbulence. In packed towers a lack of information, which would permit a separation of these two factors of area and coefficient, has led to the use of a combined coefficient 'ka', where 'a' is the transfer area per unit volume of empty or packed tower. Since the transfer coefficient and 'a' are independent functions of the liquid conditions, use of a combined coefficient makes a rational analysis difficult.

There are no direct reliable methods known for measuring the interfacial area. Most of the known methods are those based upon mass transfer, and are used for measuring the wetted area in packed towers. Grimley (11) measured the wetted area of stone-ware

ring packing by assuming uniform vertical laminar flow of the liquid and measuring its electrical resistance. The flow assumption, however, seems improbable, and the electrical resistance does not correctly average the stream cross-section. In addition, the decrease in interfacial area due to channelling is not taken into account in this method. The other work on the direct measurement of interfacial area is that of Tailby and Portalski (24), who tried to measure the increase in surface area due to rippling in falling liquid films. They recorded a two-dimensional wave-profile of the film using a capacitance technique. The method gives a very rough estimate of surface area.

In the work described in this thesis, a knowledge of interfacial area was very desirable in order to estimate the magnitude of interfacial turbulence. Surface protrusions and sonic vibrations were used to induce turbulence in the film. In this connection it would be interesting to investigate the probable flow pattern in the natural interfacial phenomena of wave motion.

Wave Motion

The phenomena of wave motion in falling liquid films was investigated very thoroughly by Grimley (11). He covered a complete range of flow rates from the inception of rippling to the onset of true turbulence. From his photographic observations the conclusions

can be summarised as under :

1. It was difficult to maintain a continuous film below Re = 20. As the flow rate was increased, the ripples started at Re = 24 and the distortions of the liquid surface became more and more violent. The motion consisted of a train of about 6 wavelets of individual wave-lengths of 0.3 cm., each train 3-4 cm. from the next. At higher flow rates the liquid surface became still more violently disturbed and separate ripples were not easily distinguished.
2. At Re = 400, the rippling started to become less violent, until at Re = 1000 rippling disappeared in the length considered. At much higher flow rates the turbulence set in, which was of a totally different nature from rippling.
3. In all cases the upper part of the film did not show any rippling, and as the liquid flow rate was increased the length of the unrippled upper part increased. It is possible that the apparent disappearance of ripples was only due to the extension of the unrippled section down the whole length of the wall. Rippling might have persisted if the tube had been longer.
4. In general the wave motion was irregular and conditions were constantly changing at any one point.

Grimley also attempted quantitative measurements of the velocity of wave motion in rippling falling liquid films. He obtained photographically a few values for the compound velocity of the ripples and deduced the ripple velocity by comparison with his experimentally determined interfacial velocity. The results were, however, not very satisfactory. Kapitsa (25) used photography with stroboscopic illumination to study the shadow of a thin layer of liquid flowing down the outer wall of a glass tube. He showed that transition from laminar to wave flow was brought about by a slight accidental or artificial perturbation. When transition took place, wave flow was the more stable form of motion. He introduced artificial, very weak, compressed air impulses synchronized with the stroboscope and thus obtained regularly periodic and stable wave motion of near sinusoidal form. He obtained another type of motion, by the application of stronger but less frequent impulses, consisting of single waves running down the film with laminar motion in between the waves. Kapitsa (25), as also Lamb (26), have put forward mathematical analysis of wave motion, but up to now no treatment has been very successful. It is useful to consider some of the conclusions concerning the mechanism of rippling in film flow :

1. The ripples progress over the moving surface in the direction of flow which is evidence that air friction is not their cause.

2. The speed of progession of the ripples is not very high, being only of the order of 15 cm./sec. This, according to Grimley, is the motion of a surface contour and does not involve the transport of material in the direction of motion.
3. Surface forces exert a predominating influence in ripple formation.
4. Because the wave peaks attain a height greater than the average film thickness, they may become the localised points of turbulence.

Art. 1.3. Flow Transition

The decisive difference between the flow in pipes and the film flow, is in the number of flow regions. While only two regions exist in pipe flow (i.e. laminar and turbulent), thorough research into the behaviour of film flow (rippling) has revealed more than two regions. In contrast to the pipe flow these regions are separated from each other not by easily recognisable transition points but merely by slight changes in the slopes of the curves for the resistance coefficients or the mass and heat transfer numbers versus Reynolds number. For each region of flow special laws are valid, and these are conditioned chiefly by the ripples occurring on the surface of falling films. Brauer (27) has shown the existence of four prominent regions divided by characteristic

Reynolds numbers for a particular liquid. He also showed that these Reynolds numbers are conditioned by a change in the wave characteristics. According to him the value of the transition Reynolds number 'Re_l' is a constant (=1600) for all liquids but that all other transition values are variable and are functions of the film number, K_F, defined as,

$$K_F = \frac{y\sigma^3}{g^2\mu^4} \qquad \ldots (1.31)$$

where 'y' denotes the specific gravity of the liquid,

'σ' the surface tension (dynes/cm.^{2}) and

'μ' the dynamic viscosity of the falling liquid.

Depending upon these characteristic quantities, the characteristic Reynolds numbers can be represented by the following relationships:

$$Re_i = 2.88\ (K_F)^{1/10} \qquad \ldots (1.32)$$

$$Re_w = 5.40\ (K_F)^{1/10} \qquad \ldots (1.33)$$

$$Re_c = 0.0720\ (K_F)^{1/3} \qquad \ldots (1.34)$$

$$Re_l = 1600$$

where Re_i, Re_w, Re_c and Re_l are the break points in the slope of curve "Re vs. resistance number" (see Ref.(27)).

In the case of smooth films, however, there are only two flow regions distinguishable, that is, the laminar and the turbulent. The transition is made evident from the plot of transfer numbers

against Reynolds numbers, which shows a change of slope when the flow changes from laminar to turbulent. For long wetted wall columns it has been reported that the slope of the curve undergoes a sharp break at the transition point. The present work on short wetted wall columns, as also the other works, indicate that the break in the curve is not very sharp and there seems to exist a small region of transition. The transition Reynolds numbers predicted by various authors vary considerably and seem to lie between 1000 and 2000. In several recent studies (15, 32), however, the Reynolds number of 1200 has been accepted as the transition point.

Art. 1.4. Mass Transfer.

Theories

The earliest theory of mass transfer is the Whitman's two-film concept (28), which assumes the existence of two stagnant films on either side of an interface. The mass transfer is supposed to take place by molecular diffusion through these films. Although the mechanism of transfer looks very unrealistic, the predictions of the transfer coefficients are very much indentical with the other theories. For reasons of its simplicity, therefore, this theory is widely used in design work. The rate of mass transfer per unit area, N_A, is given as,

$$N_A = k_G (p-p_i) = k_L (C_i-C_o) \qquad \ldots (1.41)$$

where,

k_G, k_L = individual gas film and liquid film mass transfer coefficients resp., cm./sec.,

p, p_i = partial pressure in the gas and partial pressure at the interface respectively, atmos.,

C_o, C_i = initial concentration in the liquid and the concentration at the interface resp., gm./cm.^{3}

As the conditions at the interface are unknown, it is general to use overall coefficients, and,

$$N_A = K_G (p-p^*) = K_L (C^*-C_o) \qquad \ldots (1.42)$$

where,

K_G, K_L = overall mass transfer coefficients based on partial pressure driving force and concentration driving force resp., cm./sec.,

p^*, C^* = saturated partial pressure and saturated concentration respectively at the temperature of the system.

According to the two-film theory of Whitman, then, for a liquid film controlled process,

$$k_L = \frac{D}{x_L} \qquad \ldots (1.43)$$

where,

D = diffusion coefficient of mass transfer, $cm.^2/sec.$,

x_L = the thickness of the hypothetical liquid film, cm.

A more realistic concept of the mechanism of mass transfer was proposed by Higbie (29), called the 'penetration theory'. This theory has the following underlying assumptions for a wetted wall column:

1. The liquid film* is in laminar flow with a parabolic velocity profile, having a maximum velocity at the interface and zero velocity at the solid wall. The viscous drag at the gas liquid interface is assumed to be negligible. The film is also assumed to be free from any interfacial disturbances like rippling.
2. The surface of the film is moving with a uniform velocity. A short contact time achieves this condition. The depth of penetration of the gas molecules is very small, and to the depth that they diffuse, the velocity of the laminae of the liquid may be assumed constant.
3. The surface is assumed to become saturated in the first instant of exposure, that is, the interfacial concentration has a constant value 'c*' and that there is no interfacial resistance.

---

* This designates the entire liquid layer from the solid wall to the free interface as distinguished from the hypothetical stagnant 'films' of Whitman.

4. The effect of diffusion is negligible in the direction of flow.

By applying the boundary conditions, resulting from the above assumptions, to the differential equation obtained from Fick's law, he obtained the following solution for the rate of absorption by an element of area on the surface at a time 't', as,

$$\frac{dN}{dA} = (C^* - C_o)\sqrt{\frac{D}{\pi t}} \qquad \ldots (1.44)$$

where,

N = local rate of mass transfer, gm./sec.,

D = molecular diffusivity, $cm.^2/sec.$,

C_o = zero.

Therefore, the average rate of absorption per unit area, N_A, can be obtained by integrating the expression between limits of zero and 't_c', the contact time, as,

$$N_A = \frac{1}{t_c}\int_o^{t_c} C^*\sqrt{\frac{D}{\pi t}}\, dt \qquad \ldots (1.45)$$

$$= 2C^*\sqrt{\frac{D}{\pi t_c}} \qquad \ldots (1.46)$$

In the above derivations it has been assumed that only liquid-phase resistance is controlling, the gas-phase resistance being negligible. The mass transfer coefficient 'k_L', therefore, has the value,

$$k_L = 2\sqrt{\frac{D}{\pi t_c}} = 2\sqrt{\frac{D V_i}{\pi h}} \qquad \ldots (1.47)$$

where v_i = interfacial velocity, cm/sec.

h = height of the column, cm.

Since the flow is laminar,

$$v_i = \frac{3}{2} \cdot V_{av.} = \frac{3}{2} \cdot \frac{\Gamma_v}{\delta} \qquad \ldots (1.48)$$

and

$$\delta = \left(\frac{3\nu \cdot \Gamma_v}{g}\right)^{1/3} \qquad \ldots (1.49)$$

here, $V_{av.} = \frac{\Gamma_v}{\delta}$ = average velocity of the film, cm/sec.

Γ_v = volumetric flow rate of the liquid per unit periphery, $cm.^3/cm.sec.$

δ = thickness of the liquid film, cm.

$$\therefore \quad k_L = 2\sqrt{\frac{3D\Gamma_v}{2\pi.h.\delta}} \qquad \ldots (1.410)$$

$$= 2\left(\frac{3D}{2\pi}\right)^{1/2} \cdot \left(\frac{g}{3\nu}\right)^{1/6} \cdot (\Gamma_v)^{1/3} \cdot (h)^{-1/2} \qquad \ldots (1.411)$$

$$N_A = 2\,C^*\left(\frac{3D}{2\pi}\right)^{1/2} \cdot \left(\frac{g}{3\nu}\right)^{1/6} \cdot (\Gamma_v)^{1/3} \cdot (h)^{-1/2} \qquad \ldots (1.412)$$

and

$$N = 4\,C^*\,(r+\delta)\left(\frac{\pi D}{2}\right)^{1/2} \cdot \left(\frac{9g}{\nu}\right)^{1/6} \cdot (\Gamma_v)^{1/3} \cdot (h)^{1/2} \qquad \ldots (1.413)$$

here ν = kinematic viscosity of the liquid, $cm.^2/sec.$

g = acceleration due to gravity, 981 $cm/sec.^2$

r = radius of the wetted wall column, cm.

Kramers et. al.(15) verified the validity of the penetration theory by studying the absorption of SO_2 into water flowing down the outside of a vertical tube. 'Teepol' was added to the water to eliminate rippling and short lengths of the column were used to obtain a small exposure time.

The rate of absorption was accurately measured by the difference between the inlet and the outlet gas flow rates, the outlet flow being only 5% of the inlet flow. Corrections were made for the small heat of absorption, variation in pressure, and the entry and the exit effects. It was demonstrated that the chemical reaction beteeen SO_2 and water had no measurable effect on the rate of absorption. The results showed a high degree of consistency and could be represented to the full limit of their experimental accuracy by the penetration theory.

The mathematical equations of the penetration theory were developed for a stagnant liquid of infinite depth. Danckwerts (30) introduced the concept of 'depth of penetration', arbitrarily defined as the depth at which the increase in concentration was 1/100th of that achieved at the surface. He found that its value was $3.6\sqrt{D.t_c}$. For the particular case of a wetted wall column, he obtained a graphical solution for the rate of absorption into a laminar layer of liquid flowing down a vertical wall. He found that the amount of gas absorbed in a given time to the amount absorbed in the same time by an equal area of the surface of a stagnant liquid of infinite depth, depended only on the dimensionless parameter, $J = \frac{hD\nu}{g\rho\delta^4}$. If 'J' was less than 0.1, the difference between the two was less than 5%. This condition was easily fulfilled in the work of Kramers et. al (15).

Higbie (29) had derived his theory on the assumption that each element of a liquid surface is exposed to the gas for the same length of time — the residence time of the surface. In the case of a wetted wall column, this residence time is denoted by 't_c'. This assumption is slightly unrealistic. The elements of the surface might mix into the bulk because of rippling or turbulence, or as in the case of a packed tower mixing might take place at the discontinuities and fresh liquid might come to the surface. Danckwerts (31) modified Higbie's theory by assuming a random distribution of residence times. He assumed that 'the chance of an element of surface being replaced within a given time is independent of its age'. Thus if '$\phi(\theta)d\theta$' is the fraction of the surface area, which is in the age group 'θ to $(\theta+d\theta)$', then, '$\phi(\theta)$' is the surface age distribution function, and is given by,

$$\phi(\theta) = Se^{-S\theta} \qquad \ldots (1.414)$$

where S = fraction of area renewed per unit time.

The rate of absorption into those elements of surface having age 'θ' and combined area '$Se^{-S\theta}$' is given as,

$$N = C^* Se^{-S\theta} \sqrt{\frac{D}{\pi\theta}} \cdot d\theta \qquad \ldots (1.415)$$

Hence the mean rate of absorption per unit area is,

$$N_A = C^* \sqrt{D} \int_0^{(\infty)} \frac{Se^{-S\theta}}{\sqrt{\pi\theta}} \cdot d\theta \qquad \ldots (1.416)$$

$$= C^* \sqrt{DS} \qquad \ldots (1.417)$$

$$\therefore \quad k_L = \sqrt{DS} \qquad \ldots (1.418)$$

The drawback in applying Eqn.(1.417) to experimental results is that 'S' is specific for a specific hydrodynamic system and must be determined experimentally.

In the case of wetted wall columns, if the time of contact is long enough, then the basic assumptions of the penetration theory hold no longer. If the depth of penetration of the solute molecules is comparable to the thickness of the liquid film, the velocity distribution in the film must be taken into account. The differential equation obtained from Fick's law, as also the boundary conditions, need to be modified. Although the true velocity profile has not been definitely established, it seems probable that it is nearly parabolic, with a maximum velocity at the free interface and zero velocity at the solid-liquid interface. In view of these complications, Pigford (32) modified the application of the penetration theory to long wetted wall columns. He obtained the following differential equation for the physical situation,

$$D \frac{\partial^2 C}{\partial x^2} = v_i \left[1 - \left(\frac{x}{\delta}\right)^2\right] \frac{dC}{dh} \qquad \ldots (1.419)$$

The solution of the above equation was given as under:

$$\frac{C_i - C_2}{C_i - C_1} = 0.7857 \exp(-5.121\, z) + 0.1001 \exp(-39.31\, z) + 0.0360 \exp(-105.6\, z) \qquad \ldots (1.420)$$

where,

C_2 = average outlet concentration,

C_1 = average inlet concentration,

$$z = \frac{Dt_c}{\delta^2},$$

$$\therefore \quad (k_L)_{l.m.} = \frac{v_{av.}\,\delta}{h} \ln \frac{C_i - C_1}{C_i - C_2} \qquad \ldots (1.421)$$

For short times of contact this reduces to,

$$(k_L)_{l.m.} = 2\sqrt{\frac{D}{\pi t_c}} \qquad \ldots (1.422)$$

where,

$(k_L)_{l.m.}$ = transfer coefficient based upon a logarithmic mean driving force.

If the time of contact 't_c' is long, 'z' becomes large, and all the terms in Eqn. (1.420) become negligible in comparison with the first, then,

$$(k_L)_{l.m.} = 3.41 \frac{D}{\delta} \qquad \ldots (1.423)$$

Several other modifications of the penetration theory have been proposed (33, 34, 35), which, however, give identical predictions of the transfer numbers.

Interfacial Resistance

In the analysis of absorption data it is generally assumed that phase equilibrium exists at the gas-liquid interface, but the validity of this assumption has been in doubt since Higbie's (29) pioneering gas absorption studies. In attempting to test the validity of this assumption, various previous investigators have reported conflicting results. Scharge (36) has shown theoretically that interfacial resistance does not become important except at very high rates of mass transfer, ordinarily attainable only for evaporation or condensation at reduced pressure.

Cullen and Davidson (37) concluded from jet absorber experiments that interfacial equilibrium existed in the CO_2 water system. In a companion study, employing a wetted sphere absorber (38), they confirmed this conclusion and found that it was probably also true in the absorption of a number of other slightly soluble gases. The work of Kramers (15) also suggests that the assumption of equilibrium at the interface is practically valid. Goodgame and Sherwood (39) showed experimentally the validity of adding a gas-phase resistance to a liquid-phase resistance to obtain an overall resistance. Their calculated results were in very good agreement with their experimental data obtained in a stirred vessel with a known interfacial area. Similar results were obtained by Kuznetsov (40) in a wetted wall column. Scriven and

Pigford (41) measured absorption rates of CO_2 in a short laminar jet of water noting the change in average concentration. Excellent agreement was reported with predictions based upon unsteady state diffusion assuming interfacial equilibrium. They concluded that equilibrium prevails at newly formed surfaces. Harvey and Smith (42) examined the absorption of CO_2 into quiescent water using an interferometric technique. With pure water as solvent there was no measurable resistance to solution at the interface. These experiments all suggest that the interfacial resistance has no measurable effect on mass transfer.

Some recently obtained experimental data suggests that the effect of interfacial resistance is measurable and important. Goodridge and Bricknel (43) have measured the interfacial resistance to mass transfer in CO_2 water system in the presence of mono-molecular layers of surface active materials. The experimental technique consisted of measuring gas absorption rates at constant pressure in a stirred vessel using a variety of long-chain acids and alcohols as film forming compounds. Similar interfacial studies were reported (44, 45) in the absorption of CO_2 and O_2 by water in laminar jets falling in an atmosphere of the gas. Average absorption rates were compared with rates calculated from Fick's law for unsteady state diffusion into a liquid when in rod-like flow.

In contrast to Scriven and Pigford's (41), the reported values were lower than those estimated on the assumption of no interfacial resistance. Hence there must be some interfacial resistance small enough to be overlooked and justify the assumption of interfacial equilibrium in most gas absorbers.

For the absorption of CO_2 in water, Higbie (29) attributed the deviation of his results from the penetration theory to the existence of a first order process at the interface. He described a first order process as one whose rate was proportional to the degree of unsaturation or removal from equilibrium at the interface. Danckwerts (30) used Higbie's data to calculate an accommodation coefficient thus: "If for every molecule striking the interface, calculated by the kinetic theory, a fraction 'α' of the incident molecules penetrates it, then 'α' is the accommodation coefficient".

Emmert and Pigford (32) obtained data on the absorption and desorption of CO_2 in water on both short and long wetted wall columns. They eliminated ripples by using surfactants. The rate of absorption was found to be 25% lower than that predicted by the penetration theory, and it was different from the rate of desorption. They also pointed out that Peaceman's (22) data, where absorption of CO_2 in water was carried out in very short wetted wall columns and where rippling had not started, deviated from the penetration theory. They explained their data by assuming a

finite resistance at the interface expressed as inverse of a mass transfer coefficient 'k_i' across the interface (mols. per unit time per unit area partial pressure driving force). 'k_i' was related to an accommodation coefficient 'α' and it was shown that,

$$\alpha = \sqrt{\frac{6\pi k_i}{\bar{u}}} \qquad \ldots (1.424)$$

where $\bar{u}$ = root - mean - square velocity of the gas molecules.(cm./sec.).

Danckwerts and Kennedy (46) related their results of CO_2-absorption into a water film carried by a rotating drum, by assuming a surface resistance '$1/k_s$', where 'k_s' was of the same units as 'k_i' used by Emmert and Pigford (32), and had a magnitude of 0.11 cm./sec.

The following conclusions can be drawn from the work on interfacial resistance:

1. The predictions of interfacial resistance cannot be considered conclusive because the physical properties of the solutions are not accurately known, particularly the diffusivities.
2. The total uncertainty of the experiments is of the same order as the deviation from the penetration theory.
3. It seems likely that the lack of agreement of experimental absorption data is due principally to the

inadequate knowledge of the fluid dynamics of the different flow systems employed.

4. The assumption of interfacial equilibrium seems nearly to be valid. If there is some small surface resistance to mass transfer, it may be due only to the presence of monolayers of surface active material at the interface. Thus for O_2 or CO_2 absorbing into an aqueous medium, it is claimed that a film of cetyl alcohol imposes a resistance of about 80 sec./cm., while 'Lissapol' and 'Teepol' produced resistances to CO_2 absorption (47) of about 35 sec./cm. Nevertheless, these resistances are much smaller than the usual liquid phase resistance which is of the order of 12,000 sec./cm. It remains to be confirmed by direct measurement of concentration profiles sufficiently near the interface, whether there is any removal from equilibrium at the gas-liquid interface, and if there is, whether it is sufficient to have a measurable effect on the rate of mass transfer. Interferometric techniques have been developed for measuring such concentration profiles in the case of mass transfer between a solid wall and a fluid stream (48).

Effect of Surface Active Agents

The surface active agents are known to cause a decrease

in the mass transfer rates by suppressing the following effects:

(a) the enhanced bulk mixing due to rippling.

(b) the increase in interfacial area.

It is very important here to discuss the effect of surface active agents on film flow in wetted wall columns, because, in the present work, these have been found to reduce the absorption rates very considerably, as never encountered in any previous work. The magnitude of suppression has been as much as 55% in some cases of absorption with sonic vibrations applied to the film.

The effect of adding to water measurable quantities of surfactants, such as 'Teepol', 'Petrowet', 'Lissapol' etc., upon absorption of gases has been investigated by a number of workers (49, 50, 51, 54). In long wetted wall columns, the addition of a wetting agent markedly affects both the liquid flow pattern, causing the disappearance of ripples, and the absorption rate, which is reduced considerably in the absence of ripples. In very short columns the wetting agent does not noticeably affect the rate of absorption, although it does influence the exit-end effect. The band of ripples at the exit becomes invisible by the addition of a surfactant.

Some workers have tried to find the effect of different surface agents at one or several concentrations. Ternovskaya and Belopolski (51) investigated the effect of concentration of three

different wetting agents on the absorption of SO_2 by water, and found in two cases a definite minimum for the rate of absorption. In the third case, the rate of absorption decreased down to a minimum value and then bec me nearly constant. It was recommended that such a wetting agent (Lissapol NX)was very reliable because it resultedin greater confidence in the reproducibility of results. Tailby and Portalski (52) also examined the effect of surface active agents in damping waves and ripples, by direct observation, as well as, by recording the profile of the surface of the film by a capacitance technique. In each of the cases considered an optimum concentration of the wetting agent was found for the attainment of a smooth surface.

It appears from the mass transfer tests in wetted wall columns, which are more sensitive than any hydro-dynamic tests so far devised, that the effect of rippling can be completely eliminated by the addition of a wetting agent. This has become a standard method of producing a known reproducible interfacial area, and has made it possible to test theoretical equations with confidence. As has already been discussed in connection with interfacial resistance, some authors suggest that the surface active agents introduce a surface resistance to mass transfer. However, some very reliable studies (15, 32, 53) have shown that surface active agents do not by themselves add an additional

resistance but rather decrease mass transfer by decreasing hydrodynamic activity.

Art.1.5 - Limitations

A cylind rical wetted wall column was chosen for the present study because it has several advantages over other types of absorption apparatus. There are, however, certain inherent sources of error in this apparatus which will be briefly elaborated now. The corrections for these errors have been made where necessary while making calculations,and are discussed quantitatively in later chapters. Here only the qualitative aspects will be discussed.

End Effects

At both ends of a wetted wall column, the pattern of hydrodynamics of the liquid film is different from that occurring in the middle part. The rate of mass transfer at these places is therefore different from the rest. These regions are called the regions of end effects. A correction for these effects can be made by either striking off the height of these regions from the total height, or better, by finding an equivalent height from a consideration of the hydrodynamics.

Entry Effect

If the liquid goes up through the inside of a tube and simply overflows from its top edge to form a uniform film on the

outside, we get a meniscus of liquid at the top. The liquid at this point reverses its direction of flow, and therefore, its velocity passes through zero. The surface velocity of the film in this region is different from the surface velocity in the vertical section of the wall. A combination of the effects of non-linearity of surface age distribution, and the acceleration from zero velocity, results in a surface velocity in this region which is lower than the average surface velocity on the vertical section of the column. Kramers (15) made a correction for this region by adding 3/4-radius of the tube to the effective vertical height of the tube.

Sometimes, for a better distribution of the liquid around the tube, the liquid is passed through an annular gap. The velocity profile of the film changes from fully parabolic to a semi-parabolic. There is an acceleration of the interfacial velocity from zero to maximum. Kramers estimated from an experimental model, that the length required for this transition was 1/12th of the film thickness. The magnitude of this error was negligible compared to the lengths employed, and so, no correction was made for the entry effect.

The liquid film is thicker near the entry section and tapers down to a constant thickness after traversing some length of the column. The magnitude of this length is proportional to the flow rate. No correction for this effect has been proposed

in the literature. This will be discussed further in connection with the photographic work described in this thesis.

Exit Effect

Kramers (15) observed that the liquid film became thicker just before it fell into the receiver-pool. If some aluminium powder was sprinkled on the column it seemed to accumulate as a band of 1-2 cm. height near the end, depending upon the flow rate. On careful examination, this band appeared to be stagnant. This effect was observed by several workers but Kramers was the first to make a correction for it. He observed that when '$(N_A)^2$' was plotted against 'h', the experimental points did lie on a straight line with a slope agreeing with Eqn. (1.412) but it did not pass through the origin. It intercepted the h-axis at a value of 'h' approximately the same as observed visually. He assumed that this part was not operative in the process of absorption and subtracted this from the total height.

The assumption that the absorption of gas by the stagnant height is negligible may not be valid in some cases. The height of this region varies with the increase in flow rate, increase of turbulence in the film, and by the addition of surfactants. It is rather inaccurate to subtract the same height of the end effect for all these different conditions. Also it was observed that this zone was not completely stagnant but that it had a much larger residence time than the rest of the film. With the increase in

flow rate its residence time becomes appreciable.

The cause of the exit effect was supposed to be some sort of surface contamination. When the liquid in the pool is immediately removed along with the surface of the pool, no stagnant end is observed. However, when the liquid is removed from beneath the surface of the pool, the end effect is observed. It is suggested that it is caused by a surface tension difference. When a surface is freshly created, the concentration of the surface active material at the interface will be the same as in the bulk of the solution and consequently the surface tension will be little less than that of pure water. After the surface has been formed, more surface active material will diffuse from the bulk to this surface until equilibrium is attained. Therefore, at equilibrium the surface tension will be substantially lower than that of water. The significance of this discussion is apparent when it is realised that the surface of the liquid on the wetted wall is freshly created, whereas in the receiving pool it is much older. Thus a difference in the surface tension results between the liquid in the pool and that on the wall. A force starts acting along the surface of the liquid near the bottom of the falling film where the two surfaces meet. It will resist the flow of the liquid near the surface of the film, slowing it down, and possibly bringing it to a halt.

The influence of this effect on the absorption rate becomes

appreciable when small column heights are used. In fact some workers have been misled in interpreting the influence of this effect as being caused by an interfacial resistance.

Band of Waves

Immediately above the upper edge of the stagnant region stands a band of horizontal waves. These waves decrease in amplitude up the column. The visible band is approximately 0.5-1 cm. high depending upon the flow rate. Nedderman's (55) theoretical work shows that there are no eddies beneath these waves and therefore the only way they can influence absorption is by increasing the surface area. The interfacial velocity will also be affected and in fact the increase in interfacial area might well be balanced by a decrease in the interfacial velocity. Therefore, a correction for this phenomenon was not necessary.

This wave band was used as an approximate guide in the alignment of the tube carrying the film. A horizontal stationary band showed that the liquid was uniformly distributed round the tube and that the tube was vertical.

CHAPTER II

EXPERIMENTAL APPARATUS

Art. 2.1. Choice of the Absorber

The work described in this thesis was carried out in order to improve the efficiency of absorption in packed towers. It was thought that the physical condition of the surface of a packing element, that is, the roughness or the protrusions or depressions, might give a higher rate of absorption per unit area than a plain smooth surface. The mode of absorption into a laminar falling liquid film is the same as that into a stagnant liquid exposed for a time equal to the residence time of the film. Presence of discontinuities on the surface was expected to change the mode into one of absorption into an agitated liquid, thereby improving transfer rates. With the same object in view, the film was subjected to sonic vibrations to induce mixing at the gas-liquid interface. These studies are described in Sections 2 and 3.

A short cylindrical wetted wall absorber was chosen to be the most suitable for the purposes of this work. This apparatus has the advantage of giving very short exposure times, which can be varied within a wide range, with ease. Its chief advantage lies in the fact that it represents very nearly the mode of behaviour of a single packing element of a packed absorption column. The results obtained from this absorber are easily amenable to theoretical analysis. Pure CO_2- water system was

chosen because it is liquid-film controlled, and the components can be easily available in pure form.

For the purposes of comparison, first studies were made on a smooth surface at various flow rates, temperatures, wetted wall heights etc. The details of the apparatus for this study will be described in this section. For studying the effects of surface roughness and vibrations, more components had to be incorporated into the original assembly, and these modifications are described in the corresponding studies in Sections 2 and 3 respectively.

Art. 2.2. The Wetted Wall Absorber

It was intended to obtain a ripple-free film of liquid, fulfilling, as far as possible, the demands of the penetration theory. A straight cylindrical stainless steel tube of 1/2" O.D. was chosen, with the film falling under gravity on its outside surface. The tube was 17" long, but the heights of the wetted surface used were only 8-18 cm. (heights of the wetted wall shall always be given in cm. units). The diameter of the tube was considerably larger than the thickness of the liquid film, and so, the error introduced due to the cylindrical shape of the film was assumed to be negligible. The material chosen was stainless steel because of the bright polish obtainable on the surface which remained untarnished on exposure to moist conditions. The bright surface of the wetted wall helped to make any disturbance on the gas-liquid interface easily visible. The tube was ground

for straightness and roundness up to 2/1000 inch.

The lower free end of the stainless steel tube carried a T-piece, the side link of which was used as an inlet for water and the lower limb for the drainage of water when it was required to dismount the tube. The upper free end was bevelled at an angle of 60° to give a knife-edge. Several perspex models of the tube were tried for different angles of bevel, and it was observed that an angle of 60° gave the stablest meniscus, thereby ensuring uniform distribution of the liquid around the tube. Later, when the use of an annular distributor became necessary, another similar tube with smooth polished surface was prepared with the top free end having an inside thread. An annular distributor cap could be screwed on it when required, and when it was to be used with a knife-edge distributor, a knife-edge stud could be replaced. The details of the tubes and the knife-edge stud are given in Fig.2.21.

The Annular Distributor: The liquid meniscus at the top edge was observed to be very unstable at flow rates above Reynolds number* of 800. At these flow rates, therefore, the liquid had to be distributed through an annular ring. Kramers et al (15) had mounted a plastic cap rigidly with

---

* Re has been computed throughout this thesis on 4-times the film thickness as the characteristic diameter, and is given by

$$Re = \frac{4 \Gamma_v}{\nu}$$

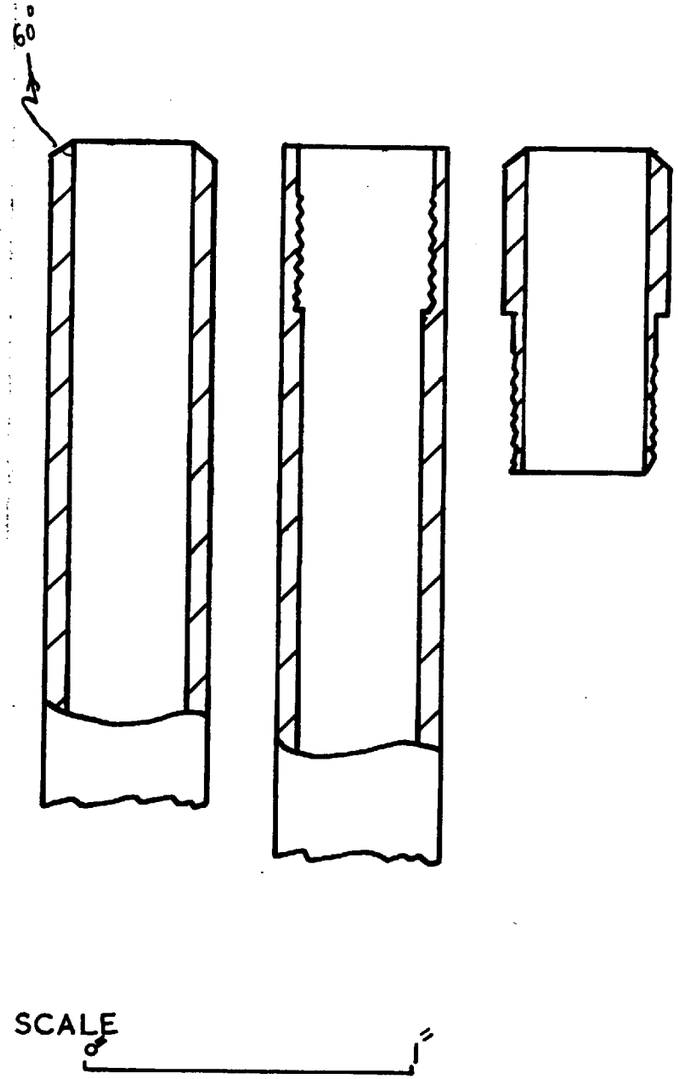

FIG. 2.21

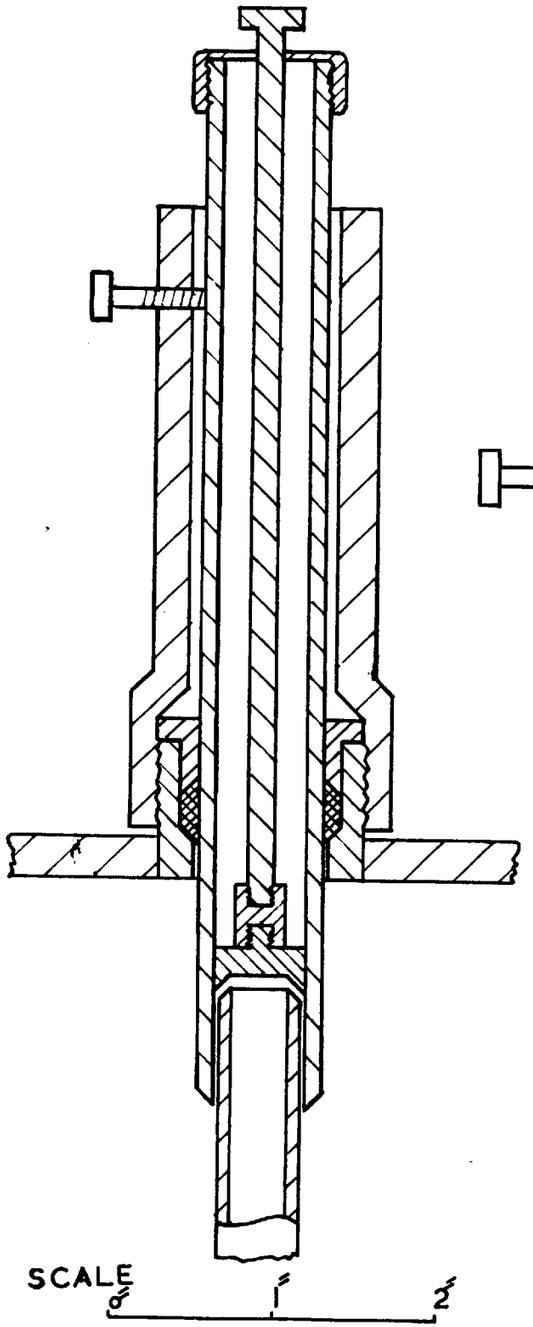

FIG. 2.22

a uniform width of clearance around the tube. Davidson and Cullen (38) had a similar annular distributor for wetting their sphere, the width of the clearance being 1/64 inch.

In the first trial of an annular distributor (see Fig.2.22), the author used a perspex tube with an inside diameter of 9/16 inch, ground with precision to 1/1000 in., and giving a clearance of 1/32 in. around the tube. The lower end of this distributor was bevelled at 45° to give a blunt edge. This reduced the possibility of water climbing due to surface tension and the consequent thickening of the film at this point. The edge was made slightly blunt to avoid damage when mounting. There was a 'P.T.F.E.' piston inside the distributor which could be moved up and down by means of a connecting rod. The details of this distributor are given in Fig.2.22. The piston served three purposes: (1) It blocked the contact of water with the atmospheric air. (2) The air trapped between the piston and the mouth of the stainless steel tube could be got rid of by moving the piston up and down. The entrapment of air was a source of trouble in the plastic cap used by Kramers (15). The trapped air prevented uniform distribution of the liquid film.

(3) The most useful advantage, from a working point of view, was the ease with which the tube could be wetted by moving the piston. It was a great trouble wetting the tube when its surface became dry. The movement of the piston served to give fluctuations to the water flow thereby facilitating complete wetting. It is to be mentioned that in actual operation the tube had to be wetted several times in one run when it became dry after a gas-purge of the absorber.

This distributor was clamped into the upper brass flange of the absorber by means of a modified 'ermeto coupling'. A screw-triad was used for aligning the distributor around the absorber column. However, this arrangement did not work very well. A lot of labour was required in obtaining a uniform width of clearance around the wetted wall. This seems obvious from a study of the design in the diagram. The distributor was, therefore, discarded.

Another distributor was designed which gave a quicker and much less laborious method of alignment. A detailed drawing of this distributor is given in Fig.2.23. The liquid films obtained with this distributor were easily reproducible. The stainless steel cap tapers down to give a clearance of 1/32 in. around the wetted wall tube.

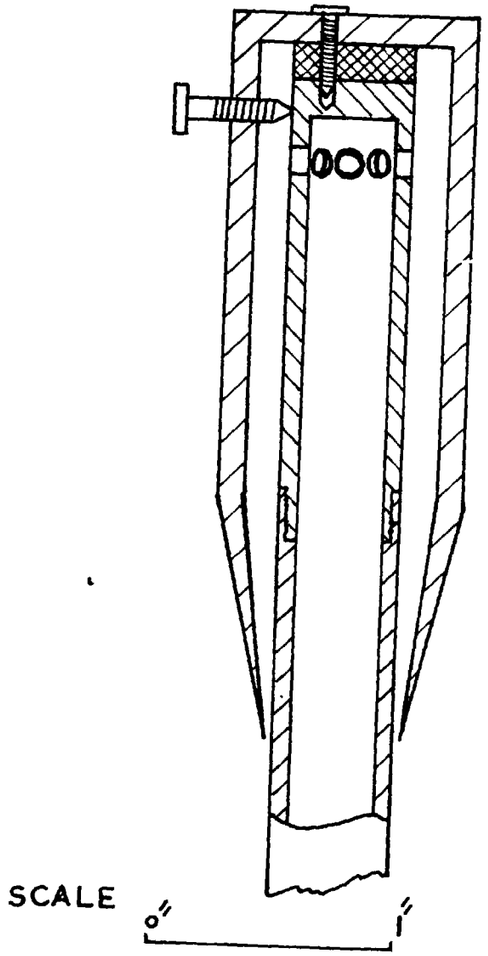

FIG. 2.23

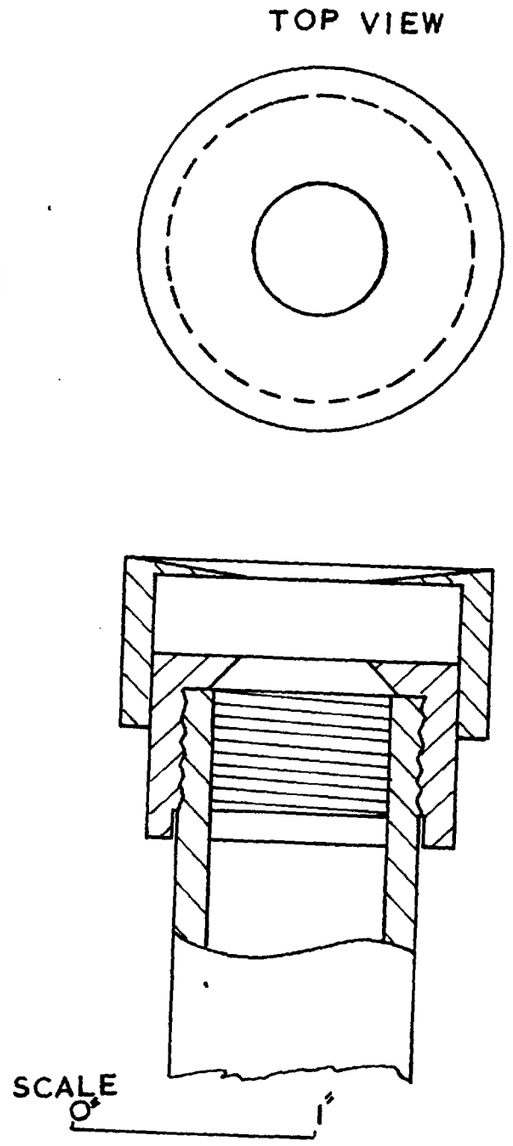

FIG. 2.24

Clearances of 1/64 in. and 1/16 in. were also tried but 1/32 in. was found to be the most suitable. The cap is coupled to the stainless steel stud by means of a screw-triad. There is a rubber gasket in between the top of the stud and the ceiling of the cap. The three screws in the side of the cap are just holding on to the stud and provide a horizontal motion of the cap round the wetted tube. These screws are used for a coarse adjustment while the small screws are used for fine adjustment. The small screws also provide a vent for the trapped air. The whole distributor could be unscrewed and fitted again without any further alignment. The water entered into the distributor through eight 1/8 in. holes in the stud.

A detailed drawing given in Fig.2.25 gives the position of the wetted wall tube in the absorber assembly. The tube was clamped at about 4 in. from its lower end to the bottom flange of liquid receiver 'R' by means of a modified 'ermeto coupling'. This coupling gave a sturdier grip than a rubber bung. The asbestos stuffing of the coupling helped to allow for an adjustment of the verticality of the tube, which was accomplished by means of a screw-triad 'D'. The two points of grip, one at the 'ermeto coupling'

and the other at the screw-triad, gave the tube a rigidity of position. The tube could be moved up and down to vary the height of the wetted wall with great ease.

The wetted wall tube was enclosed in a heavy assembly of a gas chamber 'G' and a liquid receiver 'R', the whole assembly itself resting upon a sturdy tripod stand. The sturdiness of the assembly was necessary in order to eliminate accoustic and other disturbances. Later on, when work on the application of sonic vibrations was carried out, the sturdiness of the absorber assembly was found to be very essential.

As seen in Fig.2.25, the gas-chamber consists of a thick-walled cylindrical 'Quickfit' glass section ($4^{1}/2$ in. dia x 11 in. height). This section is secured at both ends by 1/2 in. thick brass-plate flanges. The top flange has an outlet for the gas and a port for inserting a thermometer to measure the temperature of the gas. This flange carried an 'ermeto coupling' and a screw-triad also, when the perspex tube distributor was in use. The lower flange has an inlet for the gas as well as a drainage port for overflows from the wetted wall tube. The liquid receiver 'R' is coupled to this flange as shown. This receiver 'R' consists of a cylindrical perspex section ($2^{1}/2$ in. dia. x 3 in. height) secured between two brass flanges. It carries the connection for the outlet of spent liquid. The outlet liquid from here goes to an H-shaped levelling device. This device controls the height of

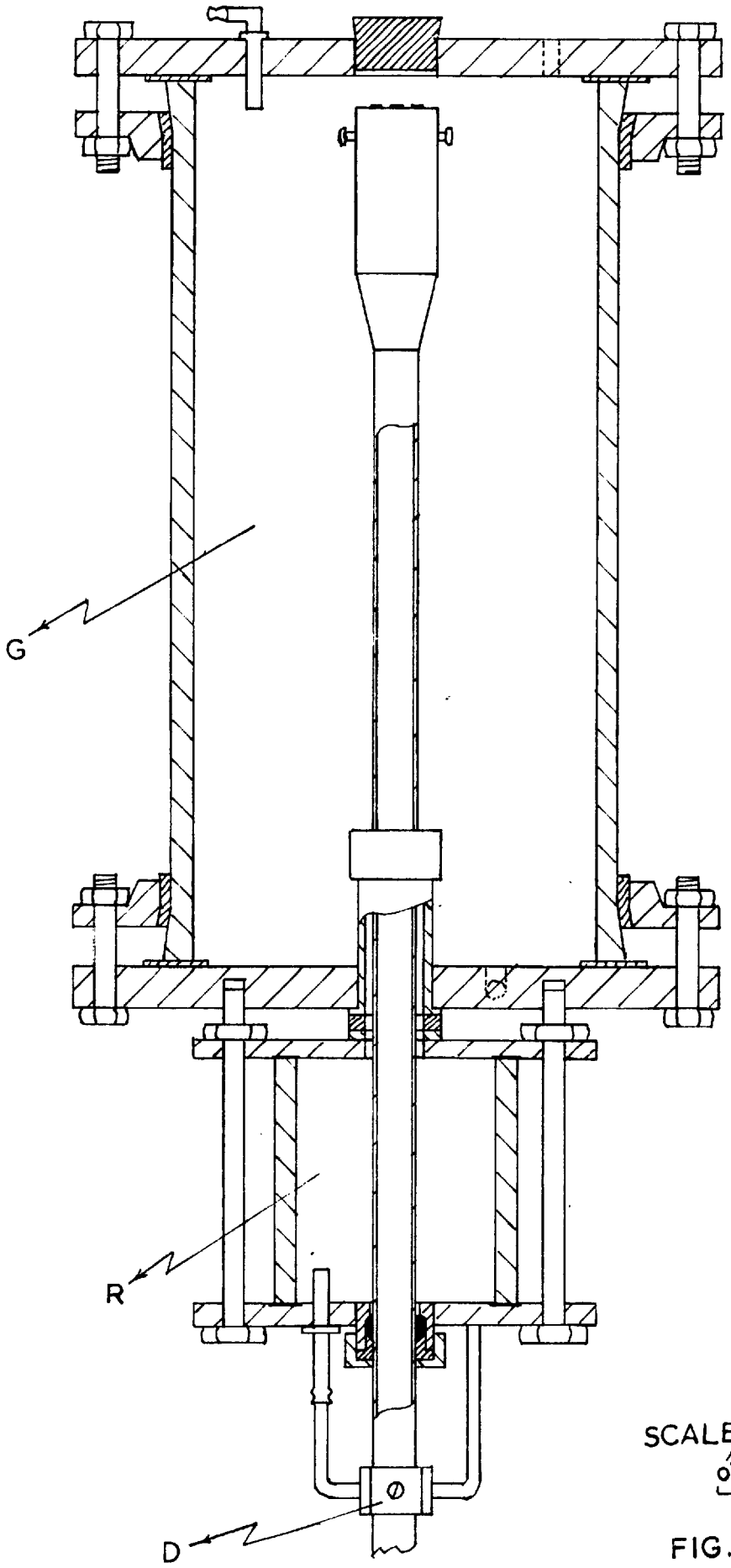

FIG. 2.25

level of the pool in the receiver. The need for a liquid receiver 'R' of a large size arose because of the observation that a small one gave rise to an end disturbance to the falling film in the pool. The large volume of liquid in the receiver seemed to cushion disturbances.

Receiving-end Device: The junction of the wetted wall and the liquid pool in the receiver was found to be subject to disturbances. These disturbances travelled into the wetted wall. The design of the 'receiving-end device' was perfected after trials of several alternative arrangements. Thus, first an open perspex tube of 3/4 in. I.D. was used, but the disturbance at the junction was so great that the pool liquid almost churned. There was a large entrapment of the gas and the pool area exposed to the gas was considerable.

A stainless steel receiving-end device was designed which was screwed on the perspex tube. It is shown in Fig.2.24. It had a 5/8" dia. hole in the centre giving an annular clearance of 1/16 in. around the tube. The results obtained with this device were better than those obtained with the open-mouth receiver, and an unnecessary pool surface exposure was reduced, but still the disturbance at the pool was quite appreciable. Another similar

cap with an annular clearance of 1/32 in. was next tried which was found to eliminate the disturbance at the pool completely but had the disadvantage of difficult alignment and caused flooding. The annular clearance in this case was too small to accept all the quantity of water at a high flow rate. The size of the annular clearance was gradually increased by grinding until a clearance of 3/64 in. was found to be very suitable. The hole was ground to a knife-edge and a bell-shaped taper given from the knife-edge downwards to a depth of 1/8 in. at an angle of 45°. This taper helped to stabilise the pool. At high flow rates, the stainless steel cap was further mounted by a shallow, funnel-shaped, perspex lid (Fig. 2.24) having a water-repellent polish. This helped to prevent any spurting of water from the receiver.

Alignment Aids: The entire absorber assembly was resting on three levelling screws of the tripod stand. The verticality of the wetted wall tube was first achieved by adjusting these three levelling screws with the help of a spirit level. The screw-triad 'D' (see Fig.2.25) was then used to obtain a uniform clearance around the tube in the 'receiving-end device'. The verticality of the column was then checked by means of a plumb-line. Pure water was then allowed to run as a film and the level in

the pool adjusted. The tripod levelling screws were then adjusted to obtain a horizontal band of waves at the exit end of the wetted wall column. This indicated that the liquid was uniformly distributed around the tube.

Art. 2.3. The Liquid Supply

Distilled deaerated water was used throughout the work described in this thesis. The still used for the supply of distilled water was actually designed for the separation of a volatile component from a binary with water. It consisted of a copper boiler-pot (1'-8" dia. x 1'-4" height) having connections of a water inlet and outlet, and a level-gauge. Inside the pot was a copper coil carrying steam. The vapours from the boiler-pot passed through six perforated plates (1/4" dia. perforations) separated by 'Quickfit' glass sections (5" dia. x 6" height). The vapour was then condensed in a vertical tubular condenser which had a connection of an air vent where vacuum could also be applied. The still had a capacity of distilling 8 gals. of water per hour. It gave a distilled water of very high quality.

The water from the still was collected in bottle 1 of a deaeration unit (see Fig.2.41). This unit consisted of three 20-litre glass aspirator bottles placed at different heights. The water was sucked into bottle 2 from bottle 1 by applying vacuum to it. A pressure-vacuum pump was used for obtaining

the vacuum and the maximum vacuum obtainable with this pump was 24" of mercury. It was found from absorption trials that a water deaerated at 20" of mercury was sufficiently free from air to give consistent results. Deaerated waters obtained at vacuums higher than 20" of mercury did not give any better absorption results. Therefore, the vacuums used throughout this work ranged from 21-23" of mercury. Water was thus sprayed into vacuum alternately in bottles 1 and 2, twice in each. It was then stored under vacuum in bottle 2 for supply to the absorber. Consistent absorption trials showed that water was sufficiently free from air after four sprays into vacuum. Bottle 3 was used in conjunction with bottle 2 only when high liquid flow rates were used in the absorber. If a surface active material was to be used, it was separately dissolved in a small quantity of water and then sucked into bottle 1 before collecting distilled water in it. This, and the subsequent spraying into vacuum, ensured thorough mixing of the addend. In the early part of this work, water from bottle 3 was used to keep the head of water constant in bottle 2. Later this method was given up because the flow of water from bottle 3 to 2 caused turbulence on the surface in bottle 2, thereby increasing air absorption. The water surface in bottle 2 was covered with a plastic sheet to avoid unnecessary exposure to air. The drop in hydrostatic head during a run at low flow rates was very small,

and the liquid flow to the absorber could easily be adjusted by means of a needle valve. At high liquid flow rates, bottle 3 was used to replenish head in bottle 2. Bottle 3 was also used as a supply vessel for pure water, when runs were being obtained with surfactant added, for the alignment of the wetted wall tube by means of the exit-end wave band. It is to be re-mentioned here that this band of waves was visible only when pure water was used.

Art. 2.4. Temperature and Pressure Control

A flow-diagram of the entire apparatus assembly is given in Fig.2.41. Both the liquid and the gas had to be brought to a particular temperature and pressure before being fed to the absorber. Water was supplied by bottle 2, and CO_2 gas was taken from a pressure cylinder (wt. of gas in the cylinder = 28 lbs., gauge pressure = 900 - 1200 lbs/sq.in). The two streams of liquid and gas passed separately through two temperature-equilibrating coils (1/4" I.D., 20 ft. long copper tubing) immersed in a constant temperature water-bath. The latter was a cylindrical copper vessel (1 ft. dia x 1'-4" height) with a stirrer. The temperature of water in this tank was controlled to a $1/4^{o}C$ by means of a toluene switch and an immersion heater. Besides the copper coil, the tank carried two glass gas-saturators.

The absorber , along with its auxilliary equipment, was placed inside a large constant temperature air-bath. The latter was a rectangular chamber (2'-0" x 1'-7" x 2'-10" height) made

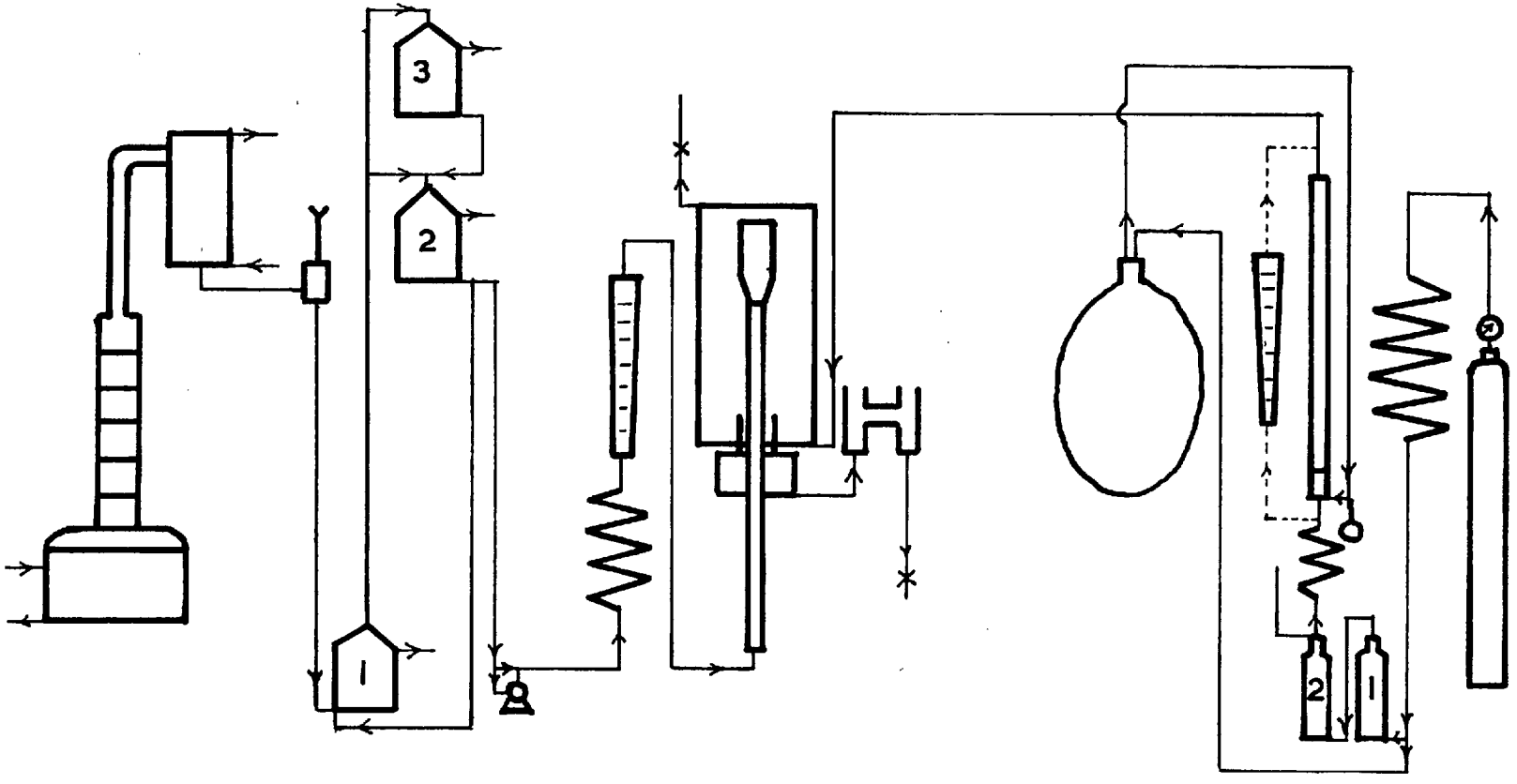

FIG. 2.41 FLOW SHEET

from Perspex sheets with the front door easily removable. This door had a window ($4^{3}/_{4}$" x $12^{1}/_{2}$") cut in it for access to the inside for manipulations while a run was underway. This arrangement minimised the temperature fluctuations. A coil of resistance wire stretched at the base of the air-bath, and covered with a hot air distributor, supplied the heat. A two-blade stirrer in the side of the chamber kept the air well stirred. The temperature could be controlled to an accuracy of $1/2^{\circ}C$. Both water and gas from the water-bath passed separately each through another 5 ft. long copper tubing, made into coils, mounted inside the air-bath. After passing through the coil in the air-bath, water was metered by a calibrated rotameter before being fed to the absorber. In the case of gas, different arrangements of feed to the absorber were employed according to requirement. Thus, when the absorber was to be purged free of air, CO_2 gas from the cylinder was first passed through the copper coil in the water-bath, then through two saturators placed in series inside the water bath, from these to the coil in the air-bath, and was finally metered through a bubble meter or a rotameter before being fed into the absorber. A slightly different arrangement was employed for an absorption run. In this case the dry gas from an atmospheric balloon was fed directly to the absorber after passing through a bubble-meter. The balloon in turn got its supply of gas direct from the cylinder. CO_2 of 99.8% purity was always used.

It was saturated with water to prevent any vaporisation of water from the wetted wall. Saturator 2 had a glass-tube, one end of which was dipping below the level of water in it, and the other end open to the atmosphere. The rise of water in this tube gave an indication of the pressure under which the gas was flowing to the apparatus. A gas pressure of 10"-22" of water was required in saturator 2 to obtain a flow in the rotameters. The balloon could not be used in this case. It was used only with a soap bubble-meter. The balloon stored gas at a maximum pressure of 1 cm. of water. Absorption results were obtained for both, (1) when the balloon was vented to the atmosphere, (2) when it was closed to the atmosphere. The difference between the two sets of results was negligible. In fact it was found that in the case of venting the balloon to the atmosphere, contamination of the gas with air occurred. Therefore, all the later work was carried out with the closed balloon.

The inlet gas rotameter (10-100 c.c. of CO_2 per minute at 25°C) was connected parallel to a bubble-meter and either could be used as desired. The outlet gas from the absorber passed through another rotameter (2-20 c.c. CO_2 per minute at 25°C) also connected in parallel with a bubble-meter. From here the gas was vented to the atmosphere. These pairs of meters were, in fact, only used in the initial runs for calibrations and refinements. In all the rest of the absorption work only one bubble-meter

was used for measuring the contraction in the volume at constant pressure of the gas due to absorption. A water manometer (U-tube) showed the gas pressure inside the absorber. The average gas pressures used were about 1 cm. of water higher than the atmospheric pressure. Temperatures of both inlet and outlet gas and liquid streams were recorded. The difference in the two sets of temperatures was found to be negligible.

Art. 2.5. Calibrations and Refinements

Calibrations

The Bubble-meter: The bubble-meter was simply a graduated Eureka glass tube (0-50 c.c. with graduations of 0.1 c.c.) carrying three limbs at its lower end. Two side limbs were connected to the gas supplies while the bottom limb carried a rubber bladder filled with 2% 'teepol' solution. When a bubble was to be introduced, the bladder was pressed to raise the level of the solution into the tube until the gas would push one thin film up the tube. Before starting an absorption run, the inside of the glass tube had to be wetted by passing a train of such bubbles through the tube. A wet wall would prevent breaking up of the bubble while travelling.

The graduated portion of the meter tube was recalibrated to determine the exact volume of gas occupied between divisions 50 and 5 at different temperatures. In all the absorption work,

time was measured for the displacement of the bubble between divisions 50 and 5. The calibration was carried out as follows:

The tube was filled with distilled water at a particular temperature and the quantity of water between divisions 50 and 5 was drained and weighed. The drainage process was made relatively slow to prevent any drops from being left sticking to the wall . The volume occupied by the liquid left as a thin film sticking to the wall could be neglected as even in an absorption run the wall had to be wetted. From the weight of the water collected, the volumes calculated were as follows:

20°C.	=	44.88 c.c.
25°C.	=	44.90 "
30°C.	=	44.91 "
35°C.	=	44.93 "

The variation in the volume of the bubble meter between division$_s$5-50 with temperature was, therefore, negligible. A volume of 45.00 c.c. was accepted for all the temperatures used. This was done because the difference between the average volume from the above calibration and 45.00 c.c. was negligible when compared with the rate of displacement of the bubble.

Liquid Rotameters: Three liquid rotameters of different ranges were used in this work. During the early part of the work,

the rotameter used had a range of 1-10 gals./hr., calibrated at 20°C. Later two other rotameters were used, one calibrated for 1-10 gals./hr. at 25°C , and the other uncalibrated (2-40 gals./hr. capacity). All three were recalibrated for temperatures of 20-40°C.

The rotameters were calibrated by noting the time required to collect a definite volume of water at the outlet from the absorber. Table-2.51 gives a sample of the results of calibrations of one of the rotameters.

Table - 2.51

Calibration Chart for rotameter (1-10 gals./hr.)

Temperature °C	Rotameter reading gals./hr.	Calibrated reading gals./hr.	Temperture. °C	Rotameter reading gals./hr.	Calibrated reading gals./hr.
20	7.000	6.826	30	4.000	4.083
"	6.000	5.824	"	3.000	3.071
"	5.000	4.889	"	2.000	2.079
"	4.000	3.901	35	7.000	7.168
"	3.000	2.917	"	6.000	6.236
"	2.000	1.932	"	5.000	5.176
25	7.000	7.008	"	4.000	4.211
"	6.000	5.977	"	3.000	3.168
"	5.000	5.012	"	2.000	2.164
"	4.000	4.020	40	7.000	7.199
"	3.000	3.023	"	6.000	6.336
"	2.000	2.020	"	5.000	5.194

Table 2.51 - contd.

Temperature °C	Rotameter reading gals/hr.	Calibrated reading gals/hr.	Temperature °C	Rotameter reading gals/hr.	Calibrated reading gals/hr.
30	7.000	7.104	40	4.000	4.304
"	6.000	6.115	"	3.000	3.259
"	5.000	5.077	"	2.000	2.256

Refinements

During early experimentation, gas rotameters were used for metering the flow rates to and from the absorber. One rotameter (10-100 c.c. of CO_2/min. at 25°C) metered the inlet gas and the other (2-20 c.c. of CO_2/min. at 25°C) metered the outlet gas. The difference in the readings of the two rotameters was the absorption rate per minute. Some 50 runs were taken with different flow rates and heights of the wetted wall. Table 2.52 records some of these runs. It is clearly seen from this table that, for the same flow rate of water, the absorption rates are different in different runs. The results were highly inconsistent. One reason for this was the small solubility of CO_2 in water. The change indicated by the rotameters for a small change in the flow rate of water (0.5 gals/hr.) was so small that the errors of the instruments themselves were comparable to it. The floats of the rotameters were very unsteady. Since wet gas had always to be

passed through the outlet rotameter, the float of this rotameter would stick to the wall and was liable to give erroneous results.

Table-2.52

Height of wetted wall = 8.70 cm.

Temperature of gas and water = 25°C (± 0.2°C)

Water flow rate gals/hr.	Rotameter 1 reading cc/min.	Rotameter 2 reading cc/min.	Rate of absorption of gas cc/min.
2.970	34.0	15.7	18.3
2.970	32.0	14.1	17.9
4.054	32.0	14.6	17.4
5.012	32.0	11.7	20.3
4.054	32.0	13.0	19.0
3.900	38.0	19.0	19.0
3.680	38.0	19.5	18.5
4.054	38.0	8.9	29.1

This, in fact, was the biggest handicap in the use of rotameters. Later, soap-film meters were used in place of rotameters but again the results were not reproducible. The technique of passing a steady stream of gas through the absorber, in order to minimise accumulation of inerts, had, therefore, to be discarded. Later tests on the influence of the accumulation of inerts on absorption, however, showed that the errors introduced in the use of a

steady-stream technique were far greater in magnitude than those due to inerts. Efforts were then made to find conditions for preventing the accumulation of inerts in a stationary-gas absorption technique as described below:

> Liquid flow was switched on to the absorber and a steady stream of saturated CO_2 at 2 litres/min. was passed through it for 2 minutes to displace the air. Gas flow was then stopped, absorber gas exit closed and the gas feed from the atmospheric balloon opened. After the conditions became steady, a soap film was introduced in the bubble-meter connected at the gas inlet of the absorber. The time was noted for the displacement of the bubble between divisions 50 and 5. The rate of displacement of the bubble gave the rate of absorption. The balloon was then disconnected, the absorber gas exit opened, and again purge-gas was streamed through the absorber at 2 litres/min. for another two minutes, at the end of which another absorption run was recorded. This process was repeated for purge intervals of two minutes until the rate of absorption reached a maximum. A graph of purge time 't purge' is plotted against the time taken for the displacement of bubble between divisions50 and 5, 't absorption', for a constant liquid

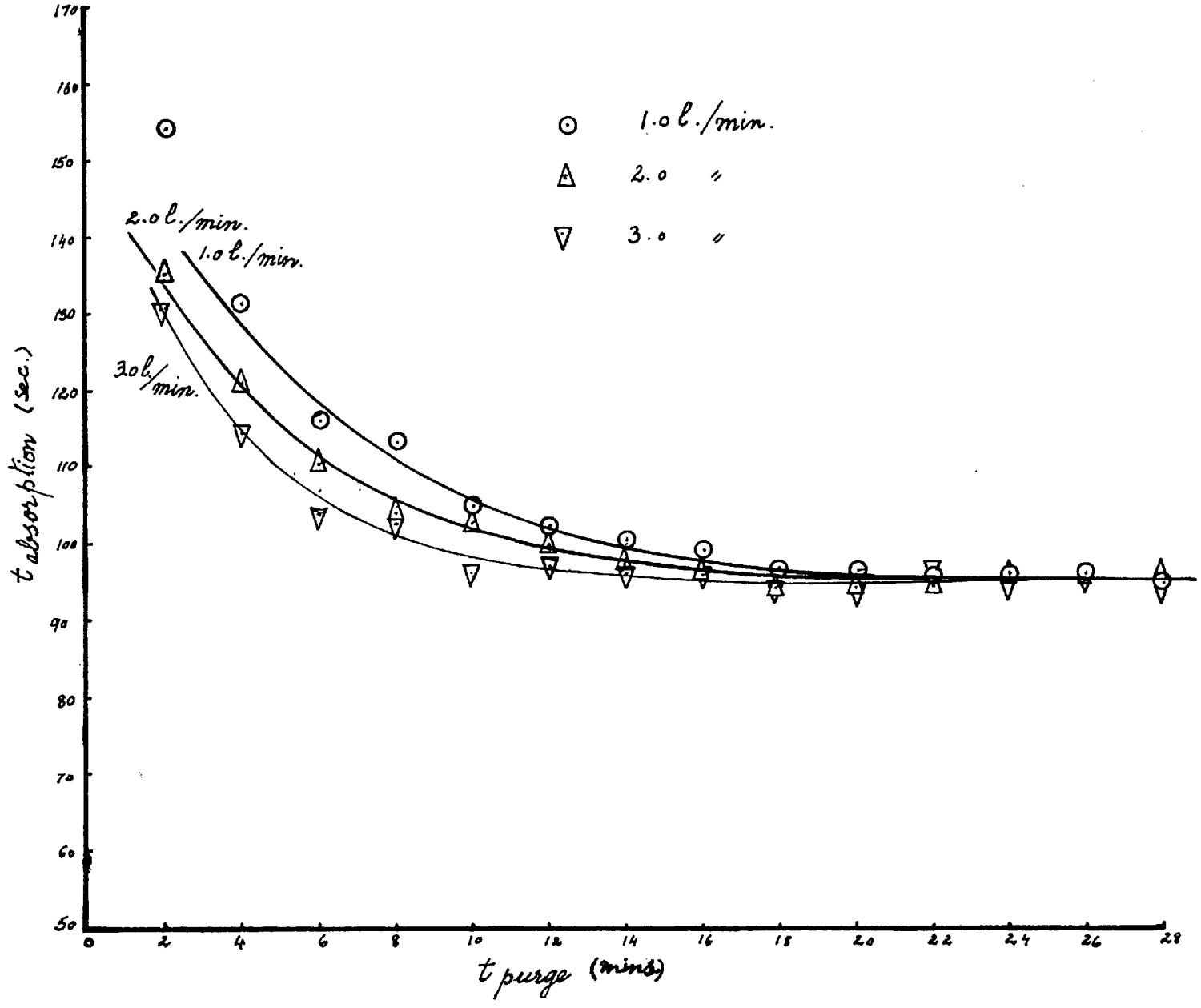
1.0 l./min.
2.0 "
3.0 "
2.0 l./min.
1.0 l./min.
3.0 l./min.
t absorption (sec.)
t purge (mins)
170
160
150
140
130
120
110
100
90
80
70
60
50
0
2
4
6
8
10
12
14
16
18
20
22
24
26
28

FIG. 2.51

flow, shown in Fig.2.51. It is seen from the graph that the absorption rate becomes constant after 17 minutes of purge.

Another two similar runs were made for purge time, 't purge' versus bubble displacement time, 't absorption', at purge-gas flows of 1 and 3 litres/min. respectively, starting with the absorber filled with air in each case. It was concluded from these studies that the purge time after which the absorption rate started to become constant was between 12-18 minutes. Therefore, in all the subsequent work, a purge-time of more than 25 minutes was always given at purge-gas flows of 2 litres/min.

Effect of the Accumulation of Inerts: The absorber was purged for 25 minutes, the gas exit of the absorber closed, supply from the balloon connected, and absorption rates determined, for a constant flow rate of water, after intervals of 5 minutes. The results are shown in Fig.2.52, where the time elapsed 't' is plotted against the time of displacement of bubble 't absorption'. The time of the first run after the purge has been taken as zero. It is seen from the graph that the first noticeable influence of the inerts becomes evident 20 minutes after the purge. The maximum effect of the inerts on absorption rate is observed at the 75th minute, after which it becomes

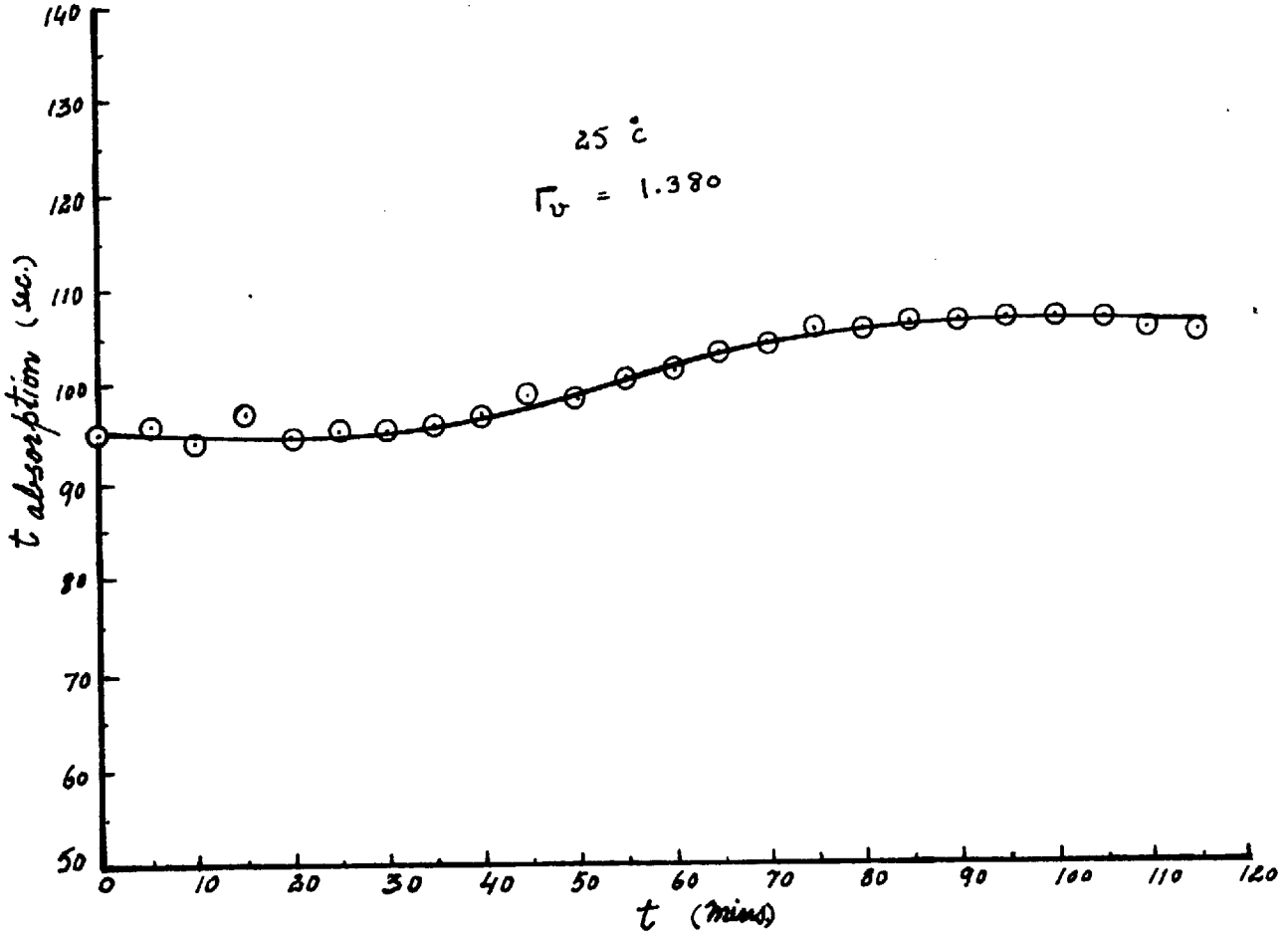
25 °c
Γ_v = 1.380
t absorption (sec.)
t (mins)
140
130
120
110
100
90
80
70
60
50
0
10
20
30
40
50
60
70
80
90
100
110
120

FIG. 2.52

constant again. Nearly identical results were obtained in another similar run at another liquid flow. It was, therefore concluded that the absorption runs should not last more than 20 minutes after the gas has once been enclosed in the absorber system. A purge of 5 minutes after every single absorption run was much preferred.

Just for a comparison of results, absorption studies were also made with tap-water, deaerated tap-water, distilled water, and deaerated distilled water. The tap-water and deaerated tap-water gave results about 2-2.5 % lower than deaerated distilled water. Results from distilled water were 0.5% lower than those from dd-water. Deaerated distilled water was, therefore, used in all the subsequent work.

CHAPTER III

ABSORPTION INTO A FALLING LAMINAR LIQUID FILM

Art. 3.1. Treatment of Data

Extensive absorption results were obtained on CO_2 - water system by varying the heights of the wetted wall, temperatures, liquid flow rates, and with either an overflow or an annular liquid distributor. The effect of the addition of a surface active agent to water was also studied. In order to analyse the results, the data obtained was treated as discussed below.

Treatment of Gas Volumes

The gas volumes of absorption were reduced to standard conditions ($0^{\circ}C$, 760 mm.), and for the sake of uniformity the volumes were calculated for a partial pressure of 760 mm. of CO_2 in the absorber. The volumetric rate of absorption is actually independent of the gas pressure inside the absorber. This is illustrated by the following example:

Let, the volume of the gas absorbed, c.c. = V

Pressure of the gas in the absorber, mm. = 771

Temperature " " " " " $^{\circ}C$ = 25

Vapour pressure of water at $25^{\circ}C$, mm. = 23.7

Therefore,

Volume of dry CO_2

absorbed, cc. = $V \times \frac{(771-23.7)}{771}$

As measured at a total pressure of 771 mm., if the same quantity of CO_2 were reported relative to a pressure of 760 mm. instead of 771 mm., its volume would be, cc.

$$= V \times \frac{(771-23.7)}{771} \times \frac{771}{760}$$

If we now ask how much CO_2 would be absorbed if its partial pressure in the absorber were 760 mm. instead of (771-23.7)mm., we have to correct the previous figure by the use of Henry's law, as, (c.c.)

$$= V \times \frac{(771-23.7)}{771} \times \frac{771}{760} \times \frac{760}{(771-23.7)}$$

$$= V$$

$\therefore$ The required volume at S.T.P. $= V \times \frac{273}{273+25}$

The density of CO_2 at S.T.P. is reliably known to be as 1.9769 gms/litre.

Height Equivalent to Meniscus

In the case of absorption results with an overflow distributor, the meniscus of liquid at the overflow was observed to vary with the liquid flow rate. Thus, at the lowest flow rate of 0.3162 $cm.^2$/sec., the meniscus was almost a flat pool, while at the highest rate of 3.1620 $cm.^2$/sec., it was approximately hemi-spherical. Therefore, the equivalent height to be added to the wetted wall height, would be, in the case of lowest flow rate (flat-pool) as $\pi r^2/2\pi r = r/2$, and in the case of

highest flow rate (hemi-spherical) as $2\pi r^2/2\pi r = r$ (r is the radius of the wetted wall tube). The variation in the HEM (Height Equivalent to Meniscus) from the lowest to the highest flow rate is, thus, $r/2$ to r. An average $3r/4$ was, therefore, added to the vertical height of the wetted wall, the justification for the use of an average value being the small magnitude of the correction.

Saturated Concentrations (C*)

The data on solubilities available in literature (56) are given as gm. per gm. of the solvent. In order to convert these data into concentration units (gm./cc.), a knowledge of the densities of aqueous solutions of CO_2 is required. However, the density of water is affected only in the fourth decimal place by the saturated solutions of CO_2, therefore, densities of pure water were used for the purpose. The following values were calculated for different temperatures:

Temperature, °C;	20	25	30	35
C* x 10^3, gm/cc.; (760 mm. partial pressure of CO_2).	1.722	1.495	1.315	1.170

Other Physical Constants

The values of the diffusion coefficients 'D' available in literature are widely different. Somewhat more reliable

values given by various workers are plotted for comparison in Fig.3.11. It is seen that at temperatures higher than 20°C , Davidson and Cullen (38) give much higher values of the diffusion coefficients than the others. In fact, when Davidson's values of 'D' were used for the correlation of the data, they were found to be much too high. Davidson and Cullen had obtained the values for absorption into a spherical wetted wall, using pure water. The present work has shown that pure water always gives higher absorption coefficients than water containing surface active material because of the presence of both visible and invisible ripples, and it may be suspected that such ripples were present on Davidson's absorber. Therefore, Davidson's values were not considered suitable. Diffusion coefficients given by Vielstich (57) were chosen to be more suitable (Fig.311).

The values of kinematic viscosity 'ν' used in the calculations are as follows (56) :

Temperature, °C ;	20	25	30	35
$\nu \times 10^3$, $cm^2/sec.$;	~~1.010~~ 1.010	8.974	7.969	7.250

Correction for the Exit-End Effect

As discussed before, the exit-end effects reduce the effective height of the wetted surface. The heights of the stagnant zones 'h_r' were measured at different flow rates by sprinkling lycopodium powder and reading through a cathetometer.

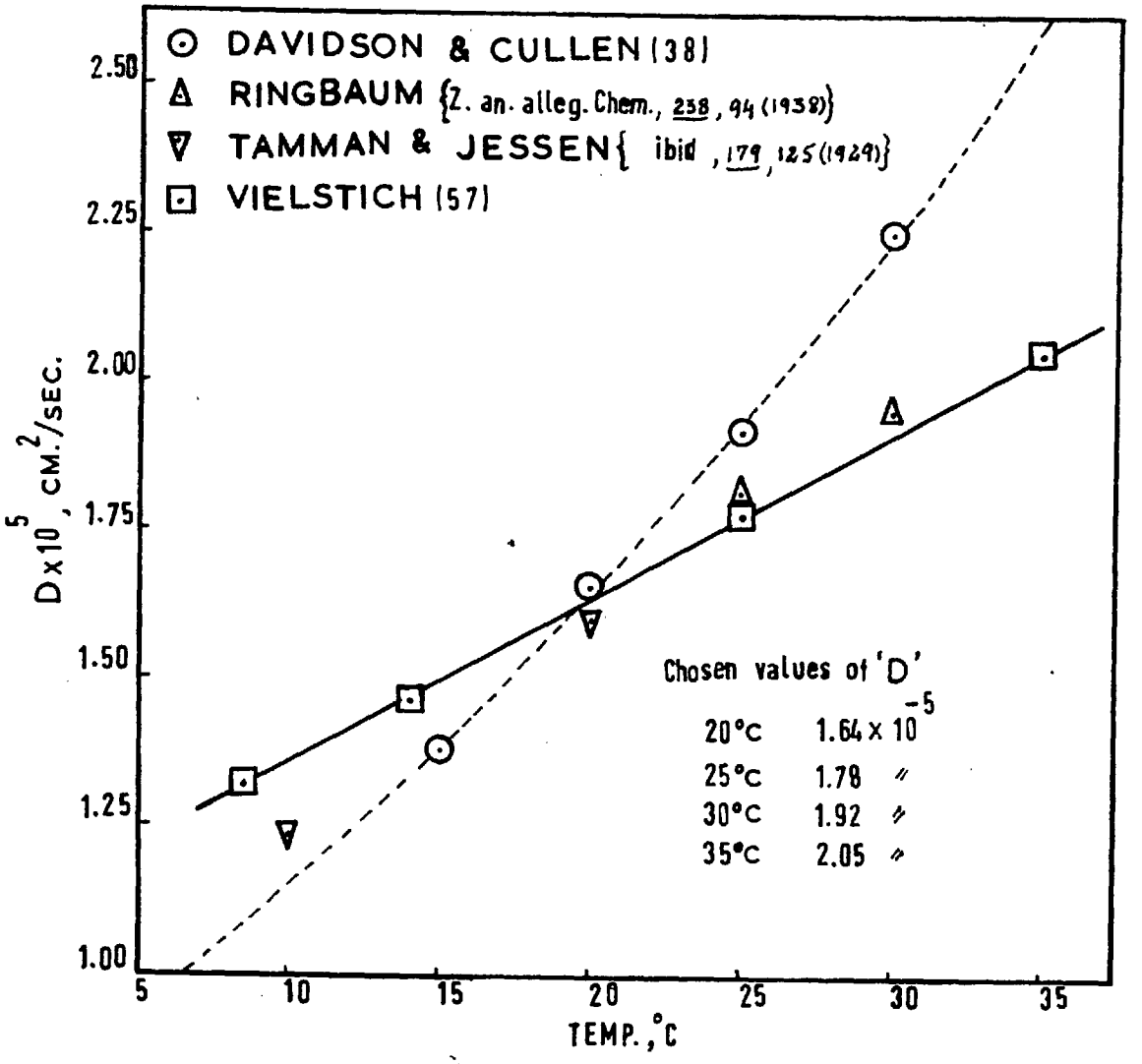
DAVIDSON & CULLEN (38)
RINGBAUM {Z. an. alleg. Chem., 238, 94 (1938)}
TAMMAN & JESSEN { ibid, 179, 125 (1929)}
VIELSTICH (57)
Chosen values of 'D'
20°C 1.64 x 10⁻⁵
25°C 1.78 "
30°C 1.92 "
35°C 2.05 "
D x 10⁵, CM.²/SEC.
TEMP., °C
2.50
2.25
2.00
1.75
1.50
1.25
1.00
5
10
15
20
25
30
35

FIG. 3.11

'h_r' was found to vary only with the flow rate and was independent of the temperature and the height of the column. The values of 'h_r' were found to be as given in Table 3.11.

Table-3.11

Γ_v cm.^{2}/sec.	0.3200	0.6369	0.9530	1.2680	1.5810	1.8850	2.2220
'h_r', cm. (Pure water)	1.00	0.60	0.45	0.35	0.20	0.05	-
'h_r', cm. (water containing Lissapol, 0.01% by vol.)	2.20	1.00	0.70	0.50	0.30	0.10	-

The effective height of absorption 'h_e' was, therefore, taken as,

$$h_e = h - h_r$$

where, for an overflow liquid distributor,

h = vertical height $+3r/4$

and, for an annular liquid distributor,

h = vertical height.

Art. 3.2. Presentation and Discussion of Results

Experimental absorption rates per unit area of the wetted surface were calculated from the following equation :

$$N_A = \frac{V.\rho_o}{2\pi(r+\delta)h_e\ t_{abs.}} \cdot \frac{T_o}{T} \qquad \ldots (3.21)$$

where,

V = volume of gas absorbed, cc.,

ρ_o = density of CO_2 at S.T.P., gm./cc.,

h_e = effective height of wetted surface, cm.,

δ = thickness of the liquid film, cm.,

r = radius of the wetted tube, cm.,

T_o = absolute temperature, 273°A ,

T = temperature of the system, °A ,

t_{abs} = time required for the absorption of V cc. of the gas, sec.

Theoretical absorption rates are given by Eqn.(1.412). When values of the physical constants are inserted in this equation, and putting $h = h_e$, we get,

$$\text{at } 20^\circ C \ , \ N_A = 5.436 \times 10^{-5} (\Gamma_v)^{1/3} . (h_e)^{-\frac{1}{2}} \qquad \ldots (3.22)$$

$$25^\circ C \ , \ N_A = 5.013 \times 10^{-5} (\Gamma_v)^{1/3} . (h_e)^{-\frac{1}{2}} \qquad \ldots (3.23)$$

$$30^\circ C \ , \ N_A = 4.680 \times 10^{-5} (\Gamma_v)^{1/3} . (h_e)^{-\frac{1}{2}} \qquad \ldots (3.24)$$

$$35^\circ C \ , \ N_A = 4.370 \times 10^{-5} (\Gamma_v)^{1/3} . (h_e)^{-\frac{1}{2}} \qquad \ldots (3.25)$$

As seen from the above equations, the effective height 'h_e' is also a variable depending upon the flow rate. However, it becomes independent of the flow rate above 1.9000 $cm.^2/sec.$, because then the height of the exit-end effect becomes negligible (see Table-3.11).

Results

It was observed that, at low flow rates, in the region of laminar liquid flow, rippling started on the film some way down the wetted wall. The height of the zone of rippling depended on the liquid flow rate. The lower was the flow rate of liquid, the higher was the zone of rippling. The lowest liquid flow rate, at which the wall could be easily wetted, was found to be 0.6585 $cm.^2/sec.$ (In some cases flow rates as low as 0.3200 $cm.^2/sec.$ could also wet the wall completely). At this flow rate the height of the unrippled region was observed to be 9.10 cm. As an unrippled film is easily amenable to theoretical analysis, and it is possible to compare the results with the results of other workers, the results shown in Table-3.21(a) were taken on a wetted wall height 'h' of 9.10 cm., using pure water.

Table-3.21

Temperature of the system, ^oC = 25

Height of the wetted tube, h, cm. = 9.10

Diameter of " " " , cm. = 1.270

Tube surface = Plain

Liquid used = Pure water

Liquid distributor used = overflow

(a)

Γ_v ($cm.^2/sec.$)	Reynolds number (Re)	$(\Gamma_v)^{1/3}.(h_e)^{-\frac{1}{2}}$	$N_A \times 10^6$ ($gm./cm.^2 sec.$)
0.6585	294	0.2983	14.86
0.8191	365	0.3183	15.40
0.9788	437	0.3360	16.09
1.1380	507	0.3515	16.74
1.2980	579	0.3655	17.30
1.4560	649	0.3787	17.81
1.6140	720	0.3901	18.34
1.7760	792	0.4014	18.91
1.9440	865	0.4140	19.39
2.1020	937	0.4245	19.98
2.2630	1009	0.4350	20.35

(b)

Γ_v	$\frac{1}{(\Gamma_v)^{1/3}.(h_e)^{-\frac{1}{2}}}$	$\frac{1}{N_A} \times 10^{-4}$
0.6585	3.351	6.730
0.8191	3.142	6.485
0.9788	2.977	6.220
1.1380	2.845	5.970
1.2980	2.735	5.780

(b) contd.

Γ_v	$\frac{1}{(\Gamma_v)^{1/3}.(h_c)^{-\frac{1}{2}}}$	$\frac{1}{N_A} \times 10^{-4}$
1.4560	2.640	5.618
1.6140	2.564	5.450
1.7760	2.491	5.290
1.9440	2.417	5.160
2.1020	2.355	5.005
2.2630	2.298	4.915

Reynolds numbers have been given in Table 3.21 (a) in order to give an easy reckoning of the flow condition. Kramers et al. (15) have given Reynolds number 1200 as the transition point of laminar to turbulent flow. It is seen from the table that the liquid flow was well within the laminar region. According to Eqn.(3.23), then, if $(\Gamma_v)^{1/3}.(h_c)^{-\frac{1}{2}}$ is plotted against N_A, a straight line should be obtained. Fig.3.21(a) gives such a plot. It is seen that the experimental results do not fit the line of Eqn.(3.23). There seems to exist some sort of a barrier to absorption.

As has been discussed in Chapter I, many authors suggest the existence of an interfacial resistance to absorption.

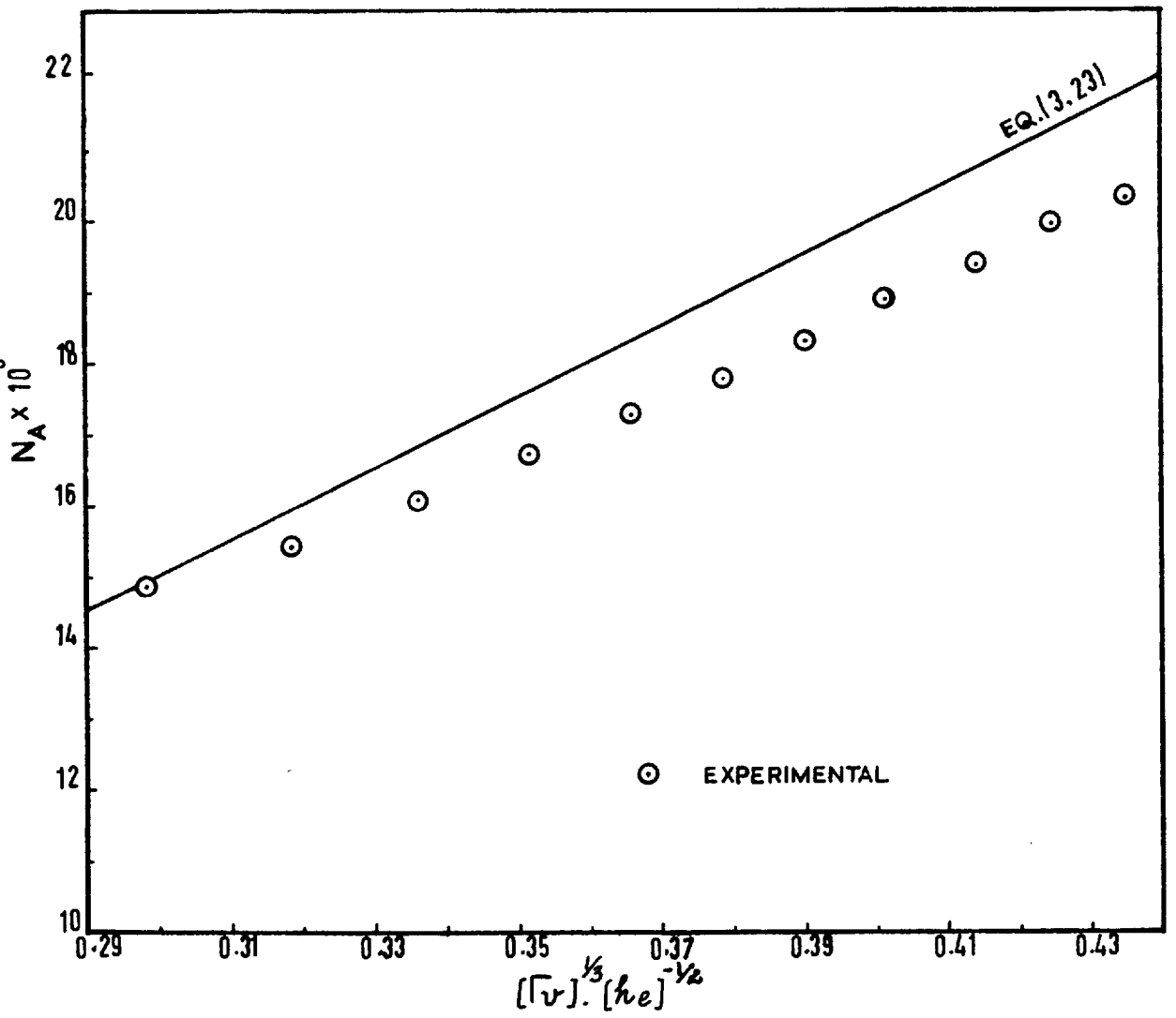
22
20
18
16
14
12
10
$N_A \times 10^6$
EQ.(3.23)
EXPERIMENTAL
0·29
0.31
0.33
0.35
0.37
0.39
0.41
0.43
$[\Gamma v]^{1/3}.[he]^{-1/2}$

FIG. 3.21 (a)

Danckwerts and Kennedy (46) correlated their results by assuming an interfacial resistance $1/k_i$, where k_i = 0.11 cm/sec. Higbie's (29) measurements of CO_2- water also indicated a surface resistance of this order of magnitude. It was, therefore, decided to compare the results obtained in this work with the results of Danckwerts and Kennedy. For this purpose, an expression of the mass transfer Eqn.(1.41) in terms of transfer resistances was obtained as follows:

Eqn. (1.41) can be written as,

$$N_A = \frac{C^*}{1/k_L} \qquad (C_o = \text{zero, and } C_i = C^*)$$

where '$1/k_L$' is a diffusional resistance to mass transfer. If '$1/k_i$' is an additional resistance to mass transfer, then, the transfer rate would be given by,

$$N_A = \frac{C^*}{1/k_L + 1/k_i} \qquad \ldots (3.26)$$

$$\text{or } 1/N_A = \frac{1}{C^*} \left\{ 1/k_L + \frac{1}{k_i} \right\} \qquad \ldots (3.27)$$

When the values of physical constants used by Danckwerts and Kennedy (46) ($D = 2.02 \times 10^{-5}$ cm.^{2}/sec. $C_i = 1.488 \times 10^{-3}$ gm./cm.^{3}, k_i = 0.11 cm/sec. at 25°C) are used, Eqn. (3.27) becomes,

$$1/N_A = \frac{1.88 \times 10^4}{(\nu_v)^{1/3} \cdot (h_c)^{\frac{1}{2}}} + 0.611 \times 10^4 \qquad \ldots (3.27a)$$

Eqn.(3.27a) has been plotted in Fig.3.21(b)along with the experimental results. The experimental values for the parameters are given in Table 3.21(b). It is seen that there is complete agreement of the experimental results with the theory, and therefore the results of the author are identical with the findings of Danckwerts and Kennedy. (There is one difference, however, in that Danckwerts and Kennedy did not correct for the exit-end effects, while in this work, corrections have been made. Probably the hydrodynamics of the exit-end of the film in their rotating-drum method might be different and a correction may not be necessary).

The above findings will now be confirmed by studies at various heights of the wetted surface, different temperatures, and with/without the addition of surface active agents to water.

Absorption at Various Heights of the Wetted Surface with Pure Water:

When the height of the wetted tube was more than 10.0 cm., rippling started on the film. Absorption rates obtained at such heights were much higher than those predicted by Eqn.(3.27). Results of a few runs are given in Table-3.22.

Table-3.22

Temperature of the system, ^{o}C	= 25
Diameter of the wetted tube, cm.	= 1.270
Tube surface	= Plain
Liquid used	= Pure water
Liquid distributor used	= overflow

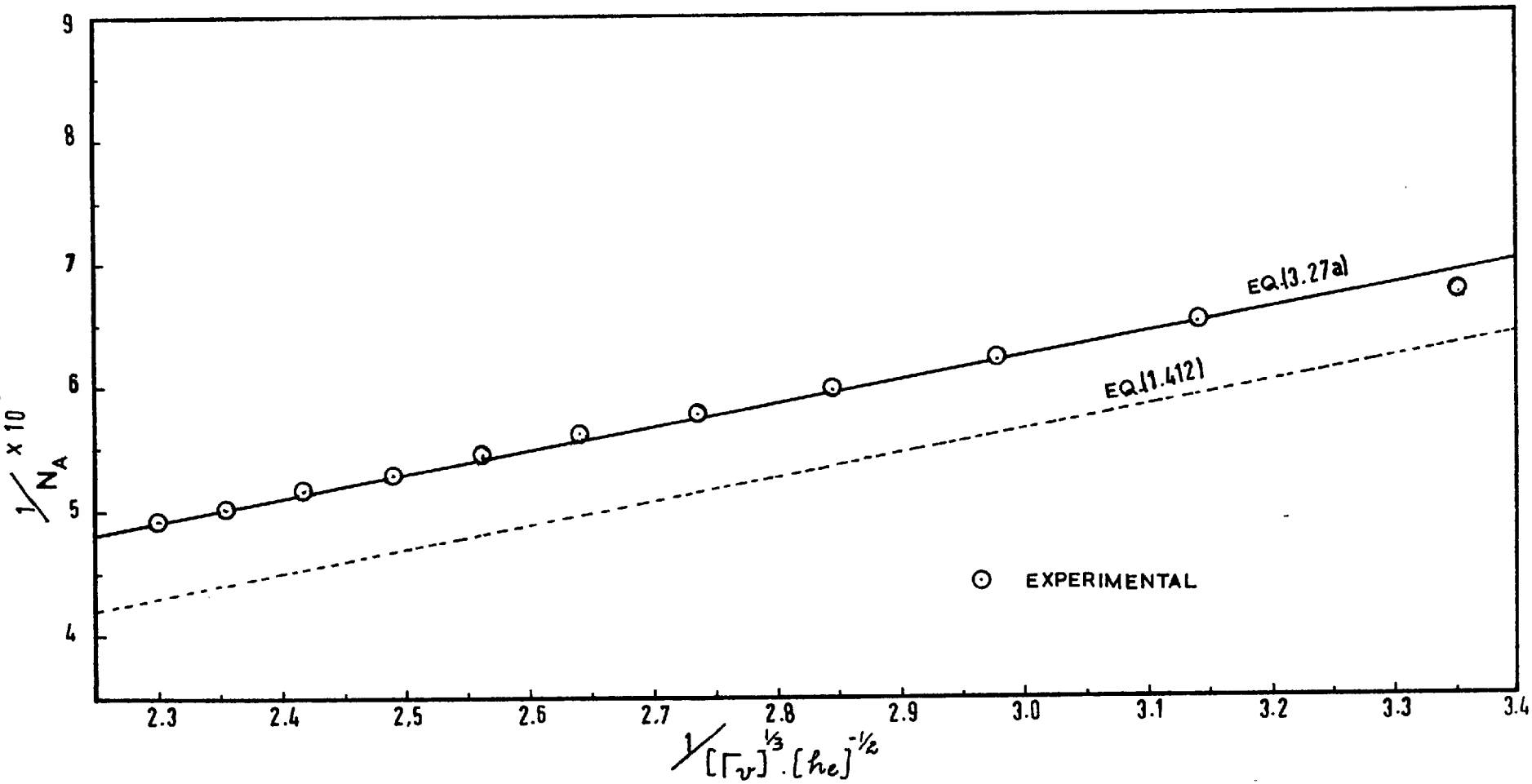
9
8
7
6
5
4
$1/N_A \times 10^{-4}$
2.3
2.4
2.5
2.6
2.7
2.8
2.9
3.0
3.1
3.2
3.3
3.4
$1/[\Gamma_v]^{1/3}.[he]^{-1/2}$
EQ.(3.27a)
EQ.(1.412)
EXPERIMENTAL

FIG. 3.21(b)

h (cm.)	Γ_v	$1/(\Gamma_v)^{1/3}.(h_c)^{-\frac{1}{2}}$	$1/N_A \times 10^{-4}$
14.1	0.6585	4.222	8.500
"	0.8191	3.947	7.972
"	0.9788	3.735	7.551
"	1.2980	3.421	7.022
"	1.6140	3.196	6.672
"	1.9440	3.007	6.410
"	2.2630	2.861	6.210
"	2.4230	2.796	6.010
15.0	0.3200	5.465	9.380
"	0.6390	4.400	7.780
"	0.9570	3.870	7.251
"	1.2730	3.530	6.930
"	1.5870	3.296	6.755
"	1.8920	3.122	6.590
"	2.2200	2.971	6.355
"	2.5300	2.845	6.060
"	2.8460	2.735	5.890
"	3.1616	2.640	5.680
18.0	0.6390	4.835	6.890
"	0.9570	4.248	6.665
"	1.2730	3.870	7.680
"	1.5870	3.613	7.610
"	1.8920	3.420	7.280

Eqn. (3.27a) was obtained by using the physical constants of Danckwerts and Kennedy. The values of physical constants used in this thesis, however, are those given in

Art. 3.1. When these values at $25^{\circ}C$ were substituted in Eqn. (3.27) the following equation was obtained,

$$1/N_A = \frac{1.994 \times 10^4}{(\Gamma_v)^{1/3}.(h_0)^{-1/2}} + \frac{10^4}{k_i \times 0.1495} \quad \ldots (3.27b)$$

The data given in Table-3.22, as well as the data for h = 9.1, from Table-3.21(b), have been plotted in Fig.3.22. The dotted line represents Eqn. (1.412), which is without an interfacial resistance. The best line passing through the experimental points and parallel to the dotted line gives the value of k_i = 0.15 cm/sec. at $25^{\circ}C$. It is seen from the graph that experimental results agree with the theoretical line with interfacial resistance, at liquid flow rates when there is no rippling. When rippling is present the experimental points are widely scattered. It is seen from Fig.3.22, that for each height of the wetted tube, the break of the experimental points from Eqn.3.27(b), which shows inception of rippling, is different. As the height of the wetted tube increases, the degree of divergence from the theoretical curve increases. It is interesting to note that, at h = 18.0, with the rippling film, the absorption rates, at Γ_v = 0.6390 and 0.9570, are higher than the absorption rate, at Γ_v = 1.2730.

Because of the complications caused by rippling, the inferences drawn above have to be substantiated further. The presence of interfacial resistance will now be confirmed by elaborate

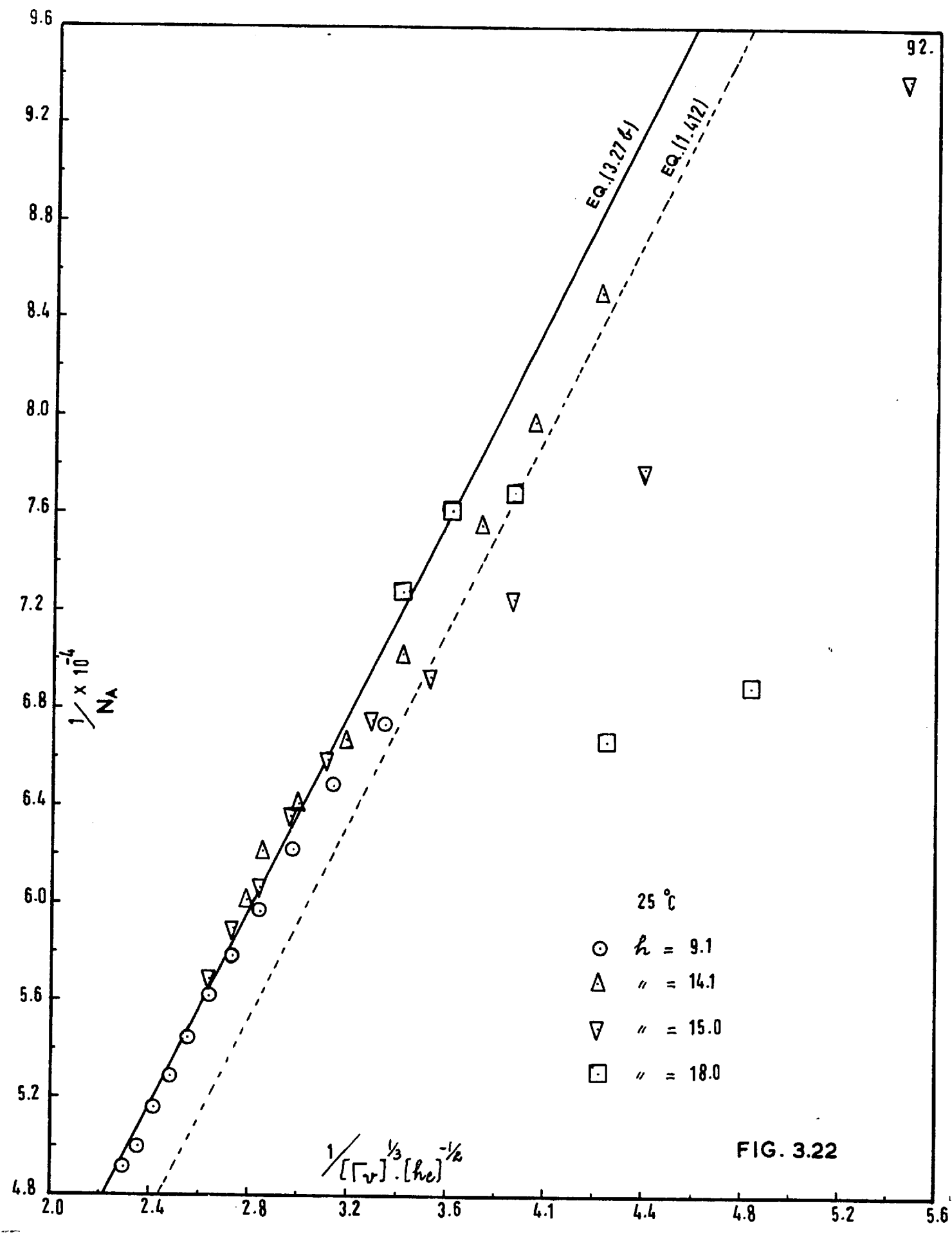
EQ.(3.276)
EQ.(1.412)
25 °C
h = 9.1
" = 14.1
" = 15.0
" = 18.0
1/N_A x 10^-4
1/[Γv]^1/3 . [hc]^-1/2
9.6
9.2
8.8
8.4
8.0
7.6
7.2
6.8
6.4
6.0
5.6
5.2
4.8
2.0
2.4
2.8
3.2
3.6
4.1
4.4
4.8
5.2
5.6

FIG. 3.22

studies on non-rippling films (using a surface active agent).

Absorption Results on Water Containing
a Surface Active Agent:

The presence of a surface active agent in water was found to eliminate rippling on the film. The absorption results obtained were accurately reproducible. Absorption results with either an overflow or an annular distributor were found to be identical for the same height of the wetted wall . Therefore, no distinction will be made in the results of either distributor from now on.

In order to find an optimum concentration of the surface active agent, absorption results were obtained at concentrations of 0.001%, 0.005%, 0.01%, 0.02%, 0.05% and 0.07% by volume of Lissapol NX. As the concentration of the agent was increased above 0.01%, a 1-3% decrease in the absorption rate was observed. Also, at these concentrations foaming took place in the liquid receiver. Below 0.01% concentration, the results were not reproducible. Therefore, a concentration of 0.01% Lissapol by volume was chosen to be the most suitable concentration. Further on, a use of 0.01% concentration of the surface active material will be denoted by 'SAM'.

Table-3.23 contains the absorption results obtained on a wetted wall height of 15.0 cm., with and without the addition of SAM. These results have been plotted for comparison in Fig.3.23.

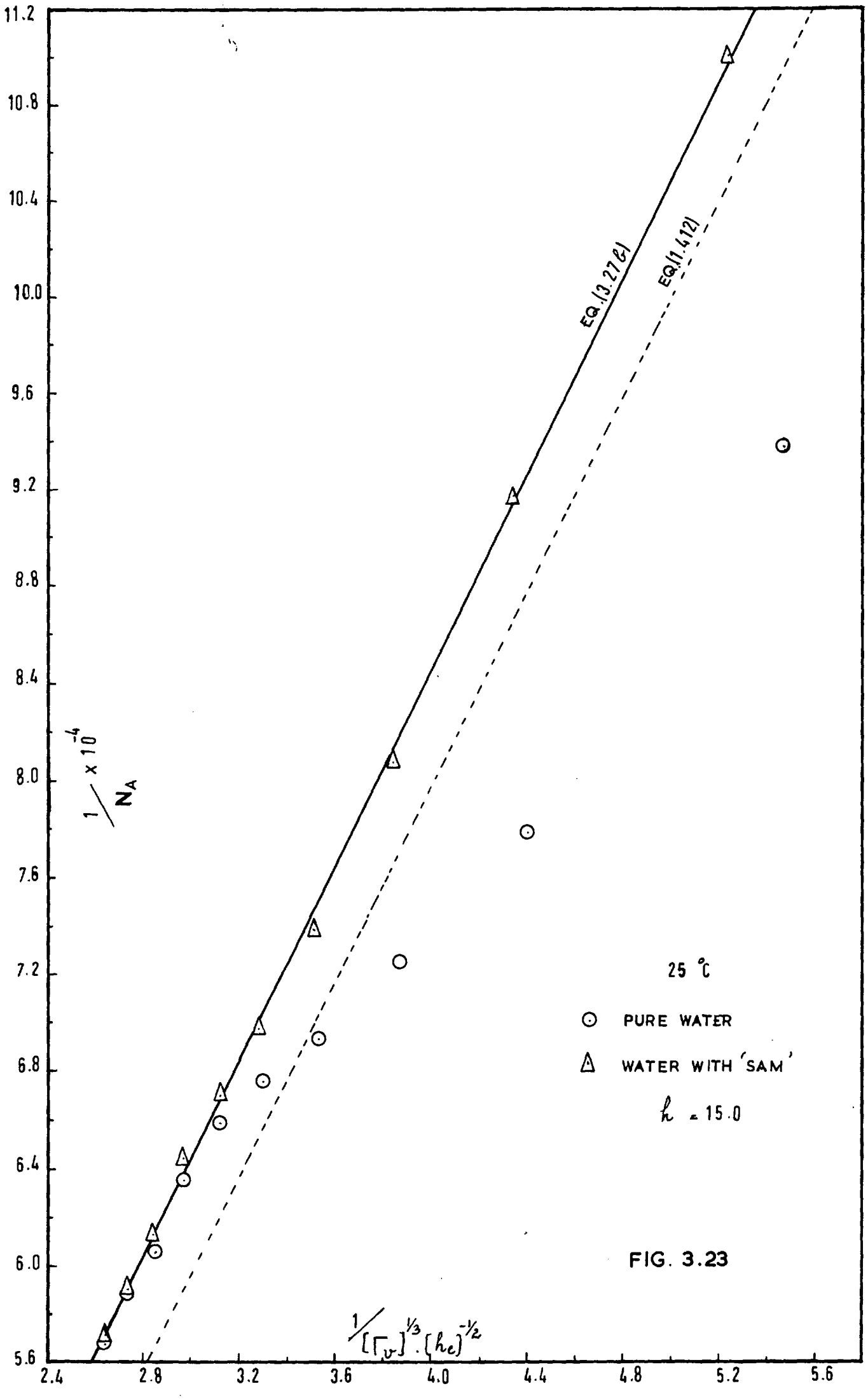
11.2
10.8
10.4
10.0
9.6
9.2
8.8
8.4
8.0
7.6
7.2
6.8
6.4
6.0
5.6
$1/N_A \times 10^{-4}$
EQ.(3.27 e)
EQ.(1.41 2)
2.4
2.8
3.2
3.6
4.0
4.4
4.8
5.2
5.6
$1/[\Gamma_v]^{1/3}.[h_e]^{-1/2}$
25 °C
PURE WATER
WATER WITH 'SAM'
h = 15.0

FIG. 3.23

Table-3.23

Temperature of the system, ^{o}C = 25

Height of the wetted tube, h, cm. = 15.0

Diameter " " " " ", cm. = 1.270

Tube surface = Plain

Γ_v	Pure Water		Water with SAM	
	$\frac{1}{(\Gamma_v)^{1/3}.(h_e)^{-1/2}}$	$\frac{1}{N_A} \times 10^{-4}$	$\frac{1}{(\Gamma_v)^{1/3}.(h_o)^{-1/2}}$	$\frac{1}{N_A} \times 10^{-4}$
0.3200	5.465	9.380	5.230	11.000
0.6390	4.400	7.780	4.340	9.170
0.9570	3.870	7.251	3.835	8.070
1.2370	3.530	6.930	3.510	7.380
1.5870	3.296	6.755	3.283	6.975
1.8920	3.122	6.590	3.117	6.705
2.2200	2.971	6.355	2.970	6.440
2.5300	2.845	6.060	2.845	6.130
2.8460	2.735	5.890	2.735	5.890
3.1616	2.640	5.680	2.640	5.720

As seen from Fig.3.23, the results with SAM at all the liquid flow rates lie on the line of Eqn.(3.27b) when k_i is of the same order of magnitude as in Fig.3.22, i.e. k_i = 0.15 cm./sec. The results for pure water also agree with this line for liquid flow rates at which there is no rippling. In the rippling region the results with pure water diverge considerably from the theoretical because of the presence of rippling. A comparison of Fig. 3.22

and Fig.3.23 indicates that the surface active material does not introduce any additional resistance to mass transfer but that the interfacial resistance already exists in the case of pure water.

Different temperatures and wetted wall heights: Tables-3.24, a, b, c, and d, record the absorption data at different heights for temperatures of 20, 25, 30, and 35°C respectively. These have been plotted respectively in Figs. 3.24, a, b, c, and d. From these plots, the following observations are noted.

Fig.3.24a, 20°C ; There is excellent agreement of the experimental points with the theoretical line for interfacial resistance, when k_i = 0.16 cm/sec.

Fig. 3.24b, 25°C ; The agreement with theoretical line for interfacial resistance is again very good. The value of k_i is found to be as, 0.15 cm./sec.

Figs.3.24c and d, 30°C , 35°C ; The agreement with the theoretical lines for interfacial resistance (Eqn.3.27) is satisfactory. The scatter of some points around the lines is due to the fact that the liquid flow was slightly unsteady at these temperatures. The values of k_i calculated from the graphs are 0.14 and 0.13 cm/sec.respectively.

It was desired to obtain a general relation of mass transfer which could predict the transfer rates based on the assumption of interfacial resistance. For this purpose, an expression for

the variation of the coefficient 'k_i' was derived in terms of a physical constant. This was done as follows:

Table. 3.25 contains the values of the saturated concentrations 'C*' and the coefficients 'k_i' derived above. C* x 10^3 was then plotted against 'k_i' (see Fig. 3.25). A straight line was obtained through the points which intercepted the k_i-axis, for C* x 10^3 = 0, at 0.068, Therefore the required expression for 'k_i' was obtained as,

$$k_i = 53.3\ C^* + 0.068 \qquad \ldots (3.28)$$

When Eqn.(3.28) is substituted in Eqn. (3.26),

Table-3.24

Diameter of the tube, cm. = 1.268

Tube surface = Plain

Liquid used = water with SAM.

(a)

Temperature = 20°C			
'h' cm.	Γ_v	$\frac{1}{(\Gamma_v)^{1/3}.(h_e)^{-1/2}}$	$\frac{1}{N_A} \times 10^{-4}$
17.45	0.9245	4.200	8.140
"	1.2360	3.830	7.480
"	1.5510	3.575	6.930
"	1.8470	3.394	6.560
"	2.1650	3.228	6.250
15.45	0.6124	4.480	8.725
"	0.9245	3.943	7.740
"	1.2360	3.604	7.110

Table-3.24 - contd.

(a)

'h' cm.	Γ_v	$\frac{1}{(\Gamma_v)^{1/3}.(h_c)^{-1/2}}$	$\frac{1}{N_A} \times 10^{-4}$
Temperature = 20°C			
15.45	1.5510	3.360	6.640
"	1.8470	3.193	6.315
"	2.1650	3.038	6.030
13.45	0.6124	4.156	7.990
"	0.9245	3.664	7.125
"	1.2360	3.353	6.510
"	1.5510	3.130	6.140
"	1.8470	2.975	5.880
"	2.1650	2.833	5.590
11.45	0.6124	3.805	7.490
"	0.9245	3.365	6.680
"	1.2360	3.101	6.120
"	1.5510	2.885	5.750
"	1.8470	2.746	5.560
"	2.1650	2.615	5.300
(b) Temperature = 25°C			
17.45	0.9581	4.145	8.660
"	1.2750	3.790	7.950
"	1.5900	3.545	7.445
"	1.8950	3.364	7.065
"	2.2220	3.203	6.710
15.45	0.6403	4.410	9.201
"	0.9581	3.892	8.212
"	1.2750	3.560	7.495

Table-3.24 - contd.

(b)

Temperature = 25°C			
15.45	1.5900	3.330	7.050
"	1.8950	3.164	6.720
"	2.2220	3.014	6.440
13.45	0.6403	4.091	8.590
"	0.9581	3.620	7.650
"	1.2750	3.315	7.050
"	1.5900	3.105	6.650
"	1.8950	2.950	6.390
"	2.2220	2.811	6.090
11.45	0.6403	3.748	7.870
"	0.9581	3.325	7.080
"	1.2750	3.070	6.390
"	1.5900	2.860	6.040
"	1.8950	2.721	5.750
"	2.2220	2.595	5.630
(c) Temperature = 30°C			
17.45	0.9731	4.125	9.400
"	1.2930	3.775	8.600
"	1.6110	3.531	7.975
"	1.9390	3.340	7.785
"	2.2530	3.184	7.340
15.45	0.9731	3.871	8.765
"	1.2930	3.544	8.105
"	1.6110	3.320	7.490
"	1.9390	3.142	7.230

Table-3.24 - contd.

(c) Temperature = 30°C			
15.45	2.2530	2.997	7.020
13.45	0.6592	4.050	9.300
"	0.9731	3.600	8.390
"	1.2930	3.300	7.750
"	1.6110	3.094	7.170
"	1.9390	2.929	6.940
"	2.2530	2.795	6.770
11.45	0.9731	3.308	7.530
"	1.2930	3.054	6.740
"	1.6110	2.850	6.380
"	1.9390	2.702	6.174
"	2.2530	2.580	5.930
(d) Temperature = 35°C			
17.45	1.0040	4.084	9.950
"	1.3350	3.736	9.180
"	1.6430	3.507	8.520
"	1.9770	3.315	8.200
"	2.2740	3.175	7.900
15.45	1.0040	3.830	9.730
"	1.3350	3.510	8.700
"	1.6430	3.298	8.240
"	1.9770	3.120	7.938
"	2.2740	2.983	7.624
13.45	0.7695	3.946	9.780
"	1.0040	3.560	8.920
"	1.3350	3.266	8.170
"	1.6430	3.072	7.750
"	1.9770	2.908	7.410
"	2.2740	2.787	7.070

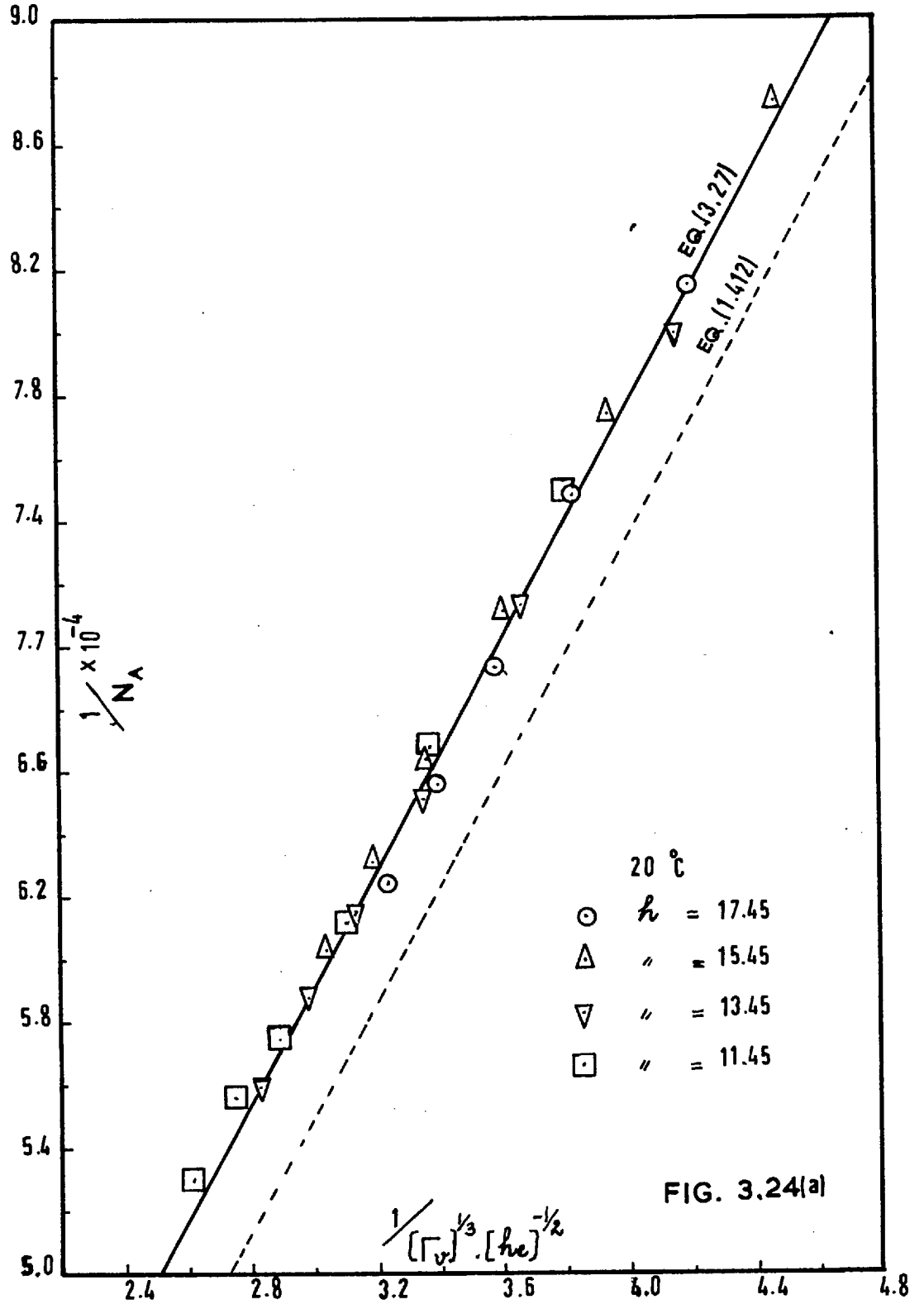
9.0
8.6
8.2
7.8
7.4
7.7
6.6
6.2
5.8
5.4
5.0
$\frac{1}{\gamma} \times 10^{-4}$
N_A
EQ.(3.27)
EQ.(1.412)
20 °C
h = 17.45
" = 15.45
" = 13.45
" = 11.45
$\frac{1}{[\Gamma_v]^{1/3}.[he]^{-1/2}}$
2.4
2.8
3.2
3.6
4.0
4.4
4.8

FIG. 3.24(a)

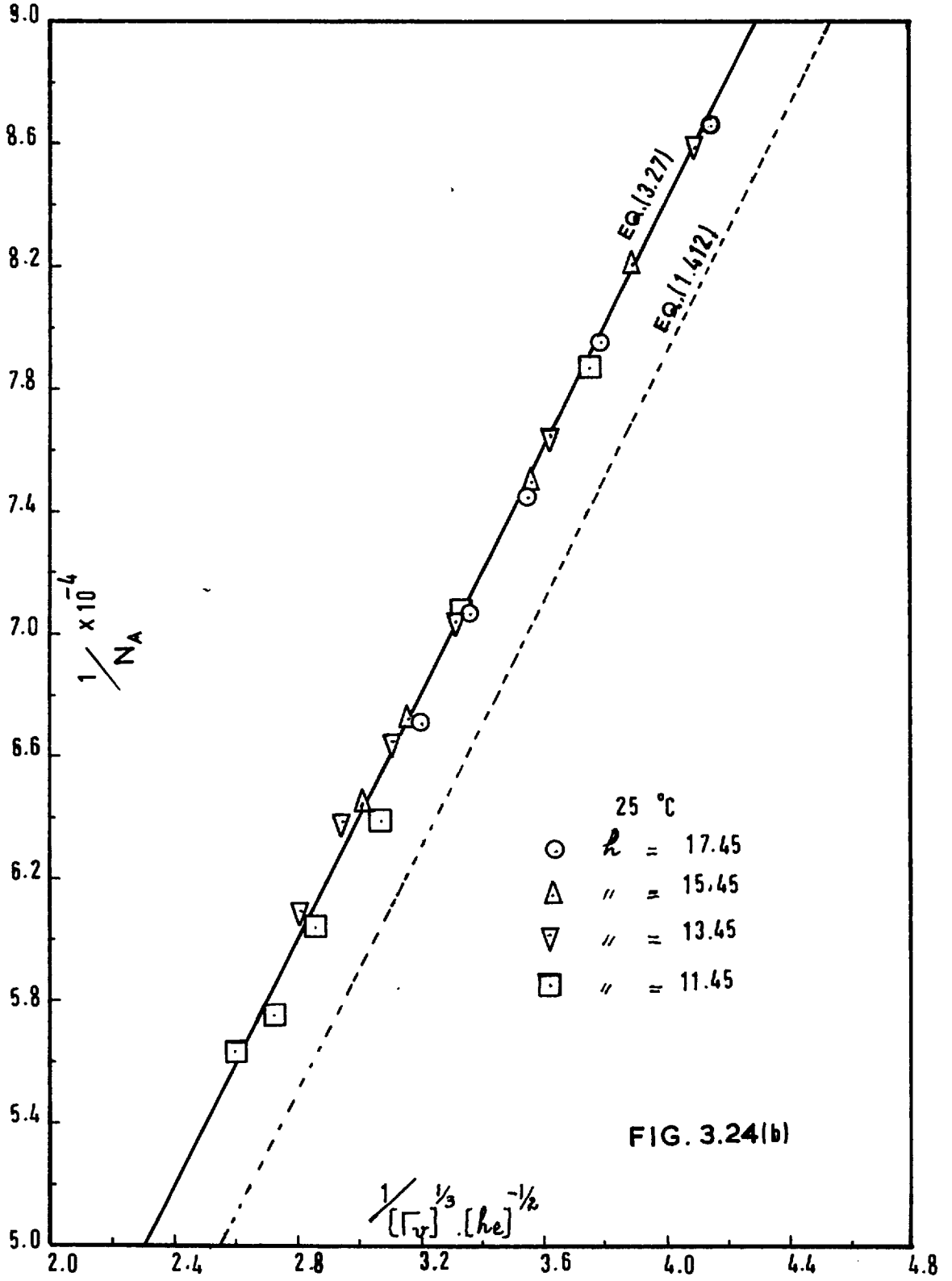
9.0
8.6
8.2
7.8
7.4
7.0
6.6
6.2
5.8
5.4
5.0
2.0
2.4
2.8
3.2
3.6
4.0
4.4
4.8
1/N_A x10^-4
1/[Γ_ψ]^1/3 . [he]^-1/2
EQ.(3.27)
EQ.(1.412)
25 °C
h = 17.45
// = 15.45
// = 13.45
// = 11.45

FIG. 3.24(b)

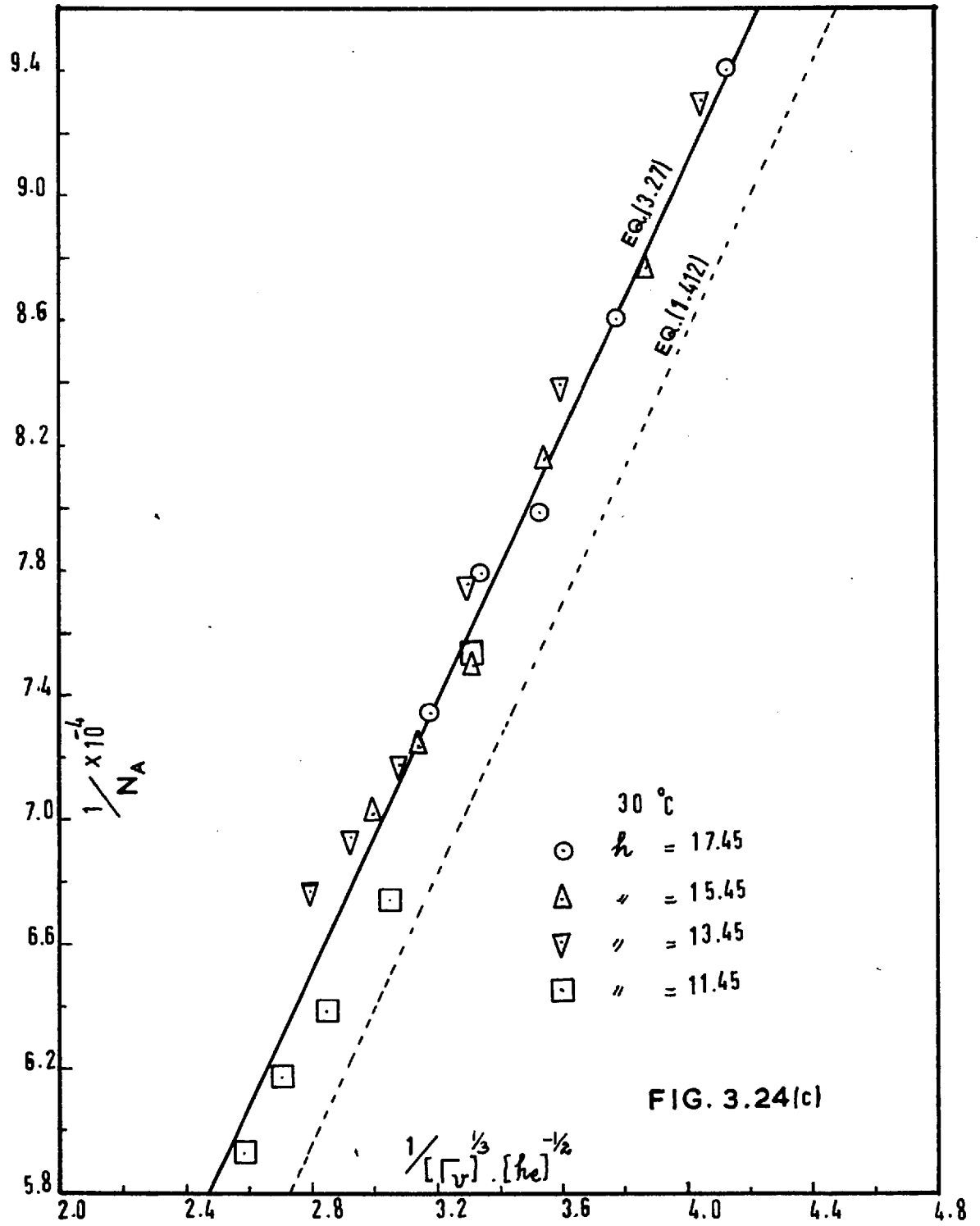
9.4
9.0
8.6
8.2
7.8
7.4
7.0
6.6
6.2
5.8
2.0
2.4
2.8
3.2
3.6
4.0
4.4
4.8
1/N_A x10^-4
1/[Γv]^1/3 . [he]^-1/2
EQ.(3.27)
EQ.(1.412)
30 °C
h = 17.45
" = 15.45
" = 13.45
" = 11.45

FIG. 3.24(c)

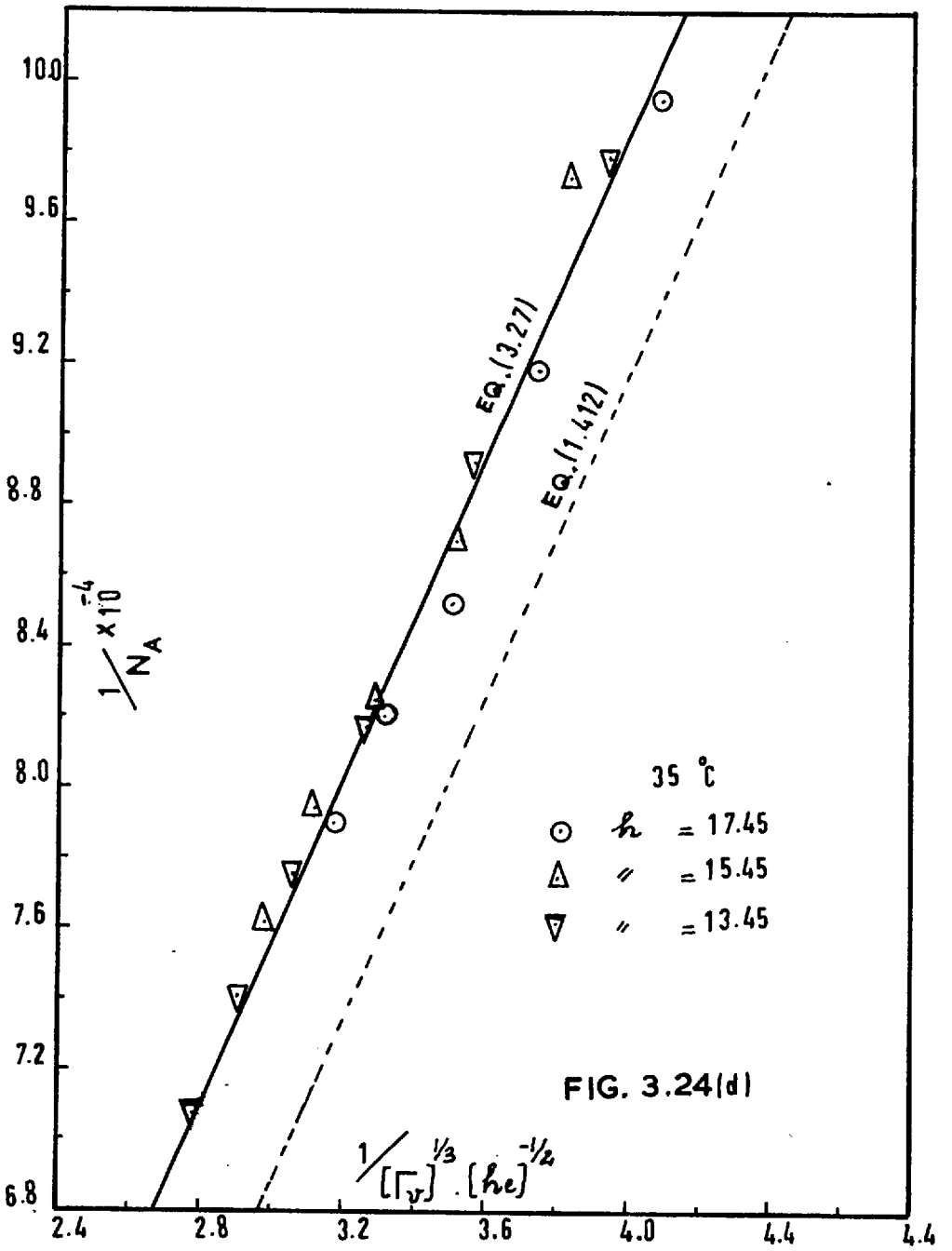
10.0
9.6
9.2
8.8
8.4
8.0
7.6
7.2
6.8
2.4
2.8
3.2
3.6
4.0
4.4
4.4
$\frac{1}{N_A} \times 10^{-4}$
EQ.(3.27)
EQ.(1.412)
35 °C
h = 17.45
" = 15.45
" = 13.45
$\frac{1}{[\Gamma_v]^{1/3} \cdot [he]^{-1/2}}$

FIG. 3.24(d)

Table-3.25

t_c, °C	20	25	30	35
$C^* \times 10^3$ gm./cm.^{3}	1.722	1.495	1.315	1.170
k_i cm/sec.	0.16	0.15	0.14	0.13

the following general expressions for mass transfer are obtained,

$$N_A = \frac{C^*}{\frac{1}{k_L} + \frac{1}{(53.3\ C^* + 0.068)}} \qquad \ldots (3.29)$$

$$\text{or } \frac{1}{N_A} = \frac{1}{C^*}\left(\frac{1}{k_L} + \frac{1}{(53.3\ C^* + 0.068)}\right) \qquad \ldots (3.210)$$

Eqn. (3.29) is a general equation for the prediction of absorption rates. All the theoretical curves drawn for interfacial resistance in the previous work are represented by Eqn. (3.210).

Conclusions:

(1) Surface active material does not introduce any additional resistance to absorption.

(2) Interfacial resistance to absorption is a dynamic property of the system and exists even in absorption into pure water.

(3) Eqn. (3.29) can be used for the prediction of mass transfer rates.

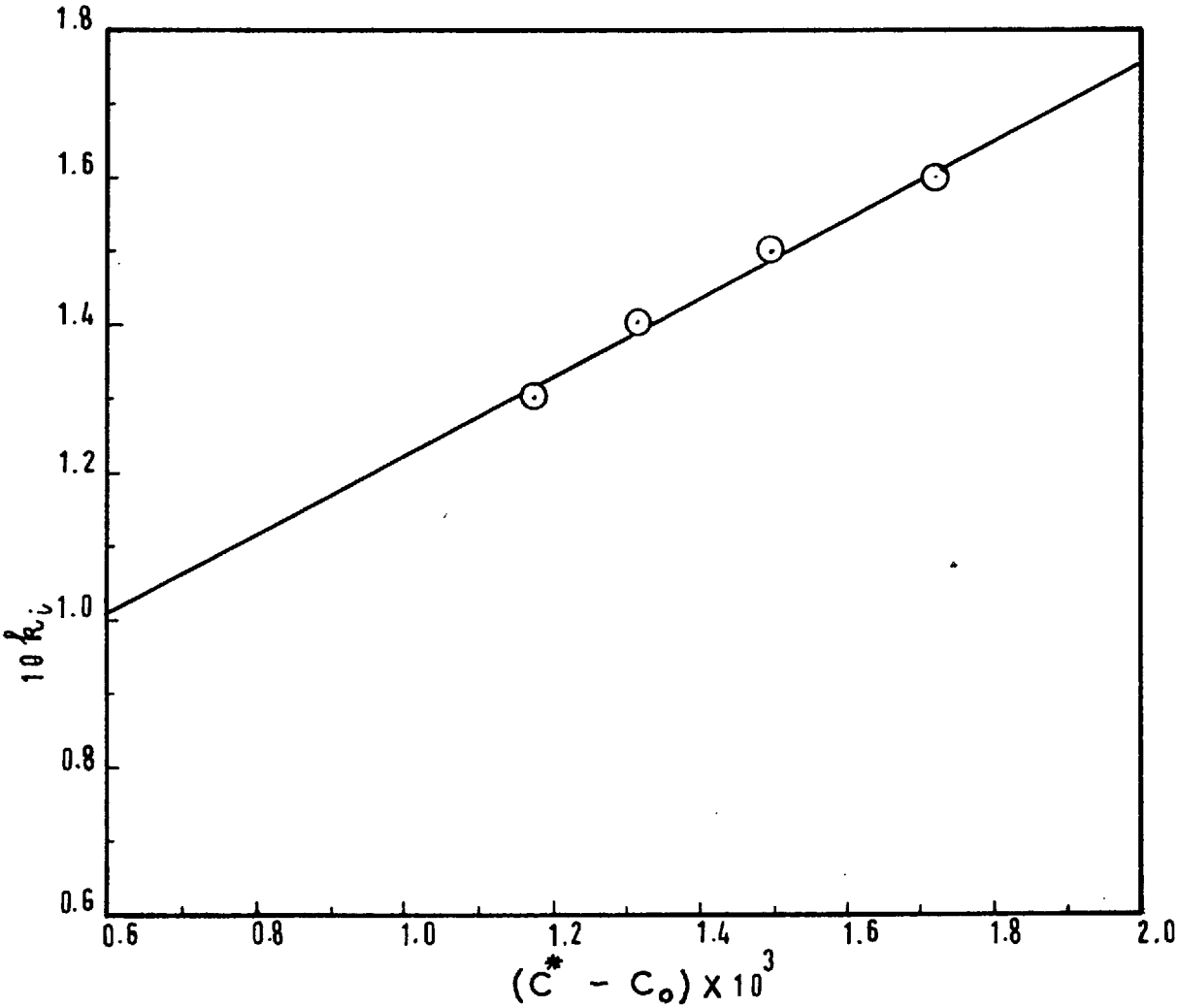

FIG. 3.25

CHAPTER IV.

ABSORPTION INTO FALLING LIQUID FILMS AT TURBULENT LIQUID FLOW RATES

Art.4.1. - General

In order to investigate the mass transfer phenomena at high liquid flow rates of the falling film, the hydrodynamic properties of the system should first be understood. The hydrodynamics of the laminar falling liquid films, discussed in the last chapter, were assumed to be explained by Nusselt's theory (2). No such theoretical analysis is available for flow rates in the turbulent region ($Re > 1200$). As has been discussed previously, the liquid film thickness is the most important parameter of the falling film. Several different approaches have been reported in the literature on the measurement of this quantity for a long wetted wall column with a wavy liquid film at turbulent flow rates. There is not a single study reported for a short wetted wall column, where the film has a smooth surface. An attempt was, therefore, made by the author to measure the film thickness for short columns at turbulent liquid flows.

Art. 4.2. - Measurement of the Film Thickness

The different methods of measuring film thickness have already been discussed in Chapter I. A method of silhouette photography was developed as an improvement on the method used by Brauer (16).

The photographic method has the advantage of leaving the flow undisturbed and is independent of such ellusive factors as influence the drainage type of measurements. He took high speed photographs of the column with water flowing and compared them with photographs of the dry column. A planimeter was used on the enlarged photographs for the linear measurements. He realised the limitations of his method and took great care (seven photographs of the wet column for each value of the Reynolds number) to obtain the best possible results. Two different cameras were used, one each for the dry and the wet tube, and the photographs were enlarged to exactly the same magnification. This operation introduced several sources of error, as enlarging the photographs to the same magnification ratio would have been very tedious, and then the two cameras used might have had different optical errors giving slightly different images. There were so many steps to be employed, with their individual errors, before the final measurement was taken, that the accumulated percentage error must have been high.

Most of the above-mentioned sources of error were eliminated in the technique used by the author. It consisted in a double exposure of the photographic plate for a small exposure time, first for the dry tube with front lighting, and second for the wet tube with back lighting. The silhouettes of the thickness of the film obtained on both sides of the tube were measured directly from the plate under a travelling microscope.

Details of Method

The front door of the perspex air-bath, as well as the Quickfit glass section of the absorber, were removed (see inside cover photograph). Deaerated water was used to form the film as the dissolved air was found to give rise to small bubbles in the film which distorted the interface. The photographs were taken with a still camera having bellows extension and mounted on a sturdy stand. The wetted tube was rigidly fixed in the heavy absorber assembly and there was no danger from small mechanical disturbances. The tube was wetted by the use of the annular distributor which was aligned to give a uniform width of annulus. F.P.3 (glass) half-plate ($4^{3}/_{4}$" x $6^{1}/_{2}$") was used and developed in D163 developer at 1:3 dilution in a 2-minute constant agitation.

The dry tube was first exposed with two 1000-watt lights projected on to the tube from the sides. The background of the tube was covered by a dark screen in order to reduce light being reflected from behind the tube. This gave an elevation image of the dry tube. The tube was wetted at a particular flow rate and temperature. The wet tube was then exposed on the same plate with the light projected from behind the tube through a slit (1.5" width). This exposure gave a silhouetted elevation of the wet tube superimposed on the image of the dry tube. The slit was used in order to minimise dispersion of light at the edges of the tube. A few plate contact prints of the

photographs taken are shown in Figs.4.21a and b. The liquid film cross-section is clearly seen on both sides of the tube. A suitable exposure time was found by trial and error as being 1/500th of a second at an aperture of 8. The magnification ratio of the image on the plate was always nearly 2.

Calculation of the film thickness: Lines perpendicular to the edges of the dry tube were drawn at 1 cm. distances along the length of the tube on the emulsion-side of the photographic plate. Four readings were taken along each line under the travelling microscope, the plate being illuminated from below, as (1) R_1, left wet boundary, (2) R_2, left dry boundary, (3) R_3, right dry boundary, (4) R_4, right wet boundary (see Fig.4.21a(i)). The actual diameter of the dry tube was measured accurately with a micrometer screw gauge. The calculations were carried out as follows:

actual diameter of the dry tube, cm. $= d$,

diameter of the dry tube on the plate, cm. $= R_2 - R_3$,

$\therefore$ magnification ratio of the image on the plate, x, $= \dfrac{(R_2-R_3)}{d}$,

actual film thickness on the left side, cm. $= \dfrac{(R_1-R_2)}{x}$

actual film thickness on the right side, cm. $= \dfrac{(R_3-R_4)}{x}$

height of the tube on the plate (from the distributor cap downwards) $= H$

$\therefore$ actual height of the tube (from the cap downwards) $= H/x$

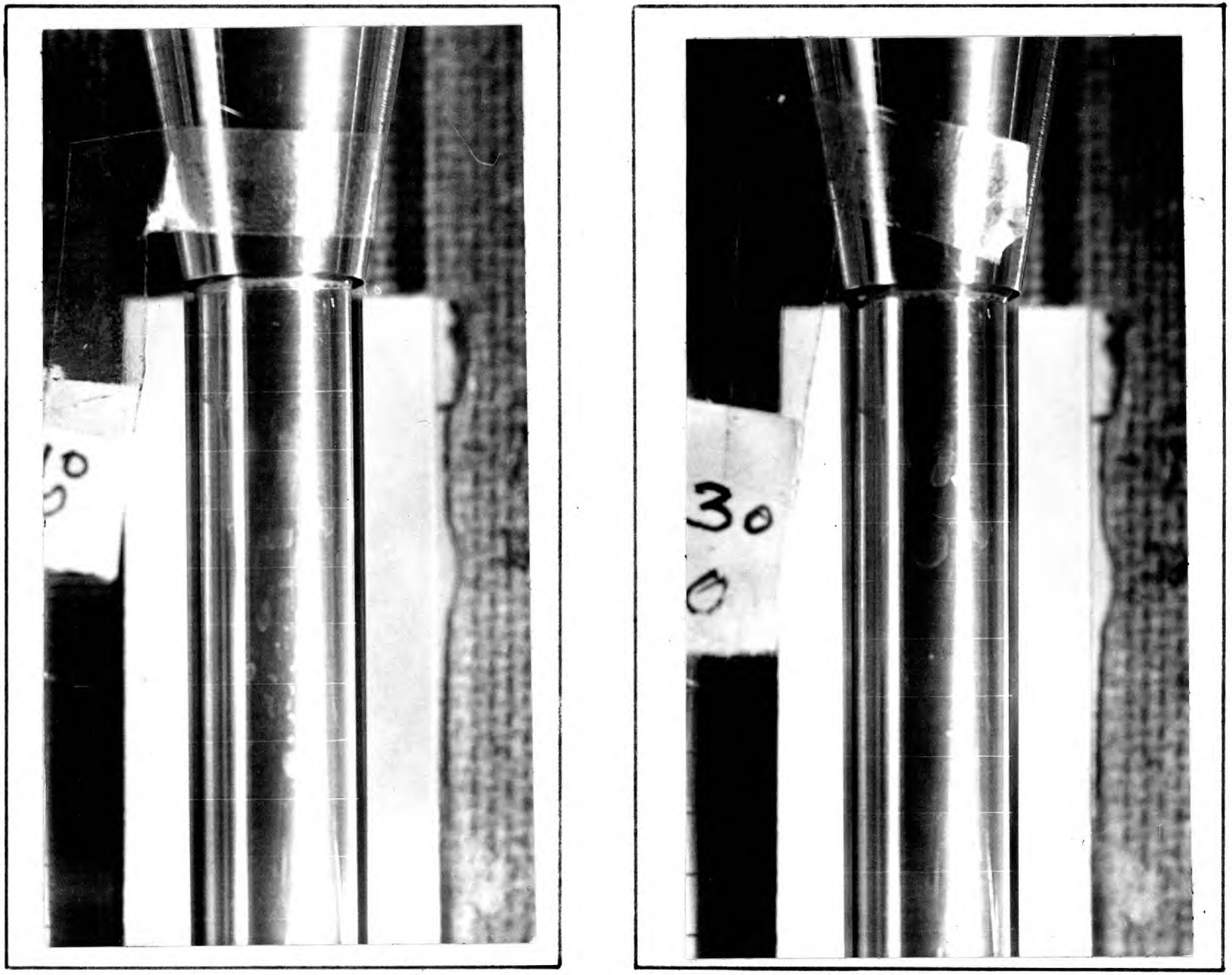

(i) 25 °C, Γ_v = 9.600 , X = 2.135

(ii) 25 °C, Γ_v = 6.824 , X = 2.153

FIG. 4.21(a)

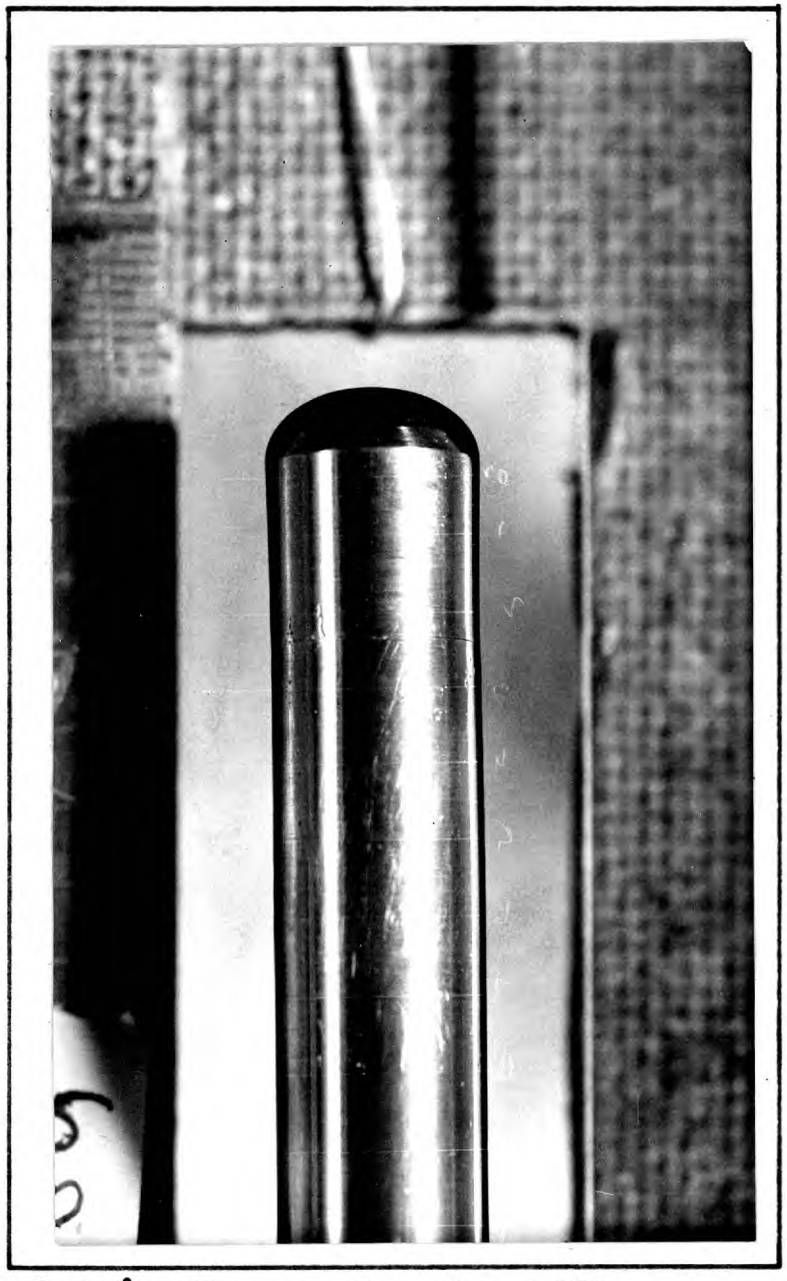

(iii) 25 °C , Γ_v = 1.179 , X = 2.102

(iv) 30 °C , Γ_v = 4.420 , X = 2.119

FIG. 4.21(b)

Both the dry tube and the annular distributor were assumed to be perfectly round. Therefore, even when (R_1-R_2) was not equal to (R_3-R_4), an arithmetic mean of these two quantities gave the film thickness that would have been obtained on both sides of the tube if the distributor annulus were perfectly uniform.

In order to visualise the cross-sectional profile of the falling film, $(R_1-R_2) + (R_3-R_4)/_2$ was plotted against H, as shown in Fig.4.22. It contains such plots at various liquid flow rates. Only one measurement of thickness was carried out in thelaminar region (see photograph in Fig.4.21b(iii)). The value of the thickness obtained was nearly identical with the prediction of the Nusselt theory. The films obtained in the turbulent region were smooth without any wavy or turbulent disturbances on the interface. Visually the pattern of flow seemed to be similar to that observed in the case of laminar films with surface active agent added. It is seen from the graphs in Fig.4.22 that the film thickness decreases downwards from the distributor cap. It was observed even in the case of laminar liquid films when the overflow distributor was used that these tapered downwards. In order to obtain an average film thickness, taking into account the shape of the profile, the area under the curve at each flow rate, A_{xy}, for x = o and y = o, was divided by x.H. Therefore,

$$\text{The average film thickness} = \frac{A_{xy}}{x.H.}$$

The value of the film thickness given by the above equation,

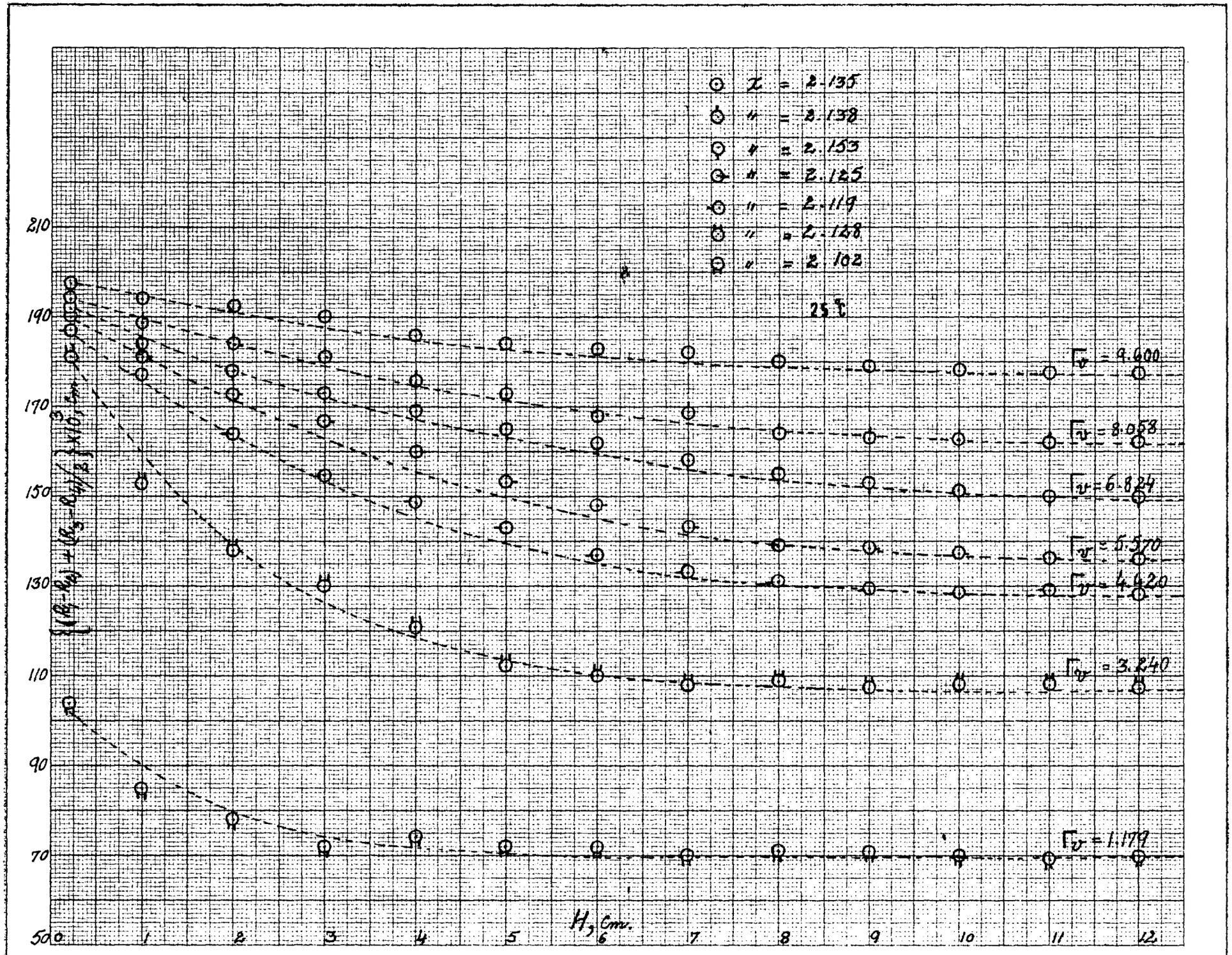
χ = 2.135
" = 2.138
" = 2.153
" = 2.125
" = 2.119
" = 2.148
" = 2.102
25°C
Γv = 9.600
Γv = 8.058
Γv = 6.824
Γv = 5.570
Γv = 4.420
Γv = 3.240
Γv = 1.179
210
190
170
150
130
110
90
70
50
0
1
2
3
4
5
6
7
8
9
10
11
12
H, Cm.

FIG. 4.22

however, depends on the height H. It was difficult to use this value of thickness for the absorption studies described later. The limiting value of the film thickness is reached when H > 12.0 cm. (see Fig.4.22), and is only slightly different from the average value. The extra thickness due to the curvature in graphs was, therefore, neglected. The limiting values, δ_i, at different flow rates are given in Table-4.21.

Table-4.21.

Temperature of water, ^{o}C = 25.

$\bar{v}$ $cm.^2/sec.$	3.240	4.420	5.570	6.824	8.058	9.600
δ_i cm.	0.0502	0.0604	0.0640	~~0.695~~ 0.0695	0.0760	0.0831

Values of the film thickness were also determined at different temperatures for a constant flow rate (4.420 $cm.^2/sec$). $(R_1-R_2) + (R_3-R_4)/2$ has been plotted against 'H' in Fig.4.23. It is seen from the graphs that the variation in the thickness with temperature is very small and that the limiting values of 'δ_i' are almost overlapping.

It was assumed in the estimation of the film thickness that the limiting value was independent of the width of the annular gap. This assumption was justified by the fact that the absorption results

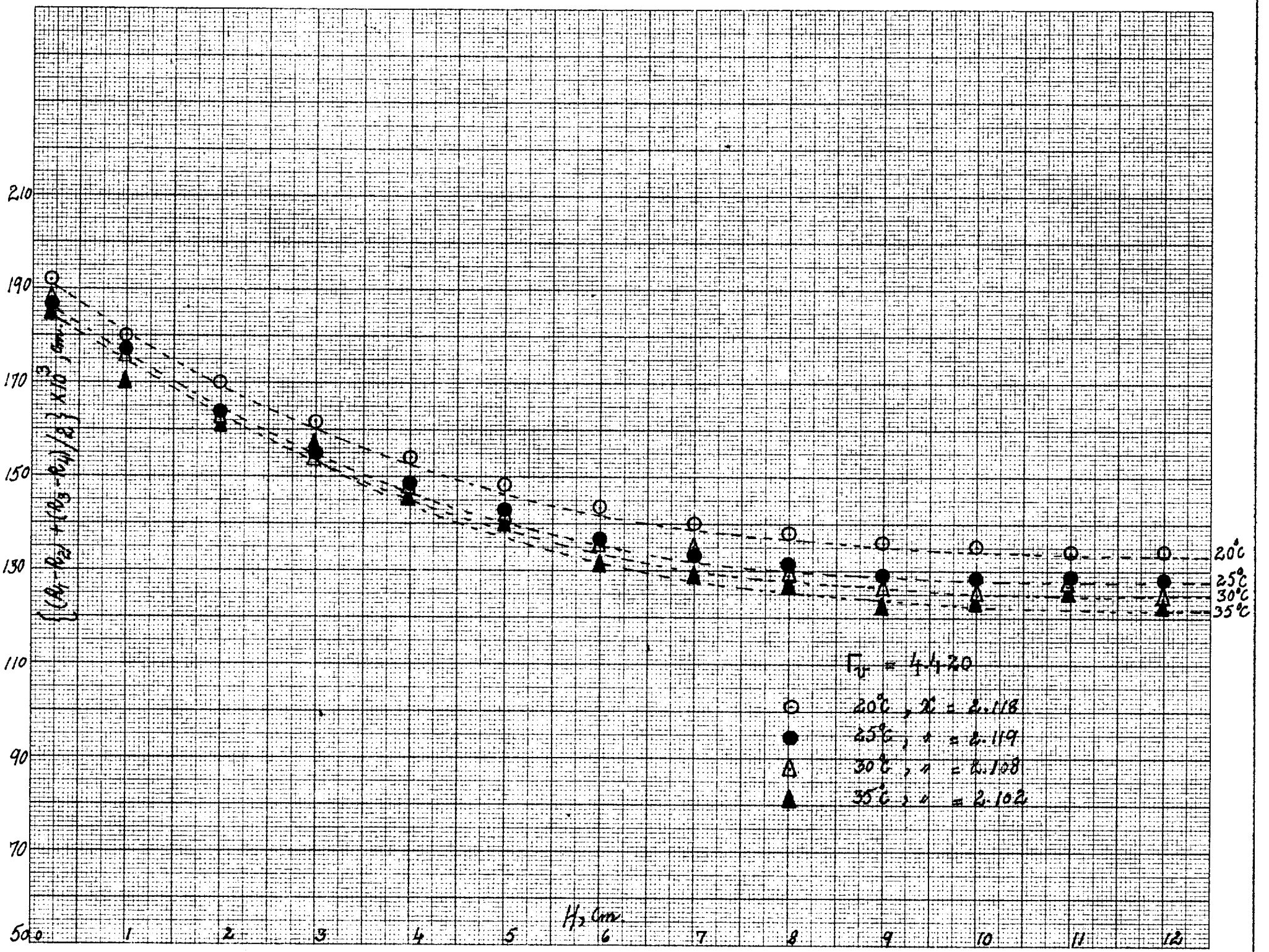
210
190
170
150
130
110
90
70
50
0
1
2
3
4
5
6
7
8
9
10
11
12
H₂ Cm.
20°C
25°C
30°C
35°C
Γv = 4.420
20°C, x = 2.118
25°C, x = 2.119
30°C, x = 2.108
35°C, x = 2.102

FIG. 4.23

on films, using different widths of the annulii, showed nearly identical rates of transfer. Also it is corroborated by the findings of many workers, who observed no change in the value of the average thickness by varying the width of the annulus.

Correlation of Results

When a liquid falls as a thin film in isothermal streamline flow down a vertical wall, it is retarded in its motion by its internal fluid friction and the resistances prevailing at the two boundary surfaces. If it is flowing in a stationary gas medium, then the resistance at the gas-liquid boundary can be regarded as negligible. At a steady state of motion, the acceleration due to the force of gravity becomes balanced by the retardation due to the frictional resistance. By applying these opposite forces to a thin laminar layer of the film and integrating the result for the entire film layer, an equation can be obtained for the film thickness 'δ',as,

$$\delta = \left[12\mu \quad \Gamma_v \left\{1-\left(\frac{v_i}{2v_{av.}}\right)\right\} \Big/ g\rho \right]^{1/3}$$

$$= \left[12\nu \quad \Gamma_v \left\{1-\left(\frac{v_i}{2v_{av.}}\right)\right\} \Big/ g \right]^{1/3} \qquad \ldots (4.21)$$

where v_i and $v_{av.}$ are the interfacial and average velocities as given in Chapter I.

When the liquid is in laminar flow, the velocity distribution in the film is semi-parabolic and therefore $v_i/v_{av.} = 3/2$. When the

liquid is flowing in the turbulent region, the bulk of the liquid film will be turbulently mixed and therefore the velocity profile will be flat except in a very thin layer next to the wall. Assume that the whole of the layer, from the wall to the gas-liquid interface is flowing in this fashion with the same velocity at every point in a horizontal plane. In this case 'v_i' would be equal to '$v_{av.}$'. Substituting $v_i/v_{av.} = 1$ in Eq.(4.21)

$$\delta_i = \left[6\nu . \Gamma_{v/g}\right]^{1/3} \qquad \ldots (4.22)$$

Eq.(4.22) obtained above is semi-theoretical in nature as is evident from its method of derivation. The photographically determined values of 'δ_i' given in Table 4.21 are plotted for comparison with Eq.(4.22) in Fig. 4.24. The agreement of the experimental points with the equation is rather poor. The consistency of Eq.(4.22) has been verified in Fig.4.25, where it is plotted as 'ν' vs. δ_i. The limiting values of 'δ_i' have been taken from Fig.4.23. The scatter of experimental points has the same range as in Fig.4.24. For reasons of its simplicity, however, this equation will be used for the film thickness in the turbulent region and in the derivation of a relation for the transfer coefficient to be described below.

Art. 4.3. - Absorption Results for Turbulent Flow of Liquid Film

The only change in the apparatus assembly, from that used in the last chapter on laminar films, was the introduction of a small

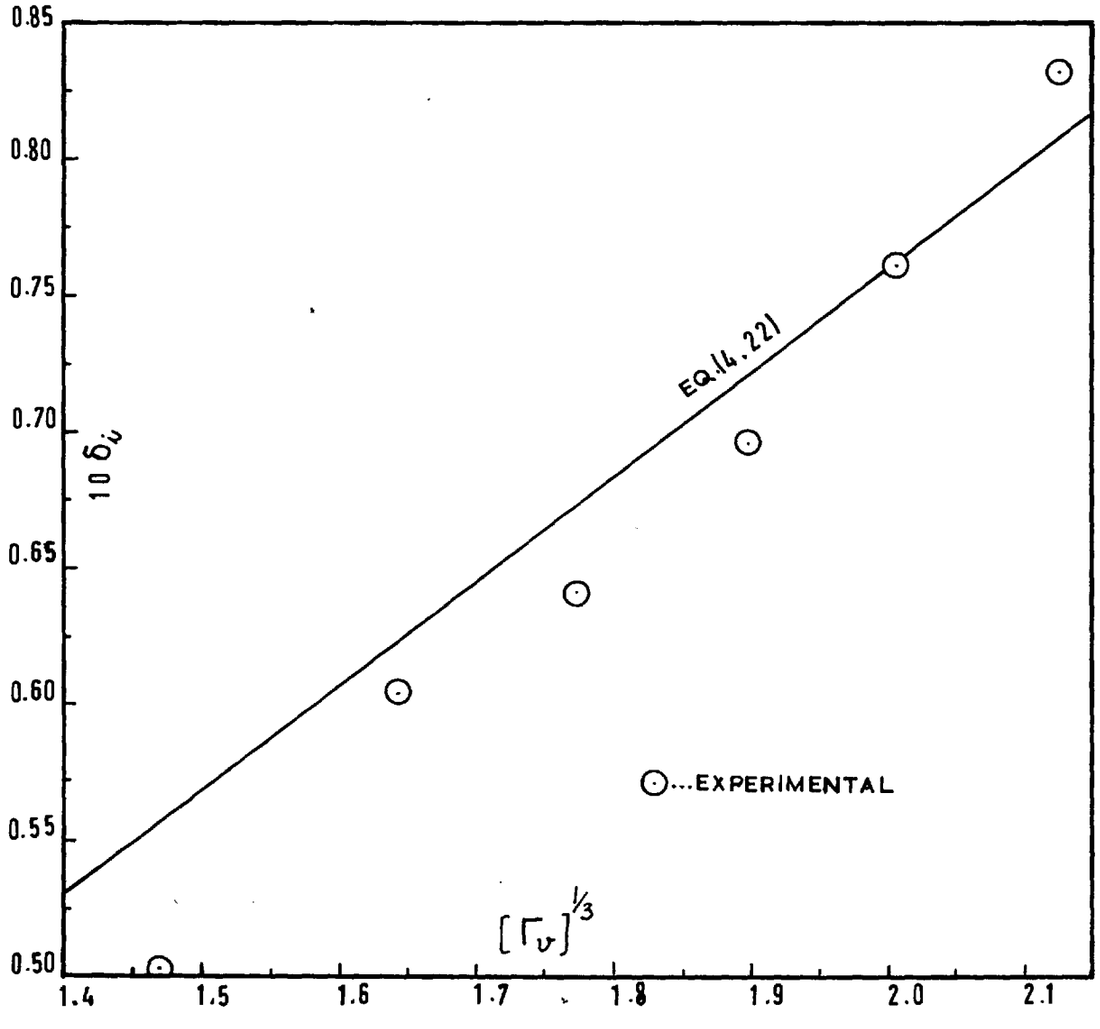

FIG. 4.24

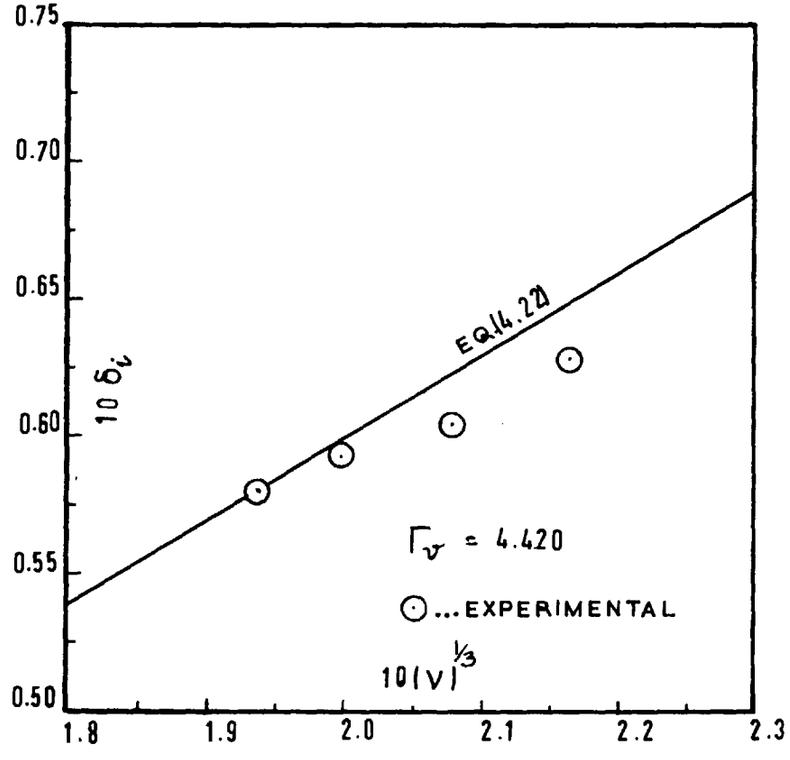

FIG. 4.25

centrifugal pump in the liquid line of feed to the absorber. Flow rates as high as 9.600 $cm.^2/sec.$ (Re = 4280) were used. Experimental absorption rates were calculated from Eq.(3.21), using values of 'δ_i' obtained from Eq.(4.22) instead of 'δ'.

Correlation of Results

The equation for predicting the value of the mass transfer coefficient for a laminar film has been derived from the penetration theory as Eq.(1.47). When the value of $v_i = \frac{\Gamma_v}{\delta}$ is inserted, it can be written as,

$$k_L' = 2 \sqrt{\frac{D\ \Gamma_v}{\pi\ h}} \cdot (\delta)^{-1/2} \qquad \ldots (4.31)$$

When the liquid flow is turbulent, the semi-theoretical equation derived previously (Eq.(4.22)) for the film thickness, in the turbulent region, δ_i, is substituted for 'δ' in Eq.(4.31), giving,

$$k_L' = 2 \left(M/\pi\right)^{1/2} \cdot \left(g/6\nu\right)^{1/6} \cdot \Gamma_v^{1/3} \cdot h^{-1/2} \qquad \ldots (4.32)$$

The molecular diffusion coefficient, 'D', has been substituted by a mixing coefficient 'M'. When the flow is turbulent, mass is transferred both by molecular diffusion and eddy diffusion. Therefore,

$$M = D + \epsilon$$

where ϵ = Eddy diffusion coefficient, $cm.^2/sec.$

'D' is a constant and depends only on temperature but the value of 'ϵ' would depend upon the intensity of turbulence also. For those hydro-dynamic systems where the intensity of turbulence

changes with the flow rate, the value of 'M' would vary with the flow rate. Eq.(4.32) should not hold for such cases.

When 'k_L'' is substituted for 'k_L' in Eq.(3.210), it is obtained as,

$$1/N_A' = \frac{1}{C^*}\left\{1/k_L' + 1/(53.3C^* + 0.068)\right\} \qquad \ldots (4.33)$$

Experimental absorption rates were plotted as $1/N_A'$ against $1/(\Gamma_v)^{1/3}$ in Fig.4.31. Table-4.31 contains the numerical values of the plot. A straight line could be drawn through the points passing through the intercept given by Eq.(4.33). The line, therefore, represents this equation. From the slope of the line, the value of 'M' was calculated as 3.175×10^{-5}. A constant value of 'M' indicates that the intensity of turbulence is independent of the liquid flow rate for a short wetted wall column. Eq.(4.33) can, therefore, predict the transfer rates in any similar hydro-dynamic system. This equation will be used later in comparing the hydro-dynamics of the turbulent films falling on rough and vibrating surfaces.

Table-4.31.

Temperature of the system, ^oC = 25

Height of the tube, cm. = 15.0
Diameter " " " " = 1.27
Liquid used = Pure water*

Γ_v	$10\left[1/\Gamma_v\right]^{1/3}$	$N_A' \times 10^6$	$1/N_A' \times 10^{-4}$
3.240	6.75	17.48	5.720
4.420	6.09	18.87	5.300
5.570	5.64	20.24	4.940
6.824	5.27	21.47	4.660
8.058	4.99	22.35	4.472
9.600	4.71	24.11	4.150

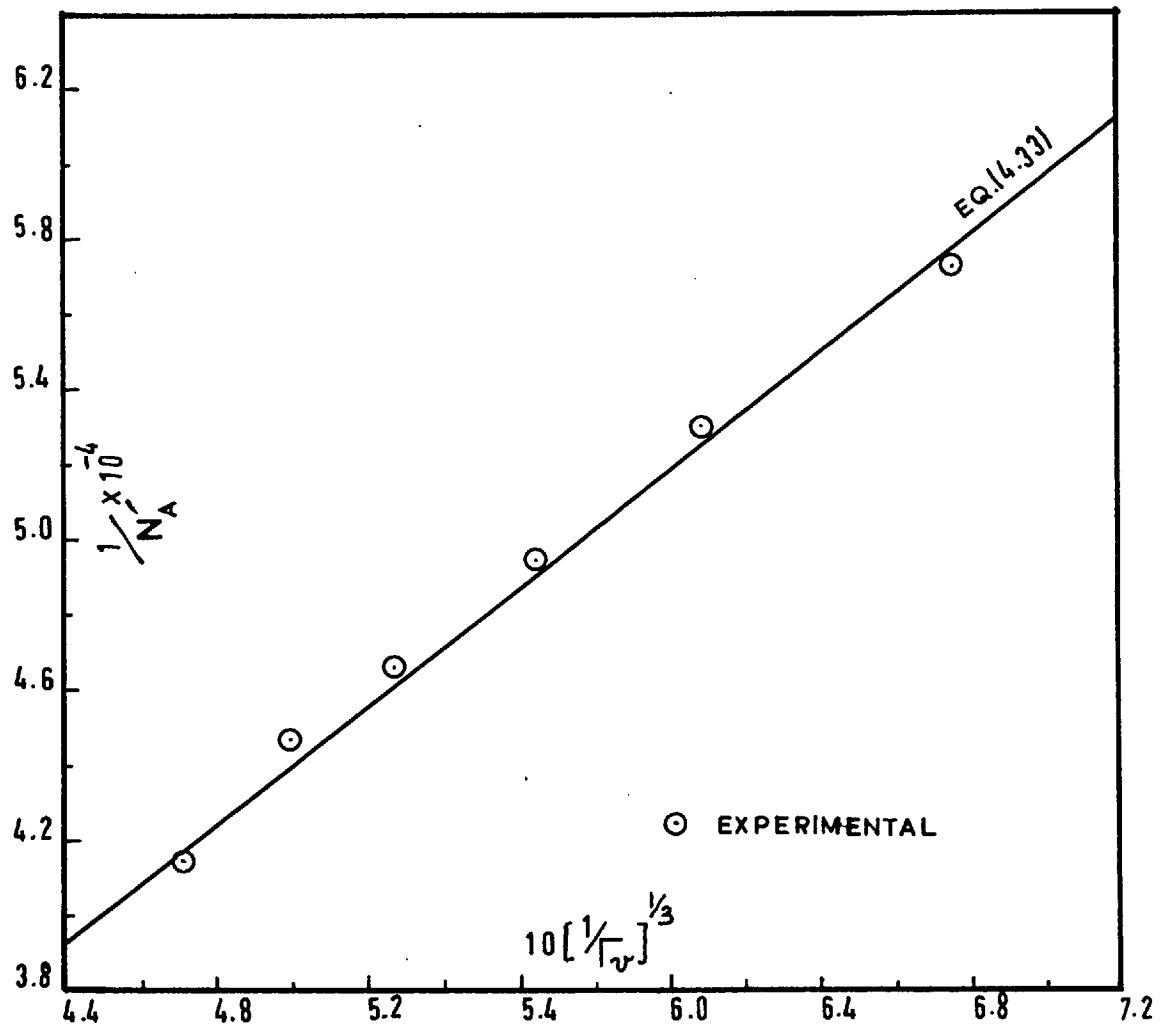
6.2
5.8
5.4
5.0
4.6
4.2
3.8
$\frac{1}{N_A} \times 10^{-4}$
4.4
4.8
5.2
5.4
6.0
6.4
6.8
7.2
$10\left[\frac{1}{\Gamma_v}\right]^{1/3}$
EQ.(4.31)
EXPERIMENTAL

FIG. 4.31

* Addition of surface active agent did not affect the rate of absorption at turbulent flow rates.

In order to compare the degree of intensification of absorption obtained with such turbulence promoters as surface roughness and surface vibration (Sec. 2 and 3), the results will be plotted as 'Γ_v' vs. 'N_A''. When the results for a smooth surface, in the absence of turbulence promoters, are plotted as Γ_v vs. N_A' in Fig.4.32, the points seem to lie on a straight line giving an intercept equal to '$N_{Ac.}$'. '$N_{Ac.}$' is the value of the absorption rate predicted by Eq.(3.29) for the laminar region at the critical flow rate (Re = 1200). Therefore an empirical equation can be derived for the turbulent region (Re $\geq$ 1200), as,

$$N_A' = 0.545\ \Gamma_v + N_{Ac} \qquad \ldots (4.34)$$

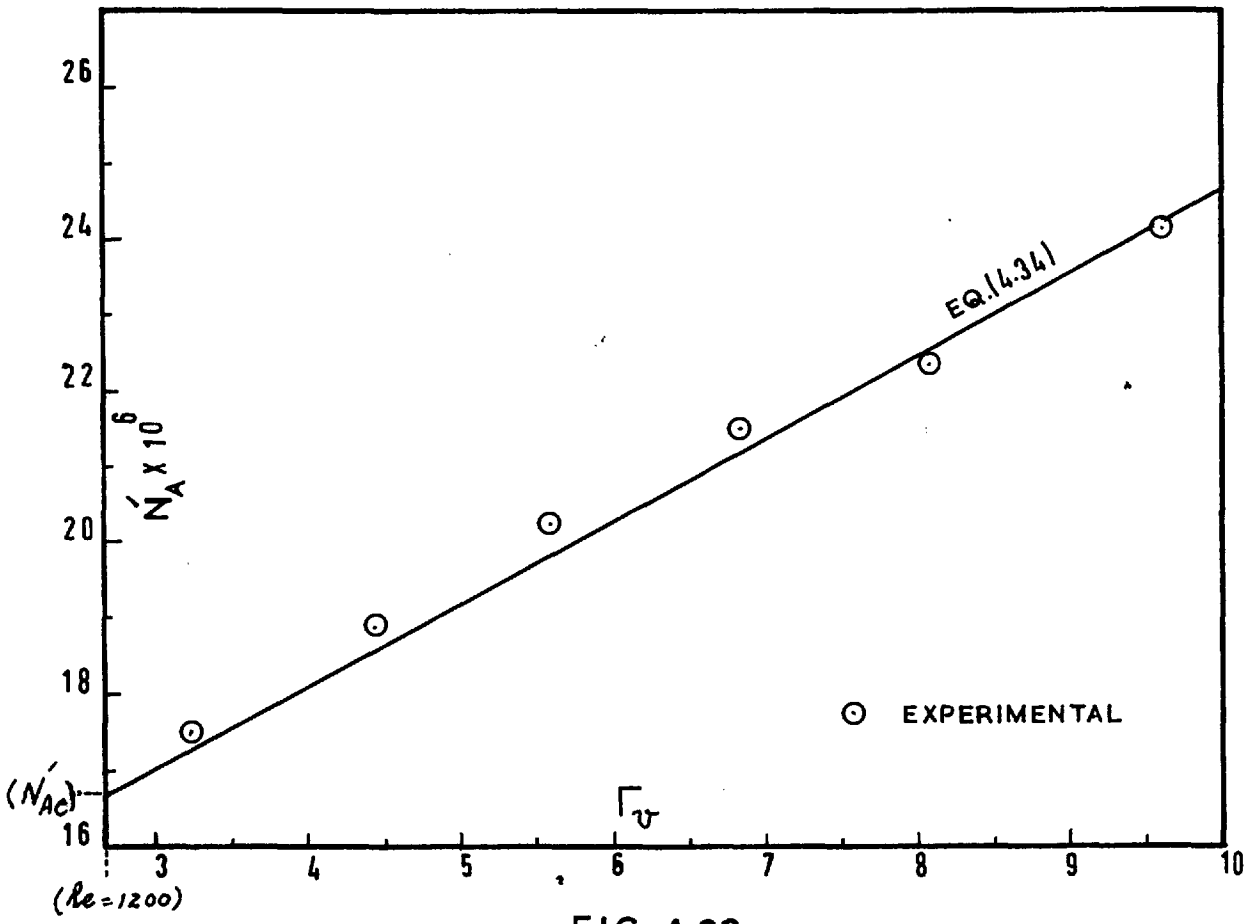
26
24
22
20
18
16
$\acute{N}_A \times 10^6$
$(\acute{N}_{Ac})$
EQ.(4.34)
EXPERIMENTAL
Γ_v
3
4
5
6
7
8
9
10
(Re=1200)

FIG. 4.32

SECTION 2.

GAS ABSORPTION INTO LIQUID FILMS FALLING OVER ARTIFICIALLY ROUGHENED SURFACES.

CHAPTER V

INFLUENCE OF WALL ROUGHNESS IN TRANSPORT OPERATIONS

Art.5.1. Momentum Transfer

Considerable work has been done on the influence of roughness of the wall in promoting turbulence, ranging from the effect of cylindrical rough elements to point-like elements, and randomly distributed roughness elements. Generally speaking, the presence of roughness favours transition to turbulence in the sense that fully developed turbulent flow is developed on a rough wall at a lower Reynolds number than on a smooth wall. That this should be so follows clearly from the theory of stability. The existence of roughness elements gives rise to additional disturbances in the laminar stream which have to be added to those generated by turbulence already present in the boundary layer. If the disturbances created by the roughness elements are bigger than those due to natural turbulence, we must expect that a lower degree of amplification will be sufficient to effect transition. On the other hand, if the roughness elements are very small, the resulting disturbances should be below the threshold which is characteristic of those generated by the turbulence of the free stream. In this case the presence of roughness would be expected to have no effect on transition. The preceding considerations show complete agreement with experiment. When the roughness elements are very large, transition will occur at the points where these are present.

Experimental evidence has shown that the effect of wall roughness on turbulence flow pattern is negligible if the relative roughness is sufficiently low. There is a minimum height of those elements below which no influence on transition exists (critical height). In the case of sand-roughness, it may be deduced from Nikuradse's(14) experiments, as,

$$u^* \cdot e/\nu < 5$$

where $u^* = \sqrt{\tau_{oe}/\rho}$ denotes the friction velocity and τ_{oe} is the frictional stress at the rough wall : 'e' is the height of the roughness elements.

Equivalent Sand Roughness: The number of parameters describing roughness is extraordinarily large owing to the great diversity of geometric forms. If we consider, for example, a wall with identical protrusions, we must come to the conclusion that its influence on frictional drag will depend upon the density of distribution of the roughness, i.e., on the number of protrusions per unit area as well as on their shape and height, and finally, also, on the way these are distributed over the surface. It took, therefore, a long time to formulate clear and simple laws which describe the flow of fluids through rough pipes. It was found that the nature of roughness can be expressed by means of a single parameter, e/D, the so-called "relative roughness", where 'e' is the height of a protrusion and 'D' denotes the diameter of the tube (or the hydraulic diameter). The resistance coefficient

of flow could be described by a relation containing this parameter for roughness.

In many other varieties of roughness, the height of the protrusions alone cannot describe the roughness, as far as the effect of frictional drag is concerned. The contribution of the form drag to the total drag might be more prominent. In order to predict the value of "relative roughness" in such cases, Nikuradse (14) measured the friction factors of flow for different values of '$^{e}/_{D}$' in pipes, by glueing sand grains on to the wall. He prepared charts of friction factor 'f' versus '$^{e}/_{D}$', from which the relative roughness can be read off directly. This value is called the "equivalent sand roughness" of the pipe. It can also be defined as that value which gives the actual coefficient of resistance when inserted into Eqn.(5.21) given later {after Colebrook's (58)}.

Chisholm and Laird (59) studied the dynamics of two-phase flow in rough tubes. Pressure-drop and saturation data were obtained for the flow of air-water mixtures in a smooth tube and several rough tubes, all of approximately 1 in. bore. The tube surfaces tested were as follows:

(a) Smooth brass tube, bore, 1.062 in., $^{e}/_{D}$, 0.000.

(b) Commercial galvanised tube, bore, 1.043 in., $^{e}/_{D}$, 0.068.

(c) Brass tube with concrete internal surface. The concrete was applied to the tube with an internal thread (tube diameter). An irregular finish was obtained; bore, 1.059 in., $^{e}/_{D}$, 0.037.

(d) Brass tube with internal thread (V-cut), bore, 1.077 in., measured $^{e}/_{D}$, 0.028, apparent $^{e}/_{D}$, 0.037.

(e) Sand distributed non-uniformly in the brass tube, bore, 1.032 in., $^{e}/_{D}$, 0.045.

(f) Sand distributed uniformly on the galvanised tube, bore, 1.018 in., $^{e}/_{D}$, 0.068.

Shellac was used to glue the sand to the tube wall. With the exception of the threaded tube, no direct measurements of surface roughness were made. The values quoted above are values from a Moody (60) chart (equivalent sand roughness) extrapolated, where necessary, corresponding to a measured friction factor in the region of complete turbulence. The results obtained on saturation and pressure-drop could be related to surface roughness by means of an equation accurate to $\pm$ 25%.

Art.5.2. Heat Transfer

Although the effect of wall roughness on fluid friction in pipes has received extensive study, investigations of the corresponding effect in heat transfer are comparatively few. The field has been broadened, and new data includes the effect of turbulence promoters and surface area extenders also.

When the magnitude of roughness is small, i.e. $u^{*}e/\nu < 5$, the influence on the turbulence flow pattern will be negligible and hence the mode of the transport process will be the same as for a smooth tube, except perhaps a slight effect associated with

the increased surface area of the wall. With increasing roughness (for sand roughness), such that $5 < u^* e/\nu < 55$, there is an increasing effect on flow pattern; among other things the effective thickness of the viscous sub-layer decreases. This decrease affects the transport process across the boundary layer, for the roughnesses cause disturbances in the viscous sub-layer which promote turbulent transport. In other words, the roughnesses increase the activity of the viscous sub-layer, already present in the case of a smooth wall. If the roughness is so great that $u^* e/\nu > 55$ (the numerical value again refers to sand roughness), the effective thickness of the viscous sub-layer is zero. The flow resistance then becomes unaffected by molecular transport of momentum, i.e., by viscosity; it is, consequently, independent of the Reynolds number. It seems reasonable to expect that a transport of heat or mass will also be unaffected by molecular transport, and so will also be independent of the Reynolds number. However, the transport of heat and mass need not follow the same pattern as the momentum transport. It is known from heat transfer measurements on cylinders and spheres exposed to a uniform flow, that the Nusselt number remains a function of the Reynolds number even when the resistance coefficient is already independent of the Reynolds number. Hence, if we consider the roughness elements to be small bodies attached to a smooth wall and exposed to a turbulent stream, in analogy to the above we may expect an effect

of the Reynolds number on the heat transfer from the wall to the fluid at any value of the Reynolds number, although these effects may perhaps be smaller than they would be for a smooth wall.

The first experiments deliberately made to study the effect of wall roughness on heat transfer were those by Pohl (61) on heat transfer to fluids flowing through rough pipes. These, however, were made with values of $u^* e/\nu$ smaller than 12; so they lead to no conclusions with respect to questions raised above.

Cope (62) carried out experiments with three different pipes, their internal surfaces being artificially roughened by a special knurling process which produced a series of pyramids geometrically similar in form but varying in absolute size from pipe to pipe. The roughness ratios (radius of pipe/height of pyramid) were approximately $^{8}/_{1}$, $^{15}/_{1}$, and $^{45}/_{1}$. The working fluid was water and the Reynolds numbers ranged from 2,000 to 60,000. The results indicate that, when fully turbulent conditions are established, the roughness has very little effect on the heat transmission coefficient, but that, in the transition region between the laminar and fully turbulent flow, the roughness may increase that coefficient to a considerably higher value than its value for a smooth pipe. The heat transmission

graphs for the three pipes are in better agreement if shearing force velocity $\left[u^* = \left(\frac{\tau_{oe}}{\rho}\right)^{1/2}\right]$ is used instead of the mean velocity for forming the non-dimensional parameters for plotting purposes. The broad conclusions, from a practising engineer's standpoint, were stated as below:

" 1. For a given pressure drop across a heat transmission apparatus, more heat will be transmitted if the pipes be smooth than if they be rough.

2. The smooth pipe is more efficient if the comparison is made on a basis of heat transmission for equal power. "

Apparently the form drag caused by mechanical roughness projections produces an inefficient type of turbulence from the heat transfer point of view. However, it has been found from several studies that the shape and configuration of the roughness projections are as important as the height of these projections in determining their effect on fluid friction and heat transfer. Colburn (63) and later Pratt (64) analysed data of metallic turbulence promoters placed within pipes to show that, in certain instances, the heat transmission performance for a given power loss was increased by such promoters.

The same is true of the extensive measurements made by Smith and Epstein (65) on heat transfer and fluid friction for air flow through a smooth copper pipe (Dia. = 0.6 cm.) and six

other commercial pipes (Dia. = 0.3 to 0.9 cm.), with roughness ratios D/e = 640 to 64, and Reynolds numbers of 10^4 to 8×10^4. Correlation of rough pipe data was achieved by means of Colebrook's (58) equation for sand-roughened pipes in the region between laminar and completely turbulent flow,

$$\frac{1}{\sqrt{f}} = 4 \log (D/e) + 2.28 - 4 \log \left(1 + \frac{4.67\ D/e}{Re\sqrt{f}}\right) \quad \ldots (5.21)$$

Some increase in heat transfer coefficeint with increasing roughness was observed but, even with the roughest pipe, the fully rough wall condition, as it applies to momentum transfer, was hardly reached at the highest Reynolds number.

More conclusive are the results of experiments carried out by W. Nunner (66). The artificial roughnesses applied to his copper tube (D = 5 cm.) by means of rings, had equivalent sand roughnesses up to 'e' = 2.28 cm. The Reynolds numbers were sufficiently high to obtain a large turbulence where the fully rough wall condition (friction factor 'f' independent of Reynolds number) occurred. Nunner was able to obtain a (Nu, Re) relation for each roughness condition. He concluded from his investigations that the effect of wall roughness on heat transfer was similar to the effect that may be expected from a variation in the Prandtl number. He used $(Pr.\ f/f_o)$ instead of 'Pr' in Prandtl's relation, f_o being the friction coefficient for a smooth pipe.

Turbulence Promoters

A number of methods have been devised for reducing the thickness of the laminar film and the transition layer which separate a heat exchanger tube from a turbulent core of fluid flowing within the tube, thereby extending the region of turbulence. Various types of turbulence promoters, such as, coiled wires, spirals of various pitches, propeller-shaped baffles, have been reported. The pins, sometimes used to extend heat exchanger surface area, also serve a similar purpose. The applicability of such devices depends upon a three-way balance between reduction in investment in heat transfer area, increase in investment and maintenance due to turbulence promoters themselves, and the net change in power consumption for the same heat transfer performance.

A typical work on the effect of turbulence promoters has been reported by Kays (67) who measured the heat transfer and friction on surfaces equipped with circular pins. It was recommended to stagger the pins and demonstrated that very compact heat exchangers were obtainable with this geometry.

Art. 5.3. Mass Transfer

There is almost no literature available on the effect of wall roughness or the effect of turbulence promoters on mass transfer. In fact the role of the solid wall in most of the mass transport processes is not very prominent. However, in mass

transfer operations, such as, drying, gas absorption in packed columns, and distillation in wetted wall columns, where transfer takes place from wetted surfaces, the investigation of the wall effect would be interesting.

The investigation described in this thesis was carried out to study the possibilities of intensification of mass transfer in packed gas-liquid absorption columns. Studies were carried out on the effect of surface roughness and surface turbulence promoters on CO_2-gas absorption into falling liquid films at relatively short exposure times (simulating the conditions in packed columns). A survey of literature revealed no very relevant work, however, the following studies are of interest:

1. Stephens and Morris (68) sought to develop a laboratory column for the prediction of liquid film coefficients, as an improvement on the wetted wall column. For this purpose, the liquid film was interrupted at short intervals during its descent, thus simulating the conditions of flow over a packing. They carried out the preliminary experiments with notched wetted wall columns. These were constructed from short thick-walled cylindrical sections bevelled at edges so as to form notches 1/8" deep. Columns were constructed with notches 1" and 4" apart respectively. It was found that the effect of the column length on the liquid film coefficient was satisfactorily eliminated. This type of column was abandoned

for the following reasons:

(a) The limiting velocity was substantially lower than that for a normal wetted wall column, being less than 5 ft/sec. at high liquid rates for a column of $^{1}/_{2}$" diameter with 1" pitch notches.

(b) The gas-film coefficient was increased by the roughness effect produced by the variation of the thickness of the liquid film in the neighbourhood of the notches. It was considered that, with columns of small diameters, this effect would vary with the physical properties of the liquid so that prediction of the gas film coefficient would be inaccurate.

A brief mention of the effect of surface roughness on absorption into a disc column is made by Taylor and Roberts (69). These authors repeated the work of Stephens and Morris (68) on a disc column, obtaining the data from a calibration point of view. In order to improve the wettability of the discs, these were roughened systematically by putting a series of criss-cross cuts on the faces and the rim. The cuts were scored with a knife-needle file (Grade 2), 20 cuts per inch in each direction and approximately $^{1}/_{50}$ - $^{1}/_{100}$ inch deep. It was also expected that this would create further turbulence in the liquid film and consequently higher coefficients would be obtained. In fact no increase in coefficients was obtained, but the wetting of the discs was so improved that these were wetted completely at flow rates below 45 lbs/hr.ft.

CHAPTER VI.

ABSORPTION STUDIES INTO LIQUID FILMS FALLING OVER ARTIFICIALLY ROUGHENED SURFACES

Art.6.1. - Apparatus and Measurements

Absorption studies on the influence of wall roughness were carried out in short wetted wall columns. As has been discussed previously, a short wetted wall column was chosen because it appears to represent the mode of absorption in a packed column. Various magnitudes and shapes of roughnesses were produced artificially on the surface of the column.

Fabrication of Roughness

Stainless Steel tubes of $^{1}/_{2}$" O.D. were used, and the roughness was fabricated at the outside surface. The roughness characteristic of a pipe wall is described by the dimensionless quantity, e/D, called the relative roughness. Here 'e' is a measure of the absolute roughness, and for simplicity is taken as equal to the height of the roughness elements, and 'D' is the diamter or the hydraulic diameter. In fact, the height of the roughness elements alone does not fully describe the roughness characteristic, and in some cases, shape of the elements is more important. There seems to be no such numerical method of describing the roughness of surface for the wetted wall columns. It can either be represented by only the height of the elements 'e', or the film thickness 'δ' might be used in place of

'D' (compare the derivation of Reynolds number for the falling films). If 'e/δ' is taken as the relative roughness it would be variable with the liquid flow rate and therefore unsuitable for use.

The roughnesses used in the present study were of two types — (i) engravings on surface, and (ii) protrusions on surface. In earlier work, the height of the roughness elements was small compared to the thickness of the liquid film, but later the height was increased to become comparable or even more than the film thickness. The latter type of roughness elements were thus similar to the turbulence promoters used in heat transfer work. The protrusions used were spherical glass beads, graded sand, and wire helix. Sixteen surfaces were fabricated on stainless steel tubes. The characteristics of these surfaces are given below. Roughness is described by the product of its linear dimension and its frequency on the surface.

(i) Engravings on surface.

Surface 1 (Fig.6.11) - There are eight diametric grooves per inch length of the tube, the depth and width of the grooves being $^1/_{1000}$" each. The cutting tool used was V-shaped. A 50-times magnified sectional view is shown in the diagram (x = magnification ratio). Roughness = $8 \times \frac{1}{2.54} \times \frac{1}{1000} \times 2.54$

= 0.008 cm.

Surface 2 (Fig.6.11) - The number of diametric grooves is 16 per inch, the depth and the width being $^2/_{1000}$" each.

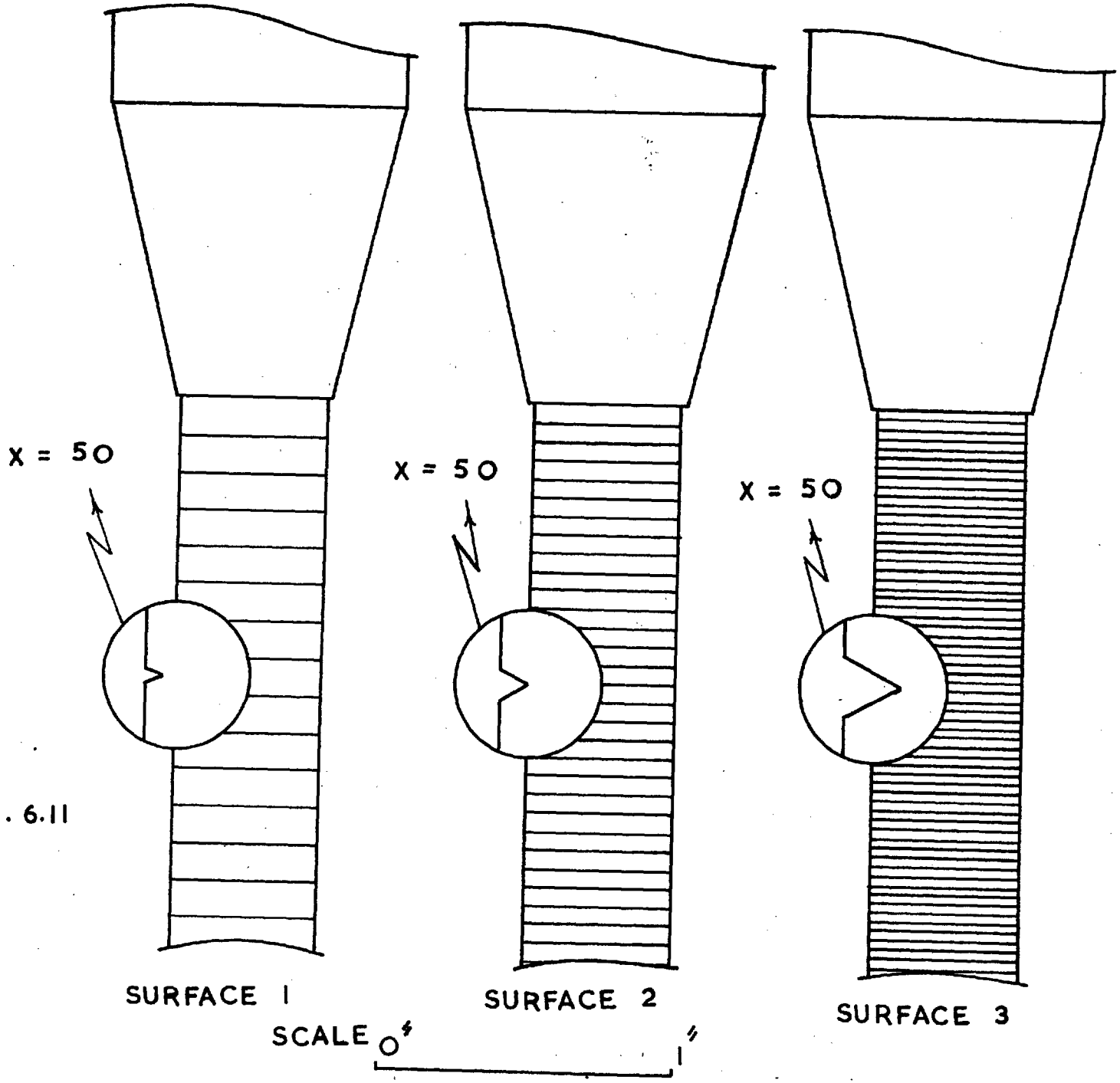

FIG. 6.11

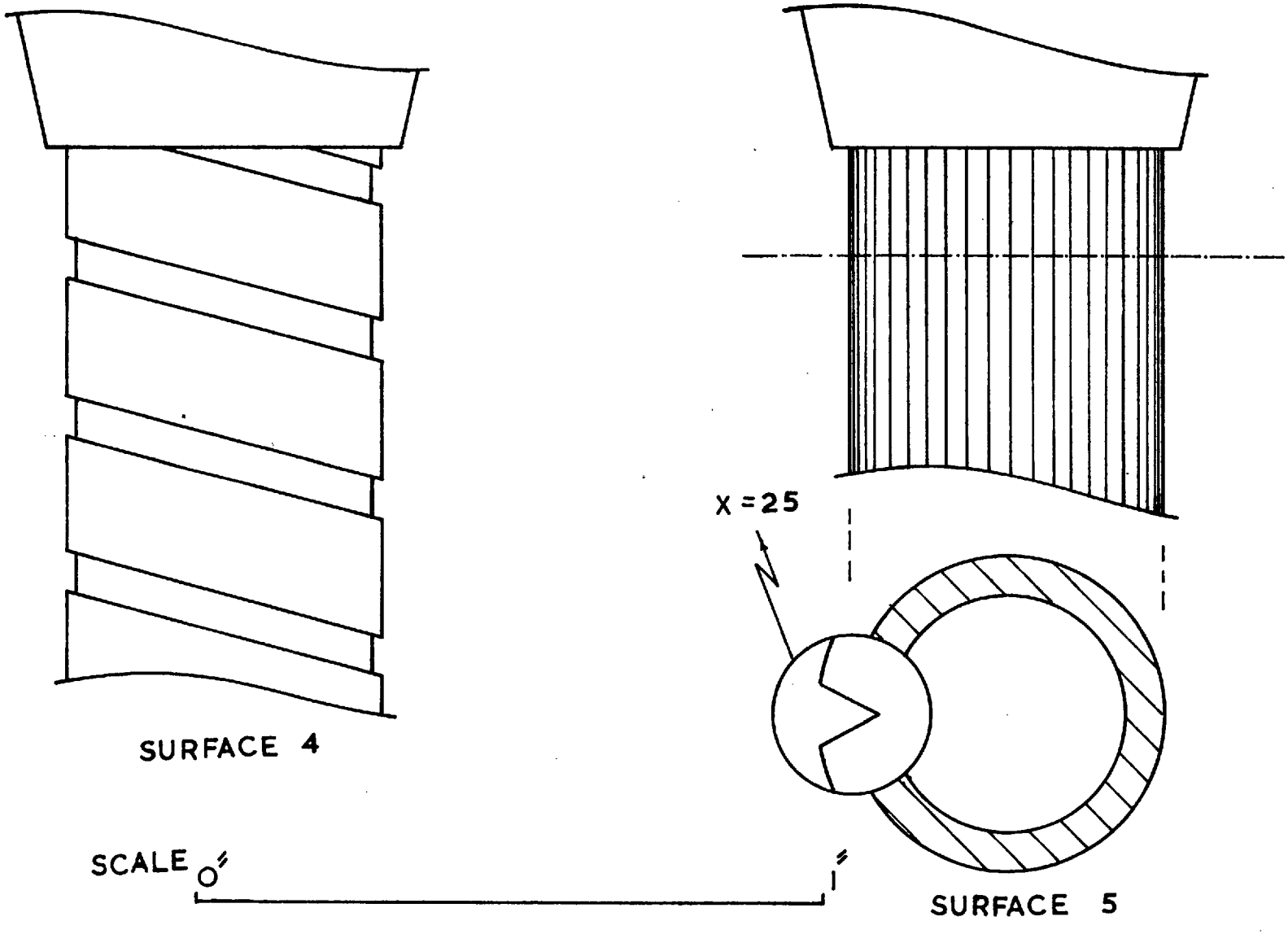

FIG. 6.12

Cutting tool was V-shaped. Roughness = 16 x $^{2}/_{1000}$ = 0.032 cm.

Surface 3 (Fig.6.11) - The grooves are diametric and 32 to an inch. The depth and the width is $^{4}/_{1000}$" each. The cutting tool was again V-shaped. Roughness = 32 x $^{4}/_{1000}$ = 0.128 cm.

Surface 4 (Fig.6.12) - The surface has a screw thread having $^{1}/_{4}$" pitch. The dimensions of the groove are $^{1}/_{32}$" depth and $^{1}/_{16}$" width. The cutting tool was rectangular. Roughness = 4 x $^{1}/_{32}$ = 0.125 cm.

Surface 5 (Fig.6.12) - There are 30 longitudinal grooves per inch of circumference. The depth and the width are $^{4}/_{1000}$" each. The cutting tool was V-shaped. Roughness = 30 x $^{4}/_{1000}$ = 0.120 cm.

(ii) Protrusions on surface.

Surface 6 (Fig.6.13) - Graded sand particles of an average diameter of 0.075 cm. are pasted on the tube surface in close packing. The cementing was done with a dilute acetone solution of transparent 'Bostik'. The tube was wetted with the solution and particles sprayed on to it. Care was taken to avoid double-mounting of particles. The adhesion of the particles to the surface was made stronger by spraying 'Bostik' solution on to the particles after the initial set. The cementing thus obtained was sufficiently strong to withstand traction of the liquid.

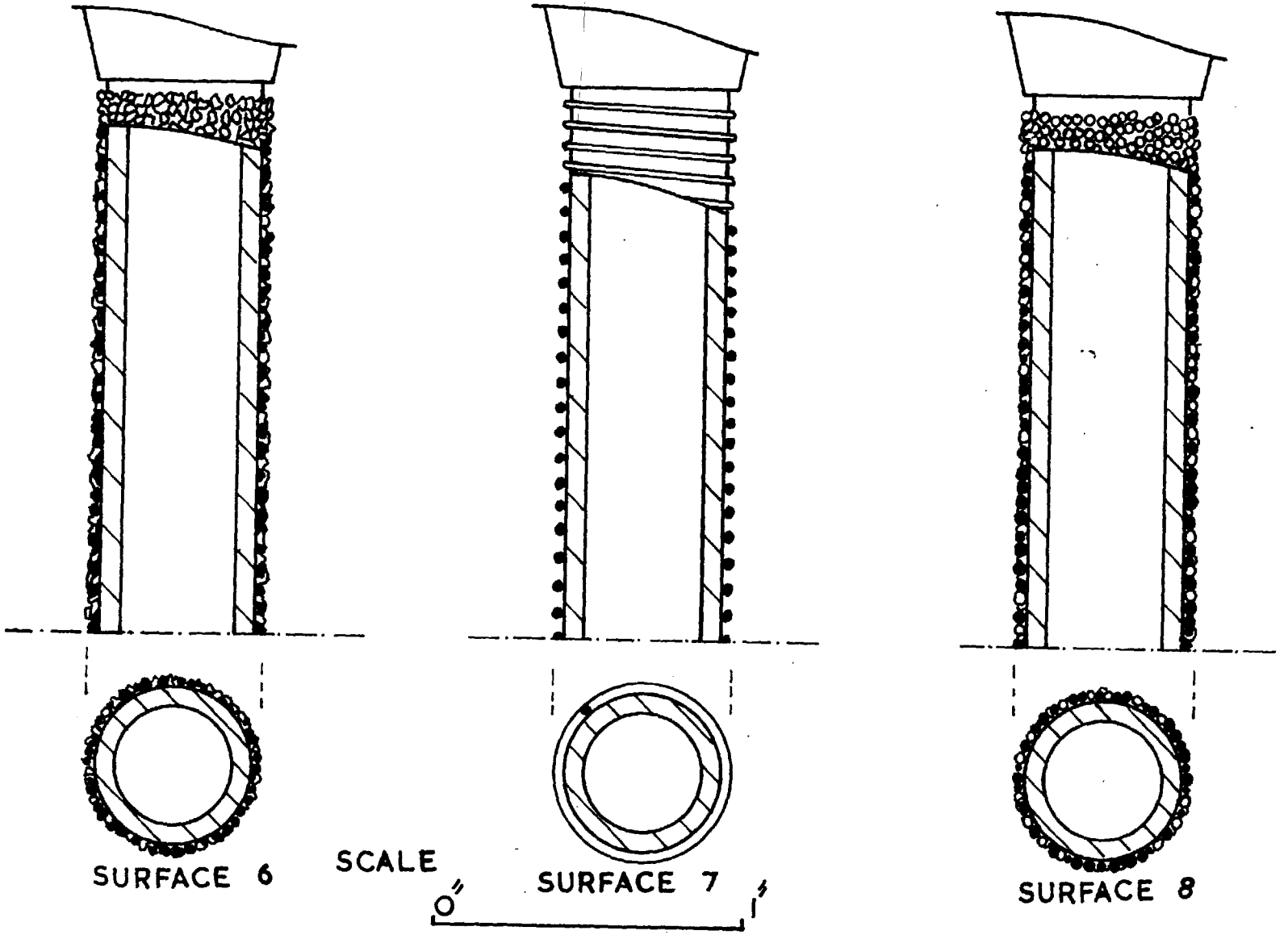

FIG. 6.13

The concentration of the particles is about 650 per sq.inch.

Roughness = $\frac{650}{(2.54)2}$ x 0.075 = 7.56 cm.

Surface 7 (Fig.6.13) - A copper wire of 0.080 cm. diameter is wound round the tube in the form of a helix, having a pitch of 0.15 cm. The wire is soldered to the tube surface at both ends to keep the helix intact. Roughness = 0.08 x $\frac{1}{0.15}$ = 0.533 cm.

Surface 8 (Fig.6.13) - Glass beads of an average diameter of 0.117 cm. are cemented to the tube surface in the same fashion as the sand in surface 6 with 'Bostik' solution. The concentration of the beads is about 58/cm^2. Roughness = 58 x 0.117

= ~~0.679 cm.~~ 6.79

Surface 9 (Fig.6.14) - Four vertical chains of glass beads (dia., 0.117 cm.) are cemented on the surface, diametrically opposite and 1 cm. apart vertically. Roughness = $4/_{\pi x 1.27}$ x 0.117

= 0.117 cm.

Surface 10 (Fig.6.14) - Two vertical chains of glass beads (dia., 0.117 cm.) are cemented on the surface, diametrically opposite and 1 cm. apart vertically. Roughness = $2/_{\pi x 1.27}$ x 0.117

= 0.058 cm.

Surface 11 (Fig.6.14) - One vertical chain of glass beads is (dia., 0.117 cm.) cemented to the wall 1 cm. apart vertically. Roughness = $1/_{\pi x 1.27}$ x 0.117 = 0.029 cm.

Surface 12 (Fig.6.15) - Four vertical chains of glass beads (dia., 0.117) are cemented to the surface diametrically opposite

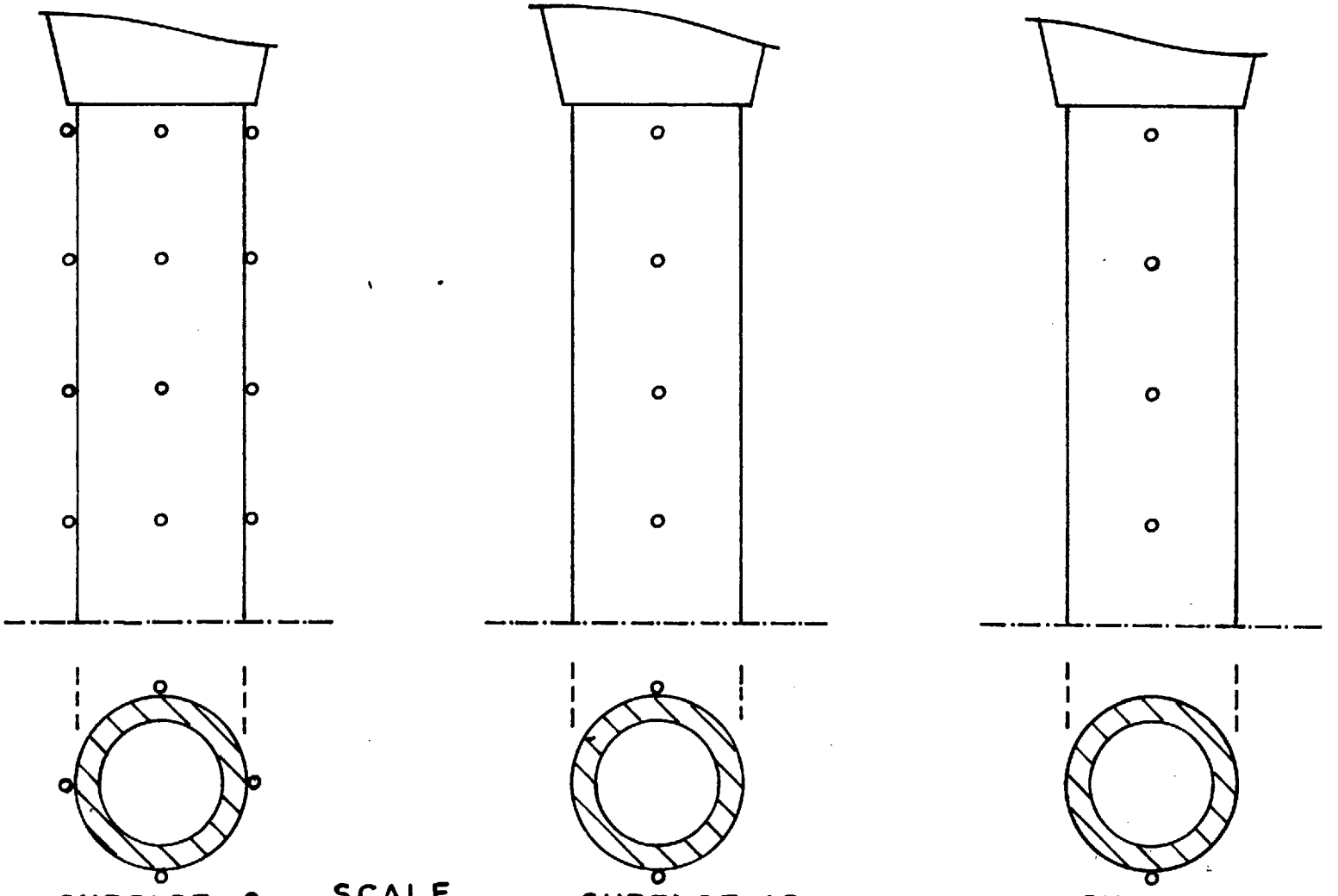

FIG. 6.14

and 2 cm. apart vertically.

Roughness = $2/_{\pi x 1.27}$ x 0.117 = 0.058 cm.

Surface 13 (Fig.6.15) - Four vertical chains of glass beads (dia., 0.117 cm.) are cemented to the surface diametrically opposite and 0.5 cm. apart vertically.

Roughness = $8/_{\pi x 1.27}$ x 0.117 = 0.234 cm.

Surface 14 (Fig.6.15) - Eight vertical chains of glass beads (dia., 0.117 cm.) are cemented 2 cm. apart vertically.

Roughness = $4/_{\pi x 1.27}$ x 0.117 = 0.117 cm.

Surface 15 (Fig.6.16) - Eight vertical chains of glass beads (dia., 0.117 cm.) are cemented to the surface, 1 cm. apart vertically. Roughness = $8/_{\pi x 1.27}$ x 0.117 = 0.234 cm.

Surface 16 (Fig.6.16) - Eight vertical chains of beads (dia., 0.117 cm.) are at 0.5 cm. apart vertically.

Roughness = $16/_{\pi x 1.27}$ x 0.117 = 0.468 cm.

Art.6.2. - Evaluation of Results

A height of 15.0 cm. of the wetted wall tube, with a particular roughness on the surface, was used for absorption at all the sixteen surfaces described above. The liquid flow rates used were both in the laminar and the turbulent ($Re > 1200$) regions. The results for each region of flow will be discussed separately. It was observed that the inception of rippling was helped by the presence of roughness at small flow rates in the laminar region. Absorption results were

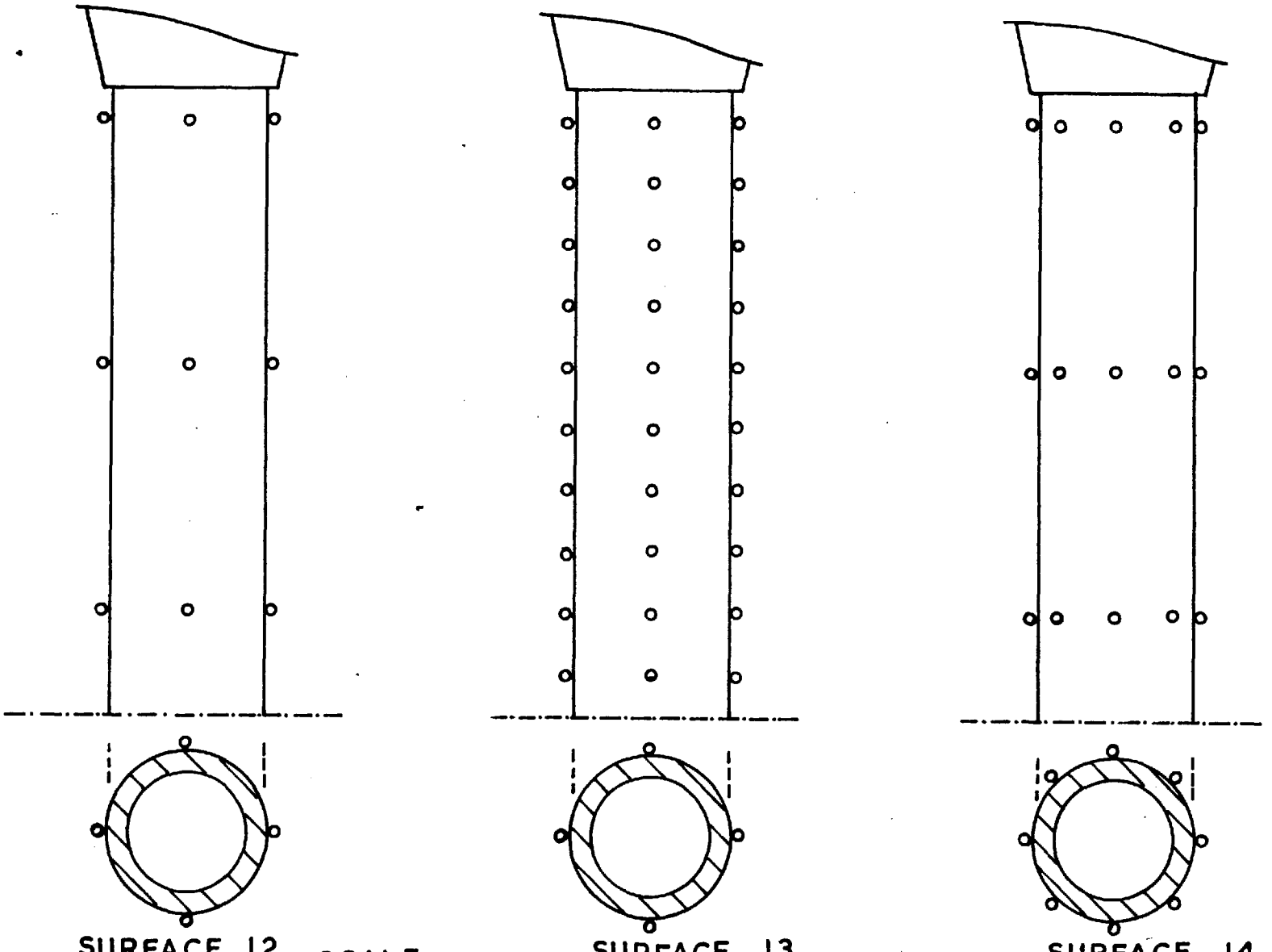

FIG. 6.15

FIG. 6.16

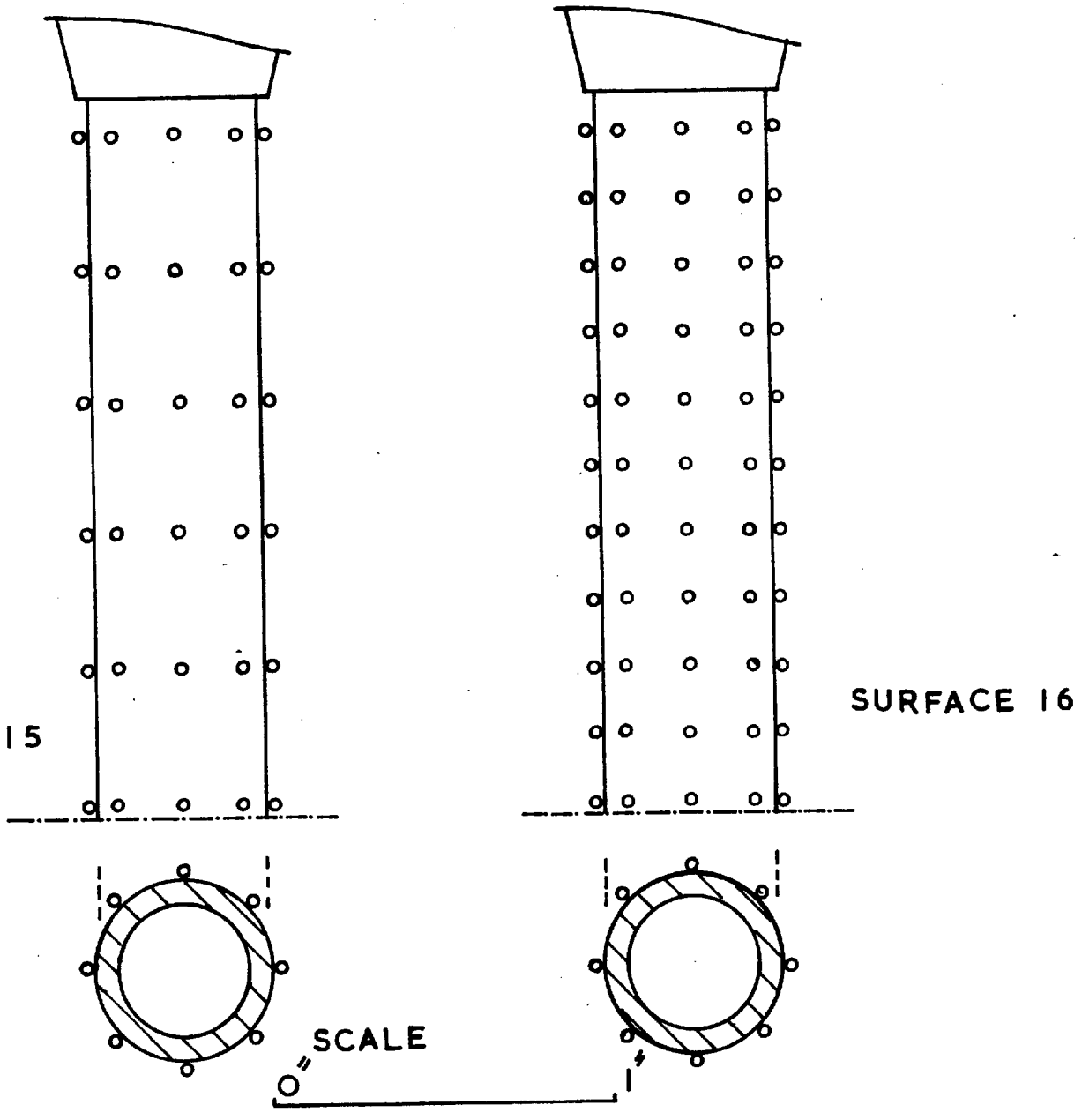

obtained both for the rippling film, as well as, the smooth film obtained by the use of surface active material in water. The presence of surface active material did not affect the absorption results at turbulent flow rates. Therefore only results for pure water are reported here for this region of flow.

Results at Laminar Liquid Flows (Re $<$1200)

(i) Engravings on surface.

The experimental absorption rates were calculated from Eq.(3.21). These are contained in Table 6.21 for both pure water, and water containing SAM. It is seen from the results for pure water that absorption rates were increased by a maximum of 3% at small laminar flow rates by the use of rough surfaces. When 'Γ_v' was more than 1.5870, rippling practically disappeared on the height of the wetted tube considered. The absorption results above this flow rate are, therefore, similar for both smooth and rough surfaces (within the range of experimental error).

Rippling was present in the case of both smooth and the rough surfaces when $\Gamma_v < 1.5870$. The slight increase in the rate of absorption on rough surfaces is attributed to two factors, (a) the zone of rippling is slightly higher, (b) the presence of roughness elements improves the mixing action of the ripples.

Table 6.21

Temperature of the System, °C = 25

Height of the wetted wall tube, cm. = 15.0

Diameter " " " " " " = 1.270

r_v	Smooth Surface		Surface 1		Surface 2		Surface 3		Surface 4		Surface 5	
	*P.W. $N_A \times 10^6$	SAM $N_A \times 10^6$	P.W. $N_A \times 10^6$	SAM $N_A \times 10^6$	P.W. $N_A \times 10^6$	SAM $N_A \times 10^6$	P.W. $N_A \times 10^6$	SAM $N_A \times 10^6$	P.W. $N_A \times 10^6$	SAM $N_A \times 10^6$	P.W. $N_A \times 10^6$	SAM $N_A \times 10^6$
0.6369	12.85	10.91	12.88	10.92	13.15	11.03	13.19	11.01	13.23	11.11	13.18	11.00
0.9570	13.79	12.42	13.81	12.43	13.98	12.50	13.90	12.52	13.92	12.58	13.90	12.52
1.2730	14.42	13.54	14.40	13.57	14.56	13.61	14.58	13.61	14.60	13.67	14.52	13.61
1.5870	14.80	14.32	14.82	14.30	14.89	14.36	14.92	14.33	14.93	14.36	14.89	14.32
1.8920	15.18	14.92	15.20	14.98	15.25	15.10	15.23	15.08	15.21	15.20	15.24	15.13
2.2200	15.74	15.53	15.72	15.54	15.76	15.61	15.75	15.60	15.74	15.65	15.72	15.60

* P.W. = Pure water.

SAM = Water containing surface active material, Lissapol, 0.01% by volume.

When the surface active agent was present in water to give ripple-free films, the rate of absorption was not affected by the nature of the surface. The small variations at different surfaces are within the range of experimental error. An interesting observation in this study was the fact that, although the interfacial areas at Surfaces 3,4, and 5, were considerably higher than those at the smooth surface, the rates of absorption were almost equal. Especially at Surface 4, where the depth of groove was more than the thickness of the film and the interface assumed a corrugated shape, a rough estimate from the height and the number of corrugations present showed that the increase in interfacial area was about 25%. The only explanation that can be given for this behaviour is that the interfacial velocity must have decreased proportionately. The latter quantity is solely responsible for the rates of absorption by molecular diffusion. The following possible reasons are suggested for a decrease in the interfacial velocity from that of a smooth surface.

1. The liquid film thickens round the roughness elements, which means that the average thickness of the liquid layer increases. This affects the average velocity of the film which decreases. The interfacial velocity is proportional to average velocity ($v_i = 3/2\ v_{av.}$) which also decreases.

Another reason for the increase in the average thickness of the film on rough surfaces is the increased area of the solid surface. It has been discussed previously that the thickness of the film is determined by a balance between the downward forces of gravity and the upward forces of internal fluid friction and the frictional resistance at the wall. This balance is disturbed by an increase in the frictional resistance at the wall due to roughness elements. The film becomes thicker in order to increase the downward gravity forces proportionately.

2. When the interface is irregular in shape, the local point values of the interfacial velocity would vary. The values of 'v_i' at crests and troughs would be 'Sin θ' times the values at a vertical surface. The average value of the interfacial velocity would, therefore, be less for an irregular interface as compared to a smooth one.

3. Presence of roughness elements increases the total periphery of the tube. Γ_v, which is the volumetric flow rate per unit periphery, decreases. As 'v_i' is proportional to 'Γ_v' ($v_i = {}^{3}/_{2} \frac{\Gamma_v}{\delta}$), its value decreases.

The above observations were later confirmed from studies of absorption on surfaces with protrustions and mechanical vibrations.

Finally it can be concluded, for non-rippling films, that the increase in interfacial area due to the presence of roughness elements does not increase the absorption over that for a smooth surface and that the mode of absorption remains essentially as molecular diffusion. When the film is rippling, the presence of roughness intensifies the transfer rate.

(ii) Protrusions on surface.

Absorption results were obtained on surfaces with protrustions (Surfaces 6-16). These were similar to the results obtained on 'engravings'.

Table-6.22

Temperature of the System, ^{o}C = 25

Height of the wetted tube, cm. = 15.0

Diameter " " " " = 1.270

Γ_v	Smooth Surface		Surface 6		Surface 7		Surface 8	
	P.W. $N_A x10^6$	SAM $N_A x10^6$	P.W. $N_A x10^6$	SAM $N_A x10^6$	P.W. $N_A x10^6$	SAM $N_A x10^6$	P.W. $N_A x10^6$	SAM $N_A x10^6$
0.6369	12.85	10.91	13.28	11.05	13.24	11.02	13.28	11.06
0.9570	13.79	12.42	13.91	12.51	13.90	12.53	13.91	12.56
1.2730	14.42	13.54	14.60	13.61	14.63	13.64	14.65	13.62
1.5870	14.80	14.32	14.93	14.36	14.85	14.35	14.84	14.33
1.8920	15.18	14.92	15.21	15.04	15.25	15.13	15.04	15.18
2.2200	15.74	15.53	15.80	15.58	15.73	15.69	15.57	15.66

Table 6.22 contains the data on three representative surfaces having protrusions of different shapes and heights. The increase in interfacial area was estimated as 18-27% as compared to a smooth surface.

The absorption rates given in the table for the rough surfaces are almost identical with those for the smooth surface. With pure water, rippling on the film was observed, as before, up to a liquid flow rate 'Γ_v' of 1.5870. This confirms the observations made previously in connection with studies on 'engravings'. It was suggested there that the decrease in the interfacial velocity was due to the thickening of the film. A double exposure photograph taken for the thickness of the film on Surface 11 is shown in Fig.6.21. The average film thickness was found to be higher than the thickness of the film on a smooth surface. A front view of the same surface is shown in Fig. 6.22. This photograph shows the distortions of the interface in the presence of protrustions. Fig.6.23 gives a view of the whole absorption column with the liquid flowing at Surface 12.

The conclusions drawn below from the study of absorption on surfaces with 'protrusions' are similar to those for 'engravings'.

1. The rate of absorption of a gas to a ripple-free falling liquid film in the laminar region of flow ($Re < 1200$) is independent of the roughness of the surface.
2. The mixing action of the ripples is slightly higher for a rough than for a smooth surface.

Results at Turbulent Liquid Flows ($Re > 1200$)

(i) Engravings on surface.

When the dimensions of the grooves were small (Surfaces 1 and 2), the visual appearance of the film was similar to that for a

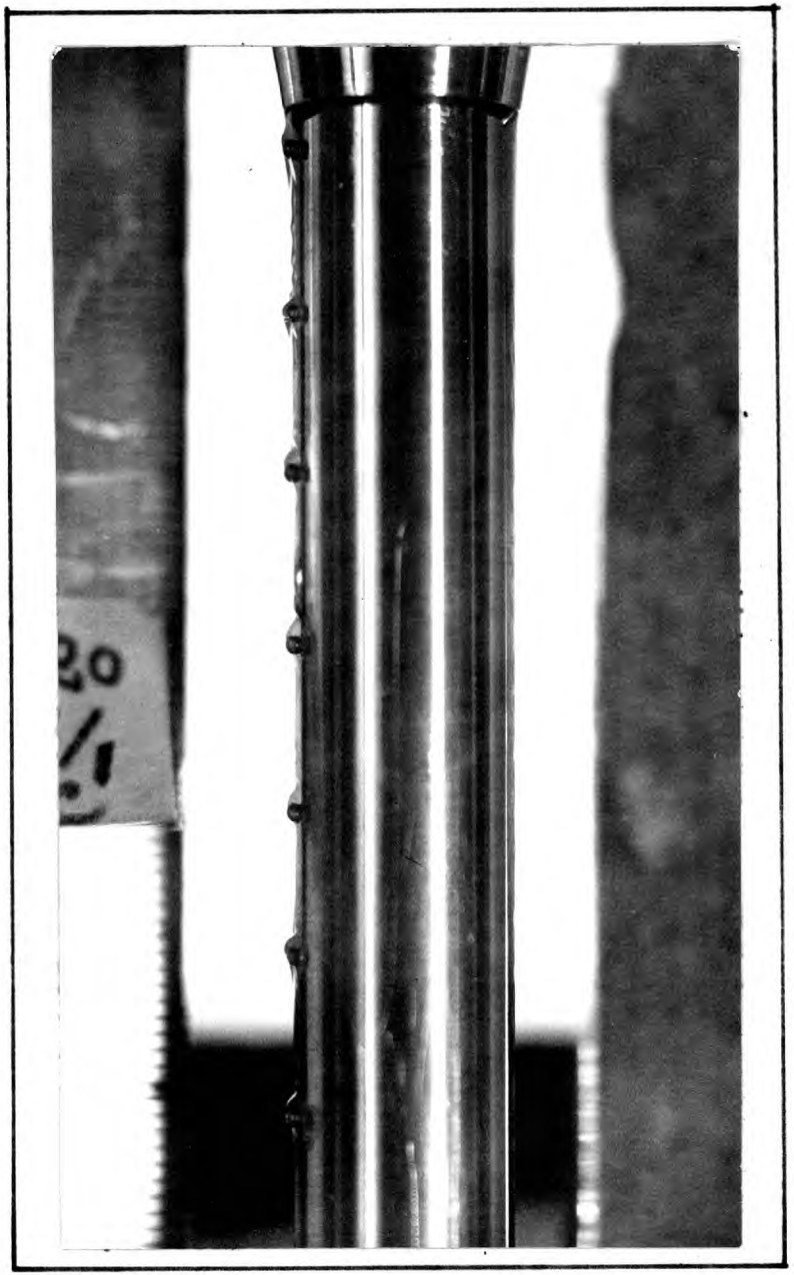

25 °C , Γ_v = 4.420 , SURFACE 11

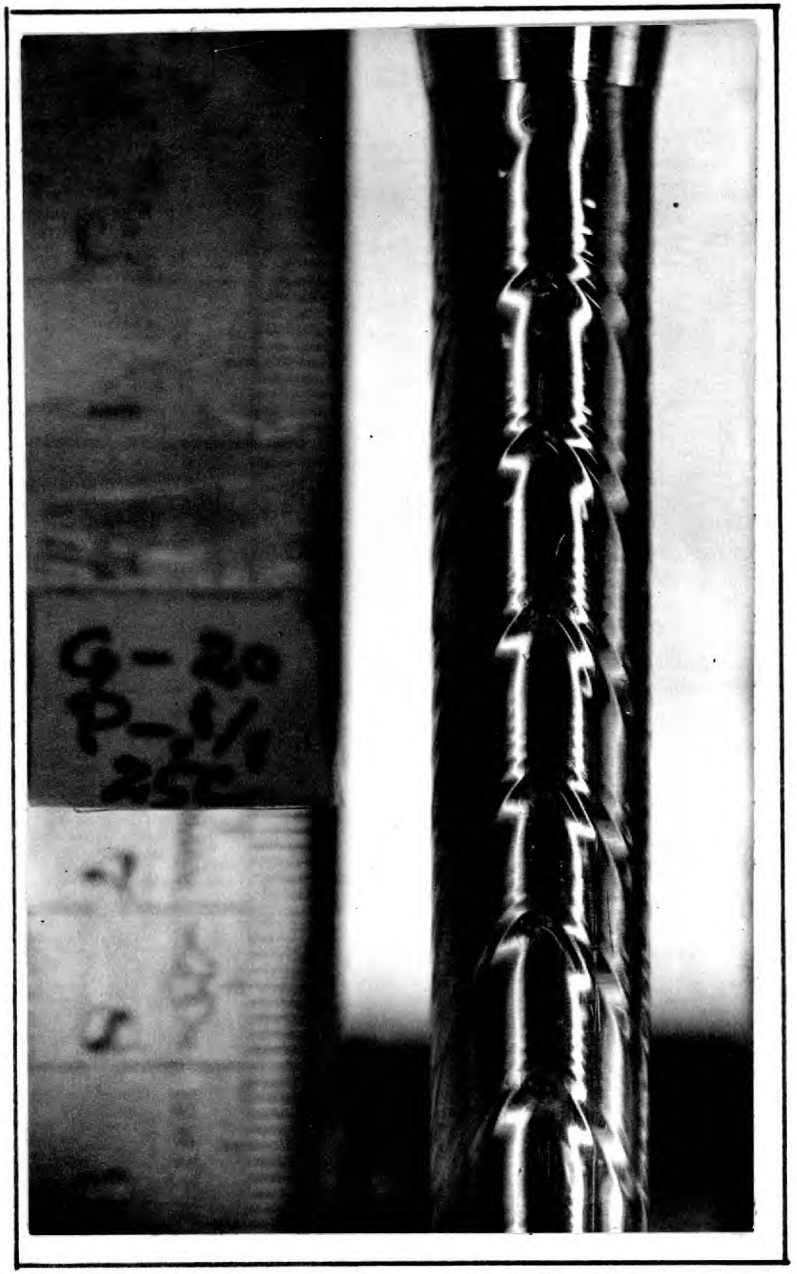

25 °C , Γ_v = 4.420 , SURFACE 11

25 °C , Γ_v = 4.420 , SURFACE 12

FIG. 6.23

smooth surface. The interface assumed a corrugated shape (criss-cross corrugations) at Surfaces 3 and 5. The dimensions of the corrugations were more prominent at these flow rates than at laminar ones. Reynolds numbers as high as 4280 (Γ_v = 9.600) were used. The absorption results have been calculated from Eq.(3.21), using value of δ_i given by Eq.4.22. The results are contained in Table-6.23. The absorption rates on all the rough surfaces are equal (within the range of experimental error) to the rates at a smooth surface.

Similar general conclusions to those derived on the effect of roughness in the laminar region of flow may be applied here. It appears that the presence of these roughness elements does not bring about any intensification of interfacial turbulence. The interfacial area was seen to be about 20-35% higher at Surface 5 as compared to a smooth surface. This means that the interfacial factors responsible for absorption decrease proportionately as the area increases so that the rate of absorption remains the same as for a smooth surface.

Table 6.23

Temperature of the System, ^{o}C = 25

Height of the wetted tube, cm. = 15.0

Diameter " " " " , " = 1.27

Γ_v	Smooth Surface		Surface 1		Surface 2		Surface 3		Surface 5	
	P.W. $N'_A \times 10^6$	SAM $N'_A \times 10^6$	P.W. $N'_A \times 10^6$	SAM $N'_A \times 10^6$	P.W. $N'_A \times 10^6$	SAM $N'_A \times 10^6$	P.W. $N'_A \times 10^6$	SAM $N'_A \times 10^6$	P.W. $N'_A \times 10^6$	SAM $N'_A \times 10^6$
3.240	17.51	17.48	17.52	17.46	17.55	17.54	17.56	17.52	17.64	17.62
4.420	18.87	18.82	18.86	18.86	18.89	18.88	18.91	18.89	18.92	18.95
5.570	20.24	20.20	20.26	20.27	20.31	20.26	20.30	20.26	20.41	20.35
6.824	21.47	21.46	21.49	21.44	21.51	21.48	21.48	21.48	21.56	21.50
8.058	22.35	22.40	22.40	22.37	22.39	22.41	22.37	22.50	22.46	22.51
9.600	24.11	24.18	24.20	24.18	24.20	24.25	24.30	24.21	24.34	24.30

(ii) Protrusions on surface.

Table 6.24a contains the absorption results at Surfaces 6, 7 and 8. Difficulty was experienced in obtaining the results at these flow rates because of the entrainment of gas in the liquid receiver. A conical brass ring was mounted on the tube inside the receiver so that the falling liquid from the wetted wall passed through an annular channel. This arrangement greatly reduced the error due to gas entrainment. Blank experiments were carried out with air-water system, where the water was saturated with air, to determine the extent of gas-entrainment. The correction was found to be between 1 and 3%. This correction was applied at the corresponding flow rates and the surfaces.

As seen from Table 6.24a, absorption is greatly intensified at rough surfaces as compared to the smooth one. The increase in the rate of absorption is as much as 130%. Sand roughness gives the highest increase. In calculating the absorption rates it was assumed that the increase in interfacial area was not responsible for the increase in absorption. Justification for this assumption has been discussed previously. The increase in absorption is, therefore, only due to increased interfacial turbulence. It is seen from the results that the presence of surface active material does not affect the rates of absorption appreciably. Further results on roughness, therefore, will be reported only on pure water.

Table 6.24a

Temperature of the System, ^{o}C = 25

Height of the wetted tube, cm. = 15.0
Diameter " " " " " = 1.270

Γ_v	Smooth Surface		Surface 6		Surface 7		Surface 8	
	P.W. $N_A' \times 10^6$	SAM $N_A' \times 10^6$	P.W. $N_A' \times 10^6$	SAM $N_A' \times 10^6$	P.W. $N_A' \times 10^6$	SAM $N_A' \times 10^6$	P.W. $N_A' \times 10^6$	SAM $N_A' \times 10^6$
3.240	17.51	17.48	25.35	25.10	22.65	20.24	28.20	28.12
4.420	18.87	18.82	31.20	31.00	28.60	28.53	30.53	30.46
5.570	20.24	20.20	38.15	38.12	33.50	33.41	33.80	33.62
6.824	21.47	21.46	43.30	43.05	38.70	38.40	38.91	37.85
8.058	22.35	22.40	48.10	47.70	43.70	436 0	45.30	45.13
9.600	24.11	24.18	55.80	55.20	50.80	50.62	50.48	50.56

The absorption results in Table 6.24a have been plotted for comparison with Eq.(4.33) in Fig.6.24. The variables of this plot are given in Table 6.24b. It is seen from Fig.6.24 that the pattern of the results does not follow the behaviour of Eq.(4.33). They seem to diverge from the line of the equation since a line drawn through the results does not pass through the intercept predicted by the equation. This means that the value of 'M' varies with the flow rate. It is also seen that the behaviour of Surface 8 is quite different from the behaviour of the other two surfaces. The photographs of the falling film with protrustions on surfaces (Figs.6.21, 6.22, 6.23) show that the pattern of turbulence varies with the height of the tube.

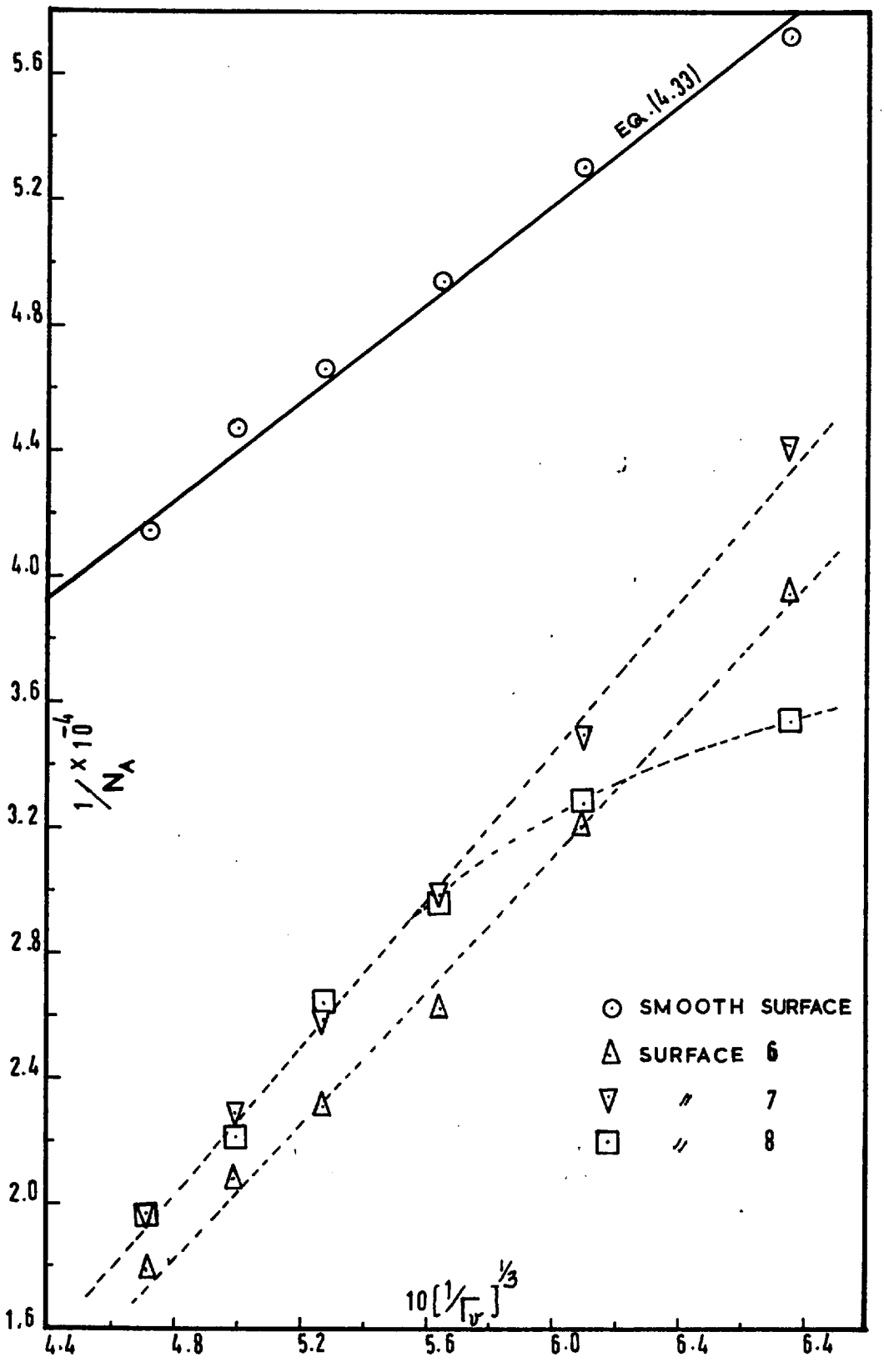
EQ.(4.33)
$1/N_A \times 10^{-4}$
$10[1/\Gamma_v]^{1/3}$
SMOOTH SURFACE
SURFACE 6
" 7
" 8
5.6
5.2
4.8
4.4
4.0
3.6
3.2
2.8
2.4
2.0
1.6
4.4
4.8
5.2
5.6
6.0
6.4
6.4

FIG. 6.24

Table 6.24b.

$10\left[1/\Gamma_v\right]^{1/3}$	Smooth Surface $1/N'_A \times 10^{-4}$	Surface 6 $1/N'_A \times 10^{-4}$	Surface 7 $1/N'_A \times 10^{-4}$	Surface 8 $1/N'_A \times 10^{-4}$
6.75	5.720	3.945	4.415	3.543
6.09	5.300	3.205	3.497	3.275
5.64	4.940	2.621	2.985	2.960
5.27	4.660	2.310	2.585	2.640
4.99	4.472	2.080	2.287	2.210
4.71	4.150	1.791	1.970	1.967

The variation in the number of projections per unit area as well as their arrangement was studied next. Glass beads were chosen as the projections because these are available in a more uniform size than the sand particles. Surfaces 8 to 16 (Figs.6.13-6.16) represent various patterns and frequencies of these beads on the surface. The absorption results for Surface 8 have already been given in Table 6.24a. The results for Surfaces 9-16 are contained in Table 6.25. The roughness results plotted in Fig.6.24 indicate no relationship with Eq.(4.33). Therefore, the results for Surfaces 9-16 have been plotted in Fig.6.25 as 'Γ_v' vs. 'N'_A', simply to compare them with the results on a smooth surface. The solid line through the results for smooth surface is represented by Eq.(4.34). Dotted curves are drawn through the results for each roughness. It is seen from these curves that the absorption ratio 'N'_A (Smooth)/N'_A(Rough)' increases

Table 6.25

Temperature of the system, ^{o}C = 25

Height of the wetted tube, cm. = 15.0
Diameter " " " " " = 1.270

Liquid used = Pure water.

Γ_v	Smooth Surface $N'_A \times 10^6$	Surface 9 $N'_A \times 10^6$	Surface 10 $N'_A \times 10^6$	Surface 11 $N'_A \times 10^6$	Surface 12 $N'_A \times 10^6$	Surface 13 $N'_A \times 10^6$	Surface 14 $N'_A \times 10^6$	Surface 15 $N'_A \times 10^6$	Surface 16 $N'_A \times 10^6$
3.240	17.51	27.80	20.05	18.02	23.75	29.60	27.61	29.40	30.80
4.420	18.84	30.45	22.60	19.96	25.55	30.05	30.28	30.20	31.64
5.570	20.24	33.25	25.10	23.25	27.50	36.15	33.40	36.30	37.80
6.824	21.47	37.60	33.25	28.95	32.80	39.10	37.40	39.05	40.10
8.058	22.35	44.50	39.70	33.95	41.40	46.30	44.60	46.20	47.20
9.600	24.11	50.60	49.00	42.40	49.60	51.10	50.81	50.80	51.20

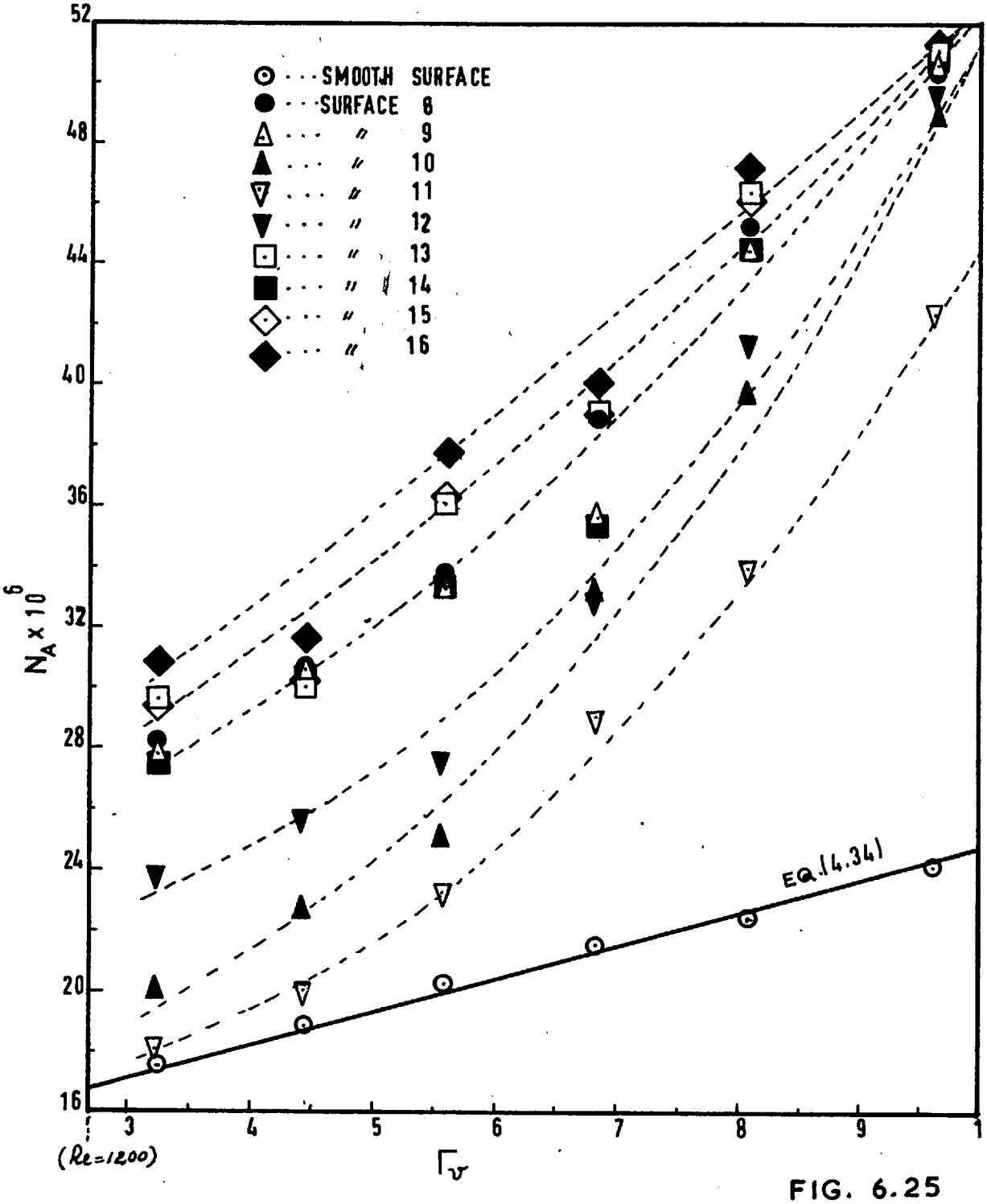
SMOOTH SURFACE
SURFACE 8
" 9
" 10
" 11
" 12
" 13
" 14
" 15
" 16
$N_A \times 10^6$
52
48
44
40
36
32
28
24
20
16
3
4
5
6
7
8
9
10
(Re=1200)
Γ_v
EQ.(4.34)

FIG. 6.25

with the increase in flow rate. Surface 10, which has one chain of beads, and Surface 11, which has twice the number of beads, do not give parallel curves. This means that the increase in absorption rate is not proportional to the number of beads. Surfaces (9, 14) and (13, 15) have coincident curves. These pairs of surfaces have the same concentration of protrusions (roughnesses 0.234 cm. and 0.117 cm. for each pair respectively) except that the arrangement differs. The increase in absorption is therefore independent of the arrangement. The curve for Surface 8, which contains closely packed protrusions, also coincides with the curve for the pair (S-9,14). The curve for Surface 16 is the highest above the line for a smooth surface. This shows that optimum intensification of absorption is reached at Surface 16 (roughness = 0.468 cm.) and that the closely packed protrusions (roughness = 6.80 cm.) are less effective.

The two photographs in Fig.6.26 give an idea of the manner of flow of the liquid film on rough surfaces. The following conclusions can be drawn from the study on surface protrusions in the turbulent region of liquid flow.

1. The rate of absorption by a falling film increases considerably (up to 130%) by the presence of protrusions on the surface. The increase is due to the increase in the mass transfer coefficient brought about by intensified turbulence.

25 °C , Γ_v = 4.420 , SURFACE 8 16

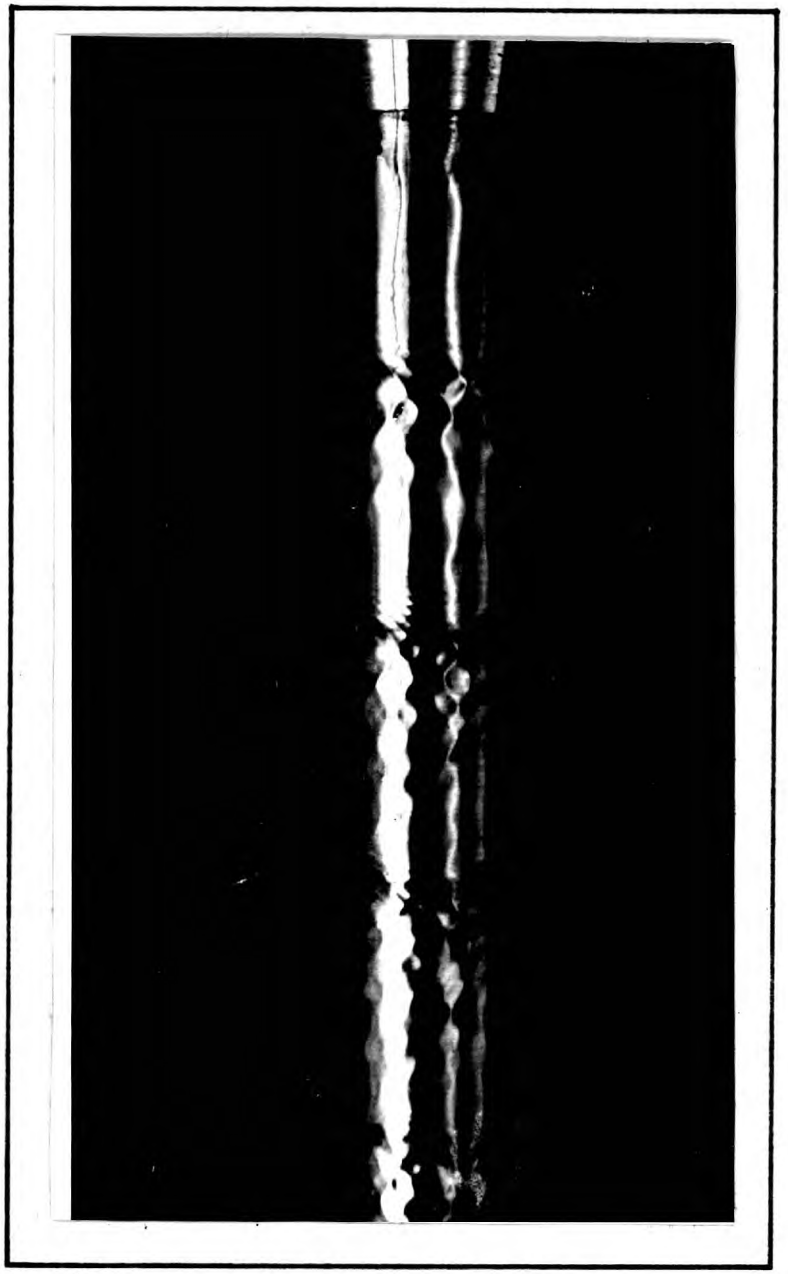

25 °C , Γ_v , 4.420 , SURFACE 14

FIG. 6

2. The increase in the absorption rate is independent of the manner of distribution of the protrusions for the same frequency.
3. There is an optimum frequency of these protrusions, represented by Surface 16, which gives the highest increase in absorption rate. If the frequency is increased further, the absorption rate decreases.

SECTION 3.

GAS ABSORPTION INTO LIQUID FILMS FALLING OVER MECHANICALLY VIBRATED SURFACES.

CHAPTER VII

INFLUENCE OF OSCILLATIONS IN TRANSPORT OPERATIONS

Art. 7.1. General

Oscillations include vibrations and pulsations. They can appear as steam or water hammer, reciprocating compressor pulses, throttling noises, etc., or,more important to this discussion, oscillatory motion can be imparted deliberately either to the medium or to the surface. The terms vibration and pulsation are often used interchangeably, although the latter is reserved for periodicity as it appears in the flow of a liquid. Variables in oscillation include frequency, amplitude and the manner of application. The last variable refers to the direction of oscillation, that is, whether the oscillation is longitudinal or transverse relative to the transfer surface or direction of flow. This also refers to whether the oscillation is applied to the fluid as with sound waves or to the surface (as with a vibrator arrangement). Although similar, these two are not the same. For the first case, any attenuation of the boundary layer next to the wall comes from without; for the second, from within. Under certain circumstances, however, the differences are quite small.

The field of inducing or intensifying physical changes by oscillations (infrasonics, sonics and ultrasonics) is of growing interest in chemical engineering. The absorption of

sonic energy has been found to improve the efficiency of transport operations. Almost all the work done in this field is essentially of an empirical nature and ranges from the use of low energy pulsations (from 10 cycles/min.) to high frequency ultrasonics (several mega cycles/sec.).

The influence of oscillations in transport phenomena is limited to heat transfer and mass transfer, no independent study being reported in the literature on momentum transfer, although occasional references are found on the modification of flow pattern due to vibration in connection with the former two operations.

Art. 7.2. Heat Transfer

One of the earliest references on the effect of vibrations on heat transfer is that of Martinelli and Boelter (70). These workers studied the effect of vibrating a horizontal heating element immersed in a tub of water on convective heat transfer from its surface. They observed an improvement in the transfer rate.

The German patent of Andreas (71) consisted in the mechanical vibration of an entire heat exchanger. He recommended vibrations with an amplitude of 1-5 mm. in the direction of the tubes with a minimum frequency of 1500 cycles/min.

Marchant (72) carried out experiments on the effect of pulsating flow in heat transfer to a fluid flowing in a tube when the pulsations were of the order of 10-60 cycles/min. It was intended to simulate the mechanism of heat transfer in an internal combustion

engine. For obtaining a pulsating flow they used a reciprocating pump giving a sinusoidal variation. Their observations are recorded below:

1. "When the flow was laminar, the values of overall heat transfer coefficients were larger than those for non-pulsed flow.
2. The overall heat transfer coefficient was not affected by pulsation of the water over the range of frequencies investigated when the flow was turbulent.
3. The increase in the overall heat transfer coefficient observed at low Reynolds numbers may be probably due to the addition of forced convection to the two normal modes (conduction and radiation) by means of which heat is transferred through what would correspond to the inner surface boundary layer under steady flow conditions".

West and Taylor (73) reported work on similar lines as above, hoping that pulsations would improve heat transver in two ways - (1) the peak longitudinal flow would be increased, which would decrease the thickness of the laminar film at the pipe wall; (2) the subsequent minimum longitudinal flow should result in radial diversion of much of the excess longitudinal kinetic energy. High flow rates, of the order of Reynolds numbers, 30,000-85,000 (overall flow), were used because in a few parallel investigations, where Re of 26 to 1375 were used, no improvement in heat

transfer was observed. Contrary to the results of Marchant (72), water film coefficients were found to increase up to 70%, with a maximum increase in power consumption of 30%, which was a moderate increase in power for the resulting improvement in heat transfer.

The study of Lemlich (74) was similar to that of Martinelli et.al. (70), involving convective heat transfer from electrically heated wires subjected to transverse vibrations in air. Marked improvement in the coefficient of heat transfer was obtained by using vibrations in the range of 39 to 122 cycles/sec., even to the extent of quadrupling the coefficient. Holding all other variables constant in turn, the coefficient was found to increase with both amplitude and frequency. The direction of vibration was without significant effect. In an effort to account for this latter observation, the concept of a stretched film surrounding the entire path of vibration was proposed. The effect of vibrational variables was correlated in terms of a vibrational Reynolds number (Re_v) defined as twice the product of amplitude, frequency, linear dimension, and density, divided by viscosity, as,

$$Re_v = \frac{D\bar{v}\rho}{\mu},$$

where $\bar{v}$ = 2 x frequency x Amp.

D = linear dimension.

In terms of quantitative results among various studies, some investigations report great increases in heat transfer coefficient from oscillations and others little, none, or even a decrease.

This is not surprising, however, in view of the many possible variations of the oscillatory variables, to say nothing of their inter-action with all the usual convective variables, such as, velocity, fluid properties etc.

A general theory and verified mathematical correlations are lacking. The only correlation available for predicting the transfer coefficient is that of Lemlich (75) for oscillations of very low frequency ($<$20 cycles/sec.), and it is of limited applicability. According to him, a system can be described as non-steady after the critical frequency of 20 cycles/sec. With the displacement amplitude held fixed, raising the frequency above the critical level usually increases the heat transfer coefficient. Each cycle of motion acts as a disturbance. Increasing the number of such disturbances per second tends to increase the overall effect on the boundary layers involved. This is by no means a complete explanation, because cases where the coefficient subsequently decreases with further elevation in frequency are not unknown. This inverse behaviour has been attributed to cyclic fluctuations in wall temperature. For a constant wall temperature, such a decrease would not be likely to occur.

The coefficient generally increases with displacement amplitude for a fixed frequency above the critical level. At low amplitude, this improvement is often too small to be detected

but the coefficient rises at an increasing rate as the amplitude is raised. At lower amplitudes, the usual forced or convective currents predominate. Not until the amplitude is raised sufficiently, do the disturbances produced become relatively significant — usually at an accelerating rate. In some cases, however, an upper limit to the particular mechanism may appear and decelerate this rate, giving the curve of coefficient vs. amplitude something of an S-shape, or even a peaked appearance. The relative effect of increasing the amplitude at constant frequency, generally equals or somewhat exceeds that of increasing the frequency at constant amplitude.

Above the critical frequency, the relative effect of oscillation, at fixed frequency and fixed displacement amplitude, is usually greater at low flow Reynolds numbers than at high and for natural convection than for forced. The reason is similar to that presented above for the increasing slope as amplitude increases, that is, when the disturbances produced by oscillation are relatively significant compared with those otherwise present, the coefficient of heat transfer is likely to increase.

For sonic vibrations applied to natural convection, improvement in heat transfer coefficients has been credited to additional currents of acoustical streaming. Such currents are produced even under isothermal conditions when sound impinges on a solid body or a body vibrates in an otherwise calm fluid.

When considering heat transfer involving a surface vibrating in a fluid, care must be taken in extrapolating from the converse case when the body is stationary and the fluid vibrates. Despite certain similarities, the two situations are not quite the same. With the first case, any alteration of the convective boundary layer comes from within, while, with vibrating surface, from without. Furthermore, with sound (the first case) the displacement amplitude is usually relatively small while, with a vibrating body such as a wire or a granule, amplitude can easily exceed the diameter of the body.

In forced convection, axial flow through a tube is a very important case. Oscillations of sufficient frequency and amplitude can substantially lower the critical flow Reynolds number and steepen the velocity profile near the wall. This amounts to increasing the level of turbulence, and by analogy of heat transfer to mass transfer, increasing the heat transfer coefficient. The oscillations can be viewed as acting at least in part as a turbulence trigger.

It has been proposed that appreciable improvement in coefficient occurs only when pulsation amplitude is large enough to allow a momentary reversal of flow during each cycle. For acoustical vibration, tuning the frequency to resonance so that standing waves are set-up within the tube, gives greater hold up to acoustical energy and larger amplitudes in the tube. This resonant effect

is so marked that even a modest detuning may stop all measurable improvement.

The heat transfer work carried out with vibrations has consisted of either oscillating the fluid or the solid surface. In the study described in this thesis on gas absorption, the surface was oscillating longitudinally to the direction of liquid flow. In heat transfer, the vibrating solid surfaces are usually heating elements. The only heat transfer study in which the mode of vibration was somewhat similar to the present study was that reported by Thompson (76). He stated that the turbulence induced by acoustical vibrations raised heat transfer rates through the laminar film on the water side of evaporators. The experimental unit consisted of a 1-in. pipe (37 in. long) co-axial with a 3-in. pipe. Water flowed continuously through the annular passage to a cooling coil and back. Electricity flowing through the pipe wall heated the 1-in. pipe. An oscillator and an amplifier powered a vibrator which was fastened by a short rod to the 1-in. pipe. The vibrator delivered energy to the pipe, creating turbulence in the water film. The range of Reynolds numbers investigated by them at various frequencies and amplitudes was 540-20,000. Some results are tabulated as under:

Table 3.1

Frequency 42 cycles/sec. Reynolds number	Amplitude (0.150 inch). Increase in coefficient (%)
540	450
1,400	280
5,000	115
12,000	30
16,000	16
20,000	10

From the foregoing results it can be seen that the lower the Reynolds number is, the more effective are the vibrations. Also that vibration helps heat transfer to some extent at all Reynolds numbers. Report is also given of studies using three different arrangements of imposing vibrations to improve heat transfer:

1. Transverse vibrations impressed directly upon the water stream flowing inside a heated tube.
2. Longitudinal vibration of the containing pipe with no vibrations impressed upon the water stream.
3. Transverse vibrations of the containing pipe with no vibrations upon the water stream.

A very recent study by Mathewson and Smith (77) on the effect of sonic pulsations on forced convective heat transfer to air and on film condensation of isopropanol, is very illustrative of the mechanism of increase in heat transfer. The interpretations of this work can possibly be applied to an analogous case of mass transfer. These authors studied the effect of very strong sonic pulsations on the rates of heat transfer with the pulse generated in the flowing stream. They used a co-axial heat exchanger, and a flat-plate siren, set in the fluid inlet line, served as a pulse generator. Effect of the flow rate of the fluid was found to be similar to that observed previously (72, 73, 75). The changes in amplitude had little or no effect on heat transfer coefficient.

This was evidenced by the fact that operation at any of the resonant frequencies gave the same results at closely adjacent non-resonant frequencies. Also the results of Lemlich (75) for the same frequency, and a much lower amplitude, were identical with these authors' results.

Effect of frequency: With a given flow rate and pulse amplitude, the heat transfer coefficient increased rapidly with pulse frequency. The following simplified model based on the penetration theory of Higbie (29) was suggested as a means of correlating the results. Application of this theory to heat transfer at a solid surface yields the following equation for the heat transfer coefficient of unpulsed air:

$$h_o = 2\sqrt{\frac{3600}{\pi}\rho.c_p.k.f_o} = 67.8\sqrt{\rho.c_p.k.f_o} \quad \ldots (7.21)$$

where, h_o = heat transfer coefficient without pulsation $\left[(B.T.U./Hr.)(Sq.ft.)\right]$,

c_p = heat capacity, $(B.T.U.)/(lb.)(F^o)$,

k = thermal conductivity, $B.T.U./Hr.ft.F^o$.

f_o = eddy renewal rate without pulsation, $sec.^{-1}$

Under the influence of pulsation, the frequency of surface renewal becomes some new average value, $f_{av.}$, and the heat transfer coefficient is given by

$$h_p = 67.8\sqrt{\rho.c_p.k.f_{av.}} \quad \ldots (7.22)$$

where, h_p = value of 'h' with pulsation.

It is now assumed that the new frequency of surface renewal, $f_{av.}$, is a weighted average of the natural frequency, f_o, and the pulse frequency, f_p, that is,

$$f_{av.} = \frac{cf_p + f_o}{1 + c} \qquad \ldots (7.23)$$

Weighting factor 'c' is assumed constant and independent of 'f_o' and 'f_p'. If 'f_o' is computed from Eqn.(7.21) and the measured values of 'h_o' and 'c' are computed from the results of at least one run with pulsations, then the effects of changes of flow rate and pulse frequency may be predicted from Eqns.(7.22) and (7.23).

The above equations do not predict values of h_p accurately when the flow is laminar. Combining Eqns. (7.21), (7.22) and (7.23), and recognising that $c \ll 1$, one gets,

$$\frac{h_p^2}{h_o^2} = 1 + \frac{c.f_p}{f_o} \qquad \ldots (7.24)$$

Equation (7.24) predicts the effect of changing pulse frequency 'f_p' and of changing 'f_o', the latter being dependent upon the Reynolds number. These authors plotted $\left(\frac{h_p}{h_o}\right)^2$ vs. $\left(\frac{f_p}{f_o}\right)$ with data taken at various pulse frequencies and Reynolds numbers. The straight line whose slope was equal to 'c' (cf. Eqn.(7.24)) agreed well, for turbulent flow, with the measured values.

A discussion of the film condensation of isopropanol with sonic pulsation, given by the above authors (77) is useful.

Isopropanol vapours were passed downwards through the central tube with countercurrent flow of water in the jacket. Vapour condensed on the wall and a thin film of liquid isopropanol flowed down the tube. Heat transfer coefficients were measured from the rate of condensate collection. As in the tests with air given above, 'f_o' in Eqn. (7.21) was found from the measured values of 'h_o'. Factor 'c' in Eqn. (7.23), dervied from the results obtained when 'f_p' was 300 cycles/sec. and the vapour rate as 1.25 lb.moles/hr., was calculated to be 0.011. From this value of 'c' and Eqns. (7.22) and (7.23), the effect of changing the flow rate on 'h_p' could be computed. There was fairly good agreement with the results when plotted. The increase in heat transfer coefficient was greatest at low vapour rates. The coefficient increased rapidly as the natural turbulence in the system increased. In all the runs the Reynolds number of the vapour was at least 30,000, and the previous results with air alone indicated that pulsation had almost no effect on transfer in such a turbulent vapour. Increases in condensation rate must have resulted from the effect of pulsation on the condensate film, through the induction of waves at the surface or turbulence in the body of the film. Since Eqns.(7.22) and (7.23) accurately predict the effect of changing flow rate, it appears that pulsation induces turbulent eddies within the condensate layer with a renewal frequency which may be estimated by Eqn.(7.23) when 'f_p' is held constant.

With vapour flow rate held constant, application of a pulse of any frequency between 50 and 330 cycles/sec., significantly increased heat transfer coefficient. Within this range of frequencies the increase was not strongly dependent on the frequency. This did not agree with the results predicted from Eqns. (7.22) and (7.23). The theory, as developed for air flow, predicts a rapid increase in coefficient with frequency, while the results obtained when isopropanol vapour was being condensed, indicate only a slow rise. The effect of pulsation on the mechanism of heat transfer under such conditions is probably different from that postulated in developing Eqns.(7.22) and (7.23). Pulsation induces eddies in the condensate film with an average lifetime different from that in an unpulsed system. This may be estimated for a given pulse frequency from Eqn.(7.23). The increase in heat transfer rate, however, probably results in large part from the penetration of these eddies into the laminar portion of the condensate layer. The magnitude of the increase may depend chiefly on the depth of penetration of the eddies and not on the renewal rate. The penetration depth in turn may depend on the flow rate and on the pulse amplitude but is apparently little affected by pulse frequency.

Effect of amplitude: With any given flow rate there appears to be a critical pulse amplitude below which pulsation has no effect on the heat transfer coefficient. This critical amplitude increased

with the vapour rate. At amplitudes just greater than the critical value, the heat transfer coefficient increased rapidly with amplitude; at very high amplitudes, the coefficient was little affected by changes in amplitude. The pulse was generated in the vapour and must have been transmitted by the vapour to the condensate before there was any effect on the heat transfer coefficient. At low amplitudes the energy in the pulse is too small to have a significant effect on the condensate film. At the critical amplitude, depending upon the amount of natural turbulence in the film, the pulse began to affect the liquid. Higher vapour rates mean greater natural turbulence in the film, and hence higher critical amplitudes. As the amplitude increases beyond the critical value, the heat transfer coefficient would be expected to rise and then level out as observed. The change in heat transfer coefficient depends on a coupling between the pulse and the natural eddies of the system. This coupling is greatest over a limited range of frequencies and amplitudes. At high amplitudes the natural eddies of the system no longer respond to increases in pulse amplitude, and the excess pulse energy is dissipated by other means.

Condensation of Isopropanol in the presence of air: The increase in heat transfer was somewhat lower than that found with isopropanol vapour alone. As with pure isopropanol, the change in heat transfer coefficient depends upon the vapour flow rate and almost not at all

on the pulse frequency. Apparently the pulsation decreases the thermal resistance of the condensate but does not affect the transfer coefficient in the highly turbulent vapour stream. If the vapour flow were laminar or in the transition region, application of a pulse should significantly increase the heat or mass transfer rates in a cooler-condenser."

Art.7.3. Mass Transfer

Most of the work done on the effect of vibration and pulsation in mass transfer has been limited to liquid-liquid extraction. A search of the literature revealed nothing for the case of a vibrating surface in diffusional mass transfer of the kind described in this thesis. The work of Lemlich and Levy (78) is the nearest case involving natural convective sublimation of naphthalene from the surface of a horizontal vibrating cylinder in still air. As has been discussed earlier in this chapter, vibrating the fluid with sound is not the same as directly vibrating the surface itself. The streaming patterns for the two types of vibratory systems were discussed by Fand and Kaye (79). Thus, at the present time, studies with insonation are only capable of limited comparison with studies involving heat or mass transfer from an oscillating surface. Lemlich et.al. used rods of 0.7-1.9 mm. diameter coated with naphthalene or d-camphor, vibrated at 20-118 cycles/sec., with amplitudes of 0.46-7.66 mm. The effect of vibration was conveniently represented by the ratio of the coefficients, $\frac{k_G(vib)}{k_G}$, or the fractional increase

$(\frac{k_G(vib.)}{k_G} - 1)$ versus the vibrational Reynolds number, $Re_v = D\bar{v}\rho/\mu$, where $\bar{v} = 2.Fy.Am.$ (cf. Art.7.2). Increases in the coefficient of up to 660% were reported. The effect of amplitude was found to be somewhat stronger than that of frequency. The results were related above Re_v of 20 (critical region) by the equation,

$$\frac{k_G(vib)}{k_G} = 0.117\ Re_v^{0.85} \qquad \ldots (7.31)$$

Both the mass and heat transfer results were related above the critical region by analogous relations, as,

$$\frac{k_G(vib.)}{k_G} = 0.038\ Re_v^{0.85}.\ Sc^{1.13} \qquad \ldots (7.32)$$

$$h_p/\ h_o = 0.038\ Re_v^{0.85}\ Pr.^{1.13} \qquad \ldots (7.33)$$

Gas Absorption

Zhavaronkov and Orlov (80) studied the effect of ultrasonic vibrations on the absorption of CO_2 by water. They carried out preliminary experiments in a beaker which was filled with water and exposed to pure CO_2. Ultrasonic vibrations with a frequency of 800 kcycles/sec. and an intensity of several watts per cm^2. were introduced through the bottom of the beaker. It was found that ultrasonic vibrations (which produced a water spout) increased the absorption rate by a factor of 1,00 as compared to the usual diffusionally controlled rate, and by one order of magnitude in comparison with the absorption rate observed when a four-blade stirrer was used at 800-1800 r.p.m. Such an increase could be attributed to a greatly increased area of phase contact, with the

contact rapidly renewed due to the formation of spray and mist, and also due to the vigorous stirring of the solution. It should be observed that in spite of strong cavitation, no degassing of solution was observed; within several minutes after the beginning of the experiment, the concentration of CO_2 in water attained its equilibrium value for the given temperature.

The experiments designed to study the continuous absorption of CO_2 were carried out in two medium sized ultrasonic film columns, (wetted wall columns) using open barium titanate cylinders as emitters. The vibrations were applied perpendicular to the direction of film flow. The heights of the absorption columns were 14 cm. and 16 cm. and internal diameters 1.22 cm. and 2.3 cm. respectively. Introduction of ultrasonic vibrations produced a substantial change in the flow pattern of the liquid in the column. Whereas in the absence of ultrasonic vibrations the liquid ran down as a smooth (or occasionally rippled) film, in the presence of the vibrations there arose a system of glittering, transverse, standing waves. In experiments carried out with one column, the waves were usually circumferential and regularly spaced at 3 mm. intervals at 800 kcycles/s.frequency or at 1 cm. intervals at 100 kcycles/s. frequency. Experiments carried out in column 2 gave short irregular rippled waves at both frequencies. When a 50 kcycles/s. frequency was used, there also appeared cavitation of the film in the form of two bands facing towards the middle of

the cylinder (length-wise). The flow rates used in these experiments were of the order of Γ_v = 0.54 - 1.15 cm.^{2}/sec.

The absorption rates were considerably increased by ultrasonic vibrations. At 50 kcs. and an intensity of 1-2 watt/cm.^{2}, a peak was obtained which was almost four times the unvibrated relative increase in the concentration of CO_2 in solution. The relative increase 'Q' was defined as,

$$Q = \frac{(C/C^*)_{\text{vibrations}}}{(C/C^*)_{\text{no vibrations}}}$$

where C^* = equilibrium concentration, and

C = conc. at the outlet.

At other frequencies the values of 'Q' were found to range from 2 to 2.5. On the basis of the visual observations, it seems that the increased interphase contact area, resulting from the wave formation, was not large enough to account for theobserved increase in the absorption rate. It seems that the increased absorption rate was mainly connected with the film turbulence caused by ultrasonic vibrations; evidently at 50 kcs. the film turbulence was also helped by cavitation.

Shirotuska and Honda (81) reported the effect of pulsations on CO_2absorption in the following two types of systems :-

1. A CO_2-air mixture in a wetted wall column with pulsed gas flow : the overall mass transfer coefficient was found to be increased with the intensity of pulsation.

2. Pure CO_2 absorption in a perforated-plate column with pulsed liquid flow : the overall capacity factor was found to be increased with the intensity of pulsation and a maximum was obtained at a specific pulsation intensity. They used pulsations of the order of 80-300 cycles/min. and amplitudes of 0.3-1.6 cm. Some empirical relations were also derived relating the effect of frequency and amplitude to the capacity factor.

Bretsznajder and Paβiuk (82) carried out experiments in a pulsed absorption column at room temperature. They pulsed the liquid (water) and the gas used was both pure CO_2 and CO_2 in admixture with air. The frequencies used were from low audible sound range at amplitudes of 0.9 mm. to 8.3 mm. Considerable intensification of absorption was reported. The absorption occurred at the free surface of water. Fresh water was supplied at the liquid surface and CO_2 solution was discharged at the bottom. On the basis of data obtained, a comparison factor 'I' was defined as,

$$I = \frac{k_L^* \cdot A^*}{k_L \cdot A} \qquad \ldots (7.34)$$

and was plotted against pulse frequency . Here,

k_L^* = mass transfer coefficient with vibrations, cm/sec.

A^* = interfacial area with vibrations, cm^2

The experiments showed that pulsation imparted to the liquid improved gas absorption at the liquid surface. The comparison factor 'I' was found to attain a maximum of 76. The maxima were thought to be related to a resonance phenomenon.

Mirev et.al. (83) studied the effect of sonic vibrations on absorption from bubbles for solutions of KOH and K_2CO_3. Gas was bubbled through a layer of liquid which was being agitated by a vibrating probe suspended in it. An intensification of mass transfer was observed. They also studied the absorption of the oxides of nitrogen under the same conditions and observed similar effects.

A very interesting study of the effect of sonic vibrations on gas absorption was carried out by Harbaum and Houghton (84). Houghton had previously carried out extensive work on the improvement of efficiencies of absorption in bubble-beds. Being led on from his results of the influence of ultrasonics in improving film boiling heat transfer, and noticing that a sound of audible frequency was emitted in film boiling, he thought that the influence of sonic frequency should be more pronounced than that of ultrasonics. Similar audible frequencies were observed to be emitted in bubble-beds during absorption, so these workers went forth to investigate the effect of sonics. They used a counter-current bubble-bed absorber in which the gas and liquid phases continuously entered and leftthe top of the column. The bottom

of the column was fitted with a polystyrene piston that could be vibrated electro-dynamically at frequencies in the range of 20-2,000 cycles per second. The amplitude of the piston vibrations was measured microscopically as a function of frequency. Comparison of absorption results showed that peaks in absorption did not correspond exclusively to peaks in amplitude, and hence could be attributed to resonance effects associated with frequency alone. The maximum increase in absorption was 70%. Vibrations were observed to increase the number of bubbles, thus increasing the interfacial area. The photographic measurement of the interfacial area was not very reliable, therefore it could not be concluded whether the increase in absorption was mainly due to the increase in interfacial area or due to a modified mechanics of bubble absorption. Their conclusions were as follows:

> "Although the effects of sound in mass transfer in beds of bubbles appear to result mainly from an increase in gas hold-up, some effects with single bubbles have been observed at higher frequencies in the range of 900-1100 c/s -- the sound causes the bubble boundary to break up giving the bubble a frothy appearance. By slight variations in the frequency, the frothy bubble could be held up, or moved up and down in the liquid. Eventually, the sound would cause the bubble to disintegrate into a number of smaller ones

which then rose to the liquid surface. Similar effects have been reported by Gibbon and Houghton (85) in boiling on a heated platinum wire under the influence of sonic vibrations. However, when a large number of bubbles were present in the liquid, frothy bubbles were not observed, presumably because the sonic power available was too small as a result of scattering effects. Since ultrasonic sources could provide greater power at high frequency, it might be possible to produce an increase both in the mass transfer coefficient and the interfacial area."

CHAPTER VIII.

ABSORPTION STUDIES INTO LIQUID FILMS FALLING OVER MECHANICALLY VIBRATED SURFACES

Art.8.1. - Apparatus and Measurements

Vibration studies described here were carried out in short wetted wall columns for reasons discussed in the last section. The absorption apparatus used was the same as was used in the previous studies except that the base of the wetted wall tube was connected to a 150W. moving-coil vibrator (Goodman's type 790). This was powered by a variable gain 120W. audio amplifier fed by a calibrated audio oscillator. The tube could be vibrated at sonic frequencies in the range of 15-2000 cycles/sec. The highest amplitude of vibration obtained in the set-up was 0.1800 cm. It could be varied at the same frequency by varying the power output from the amplifier. Vibrations given to the wetted wall were longitudinal, that is, in the plane of the liquid flow. The tube was held in a vertical position, both near its lower end and at the top end, between screw-triads. The tips of the screws were holding on lightly to the tube and were made from P.T.F.E. to reduce friction. The 'ermeto coupling' at the bottom of the liquid receiver (see Fig.2.25) was replaced by a rubber bellows.

Frequencies of vibration were given by the frequencies of pulses in the audio oscillator. Amplitudes were measured microscopically as a function of frequency. This was done by printing a hairline on the lower end of the tube, which, when vibrated, was seen as a band

through the cathetometer. The width of this band minus the diameter of the hairline gave the amplitude of vibration.

Art. 8.2. - Evaluation of Results

Absorption results with vibrations were obtained at two wetted wall heights of 18.0 cm. and 15.0 cm. The rates were calculated, as before, from Eq.(3.21). The value of the interfacial area was assumed to be the same as for a smooth film. Justification for this assumption has been discussed in Section 2.

The first investigation was carried out at a height of 18.0 cm. with a rippling water film in order to study its absorption behaviour as a function of vibration parameters. The height was increased to 18.0 cm. from 15.0 cm., the latter being the standard height used in the studies on roughnesses, in order to obtain a longer region of rippling. The liquid flow rates used were in the laminar region of flow ($Re < 1200$). Other studies were carried out at wetted heights of 15.0 cm., both at the laminar and turbulent liquid flows, and with and without the addition of surface active agent.

Results at Laminar Liquid Flows ($Re < 1200$)

(i) Pure Water.

The absorption results obtained on an 18.0 cm. height of a stationary wetted tube have previously been discussed (see Fig.3.22). It is seen that the absorption rates are considerably higher than the theoretical line of Eq.(3.210) because of interfacial mixing due to rippling. The application of vibrations was found to intensify this

mixing action, so that considerably higher absorption rates were obtained. As has been discussed in Section 2, the increase in interfacial area due to the distortion of the interface is not responsible for the increase in absorption. Increased absorption results only from increased interfacial turbulence. Therefore, any intensification of absorption rates due to vibrations will be considered as arising only because of an increased interfacial mixing, and the rate will be calculated on the basis of an unvibrated interfacial area. When the tube was vibrating, the liquid film appeared fuzzy when seen through the microscope.

It was found difficult to keep the amplitude constant and vary the frequency but the reverse was easy. From preliminary experiments it was found that the absorption rates suddenly shot up at certain frequencies. These frequencies were the resonance frequencies because the pitch of the sound emitted by the tube became more audible. The absorption results given in Table-8.21 are those for a constant frequency and a varying amplitude. The frequency of 35 c/s is non-resonating while 78 c/s is resonating. It is seen from the table that a variation in the amplitude in the range 0.0868-0.0463 cm. at the non-resonating frequency affects the absorption rate negligibly. The rate of absorption is relatively more sensitive to amplitude at the resonating frequency of 78 c/s. There is also a minimum amplitude where the rate of absorption is not affected by vibration (Fy. = 35, Am. = 0.0008).

Table 8.21

Temperature, ^{o}C = 25

Height of the wetted tube, cm. = 18.0
Diameter " " " " = 1.270

Liquid used = Pure water
γ_v, $cm.^2/sec.$ = 1.2730

Frequency (Fy.)	Amplitude (Am.) cm.	0.0956	0.0868	0.0832	0.0812	0.0758	0.0463	0.0125	0.0058	0.0008	0.0000
35 c/s.	$N_A \times 10^6$	19.88	19.12	19.36	19.18	19.16	18.70	17.88	17.52	13.05	13.02
Frequency (Fy.)	Amplitude (Am.) cm.	0.0938	0.0845	0.0732	0.0589	0.0424	0.0385	0.0267	0.0123	0.0075	0.0000
78 c/s.	$N_A \times 10^6$	26.16	26.20	26.66	23.80	22.40	21.64	20.76	18.98	17.62	13.02

The behaviour of absorption was studied next with both frequency and amplitude varying simultaneously at a constant flow rate. The results are contained in Table 8.22. The measured amplitudes are given along with the frequencies. The power output from the audio oscillator was kept constant and the frequency varied. The amplitude was found to decrease with an increase in the frequency for a constant power output. Two series of amplitudes (Am.(1) and Am.(2)) at different power putputs are given in the table for the first two flow rates. The amplitudes as well as the absorption rates have been plotted against frequencies in Fig.8.21. It is seen from the table that at small flow rates when the film is very thin ($r_v \leq 0.9570$), a frequency of 100 c/s is the highest to affect absorption rate. As the thickness of the film increases, absorption rates are seen to be affected up to 150 c/s.

Fig. 8.21(a,b) contain five plots of absorption against the vibration parameters at the five liquid flow rates used. Amplitude (Am.) versus Frequency (Fy.) has also been plotted along-with, shown by dotted curves. Am.(1) and Am.(2) are two series of amplitudes used at the first two flow rates. A maximum of about 90% increase in the absorption rate is observed. The variation in absorption with vibration follows irregular patterns. There are peaks in absorption at certain frequencies. However these peaks have no relation with the peaks in the amplitude. Also the peaks in absorption do not occur at the same frequency for each flow rate. This is explained by the fact

Table 8.22

Temperature, ^{o}C = 25
Height of the wetted tube, cm. = 18.0
Diameter " " " " " = 1.270
Liquid used = Pure water.

Γ_v = 0.6390		Γ_v = 0.9570		Γ_v = 1.273	
* Fy. : Am.	$N_A \times 10^6$	Fy. : Am.	$N_A \times 10^6$	Fy. : Am.	$N_A \times 10^6$
(1)		(1)		(1)	
0 : 0	14.52	0 : 0	14.99	0 : 0	13.02
50 : 0.0746	17.24	50 : 0.0746	18.79	20 : 0.1791	15.70
52 : 0.0583	18.32	55 : 0.0432	21.68	25 : 0.1620	18.08
54 : 0.0436	18.39	58 : 0.0403	23.23	30 : 0.1530	18.33
55 : 0.0432	18.85	60 : 0.0482	23.18	35 : 0.1180	18.48
56 : 0.0432	18.82	70 : 0.0234	19.86	37 : 0.0964	18.18
58 : 0.0403	18.30	78 : 0.0182	19.22	40 : 0.0812	18.17
60 : 0.0482	18.32	80 : 0.0112	18.70	45 : 0.0823	18.14
62 : 0.0412	17.59	90 : 0.0063	17.11	50 : 0.0746	19.13
64 : 0.0382	17.34	100 : 0.0031	15.34	52 : 0.0583	20.45
70 : 0.0234	16.09	(2)		55 : 0.0432	21.30
78 : 0.0182	15.40	15 : 0.1362	18.06	60 : 0.0482	21.55
80 : 0.0112	15.00	20 : 0.1162	17.99	62 : 0.0462	21.86
85 : 0.0093	14.53	25 : 0.1032	17.99	66 : 0.0386	23.23
90 : 0.0063	14.50	30 : 0.0983	19.46	70 : 0.0234	23.90
(2)		35 : 0.0821	19.94	72 : 0.0162	24.14
15 : 0.1362	17.13	40 : 0.0736	19.48	75 : 0.0172	24.42
18 : 0.1281	16.14	45 : 0.0686	18.84	78 : 0.0184	24.83
20 : 0.1162	16.46	50 : 0.0621	17.85	80 : 0.0113	23.15
25 : 0.1032	17.72	52 : 0.0432	19.18	90 : 0.0063	18.28
30 : 0.0983	17.13	55 : 0.0316	20.22	100 : 0.0031	15.18
35 : 0.0821	16.84	60 : 0.0313	20.40	150 : 0.0019	13.82
40 : 0.0736	17.26	65 : 0.0213	19.87	200 : 0.0008	13.06
50 : 0.0621	16.33	70 : 0.0185	17.85		
55 : 0.0316	17.90	80 : 0.0091	17.44		
56 : 0.0303	18.23	90 : 0.0021	16.52		
57 : 0.0307	17.90	100 : 0.0013	14.91		
60 : 0.0313	17.84				
70 : 0.0185	15.02				
80 : 0.0091	14.84				
90 : 0.0021	14.51				
100 : 0.0013	14.56				

* Fy. = Frequency, c/s.
Am. = Amplitude, cm.

Table 8.22 - contd.

Γ_v = 1.587		Γ_v = 1.892	
Fy. : Am.	$N_A \times 10^6$	Fy. : Am.	$N_A \times 10^6$
(2)		(2)	
0 : 0	13.16	0 : 0	13.70
15 : 0.1362	18.85	15 : 0.1362	17.70
17 : 0.1290	15.85	20 : 0.1162	15.09
20 : 0.1162	15.75	25 : 0.1032	18.06
22 : 0.1158	15.83	30 : 0.0983	16.75
23 : 0.1152	15.84	35 : 0.0821	16.89
24 : 0.1058	17.58	40 : 0.0736	17.56
25 : 0.1032	18.75	45 : 0.0686	18.47
26 : 0.1018	18.94	50 : 0.0621	18.95
28 : 0.0987	18.12	55 : 0.0316	17.42
30 : 0.0983	17.30	60 : 0.0313	17.06
35 : 0.0821	16.52	66 : 0.0201	17.45
40 : 0.0736	17.88	68 : 0.0198	17.70
42 : 0.0712	18.91	70 : 0.0185	17.70
45 : 0.0686	19.76	75 : 0.0126	16.28
46 : 0.0643	20.13	80 : 0.0091	15.76
48 : 0.0628	19.76	85 : 0.0036	15.74
50 : 0.0621	19.56	90 : 0.0021	16.11
52 : 0.0432	17.93	100 : 0.0015	15.52
60 : 0.0313	19.08	120 : 0.0013	14.67
65 : 0.0213	20.50	150 : 0.0011	13.78
68 : 0.0198	20.70		
70 : 0.0185	21.25		
75 : 0.0126	21.22		
78 : 0.0108	20.77		
80 : 0.0091	20.21		
85 : 0.0036	17.13		
90 : 0.0021	16.52		
100 : 0.0015	14.15		
120 : 0.0013	13.76		
150 : 0.0011	13.64		

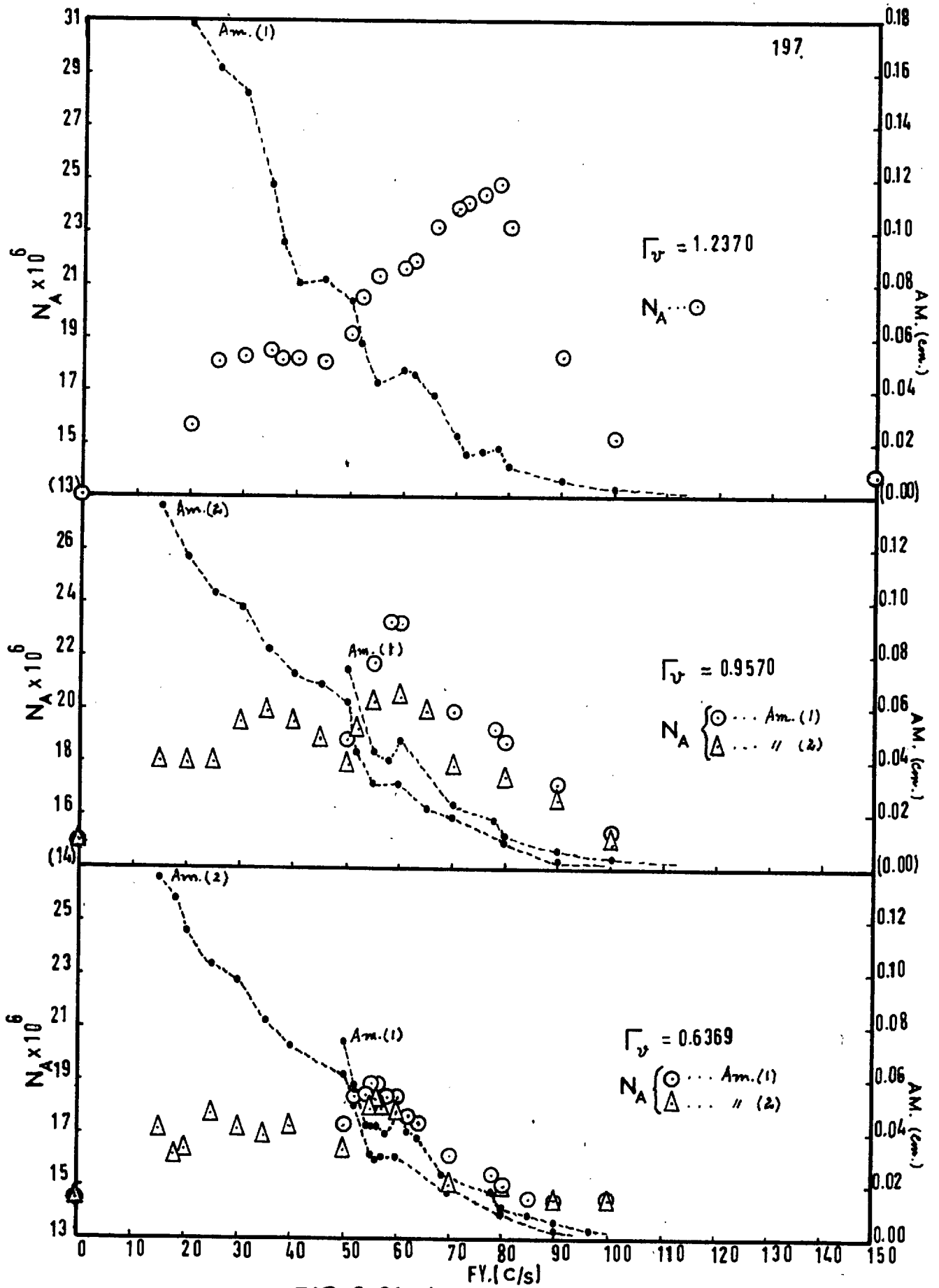
197
Am.(1)
Γ_v = 1.2370
N_A ··· ⊙
(13)
Am.(2)
Am.(1)
Γ_v = 0.9570
N_A ⊙ ··· Am.(1)
△ ··· // (2)
(14)
Am.(2)
Am.(1)
Γ_v = 0.6369
N_A ⊙ ··· Am.(1)
△ ··· // (2)
$N_A \times 10^6$
AM.(cm.)
FY.[C/s]
0 10 20 30 40 50 60 70 80 90 100 110 120 130 140 150

FIG. 8.21(a)

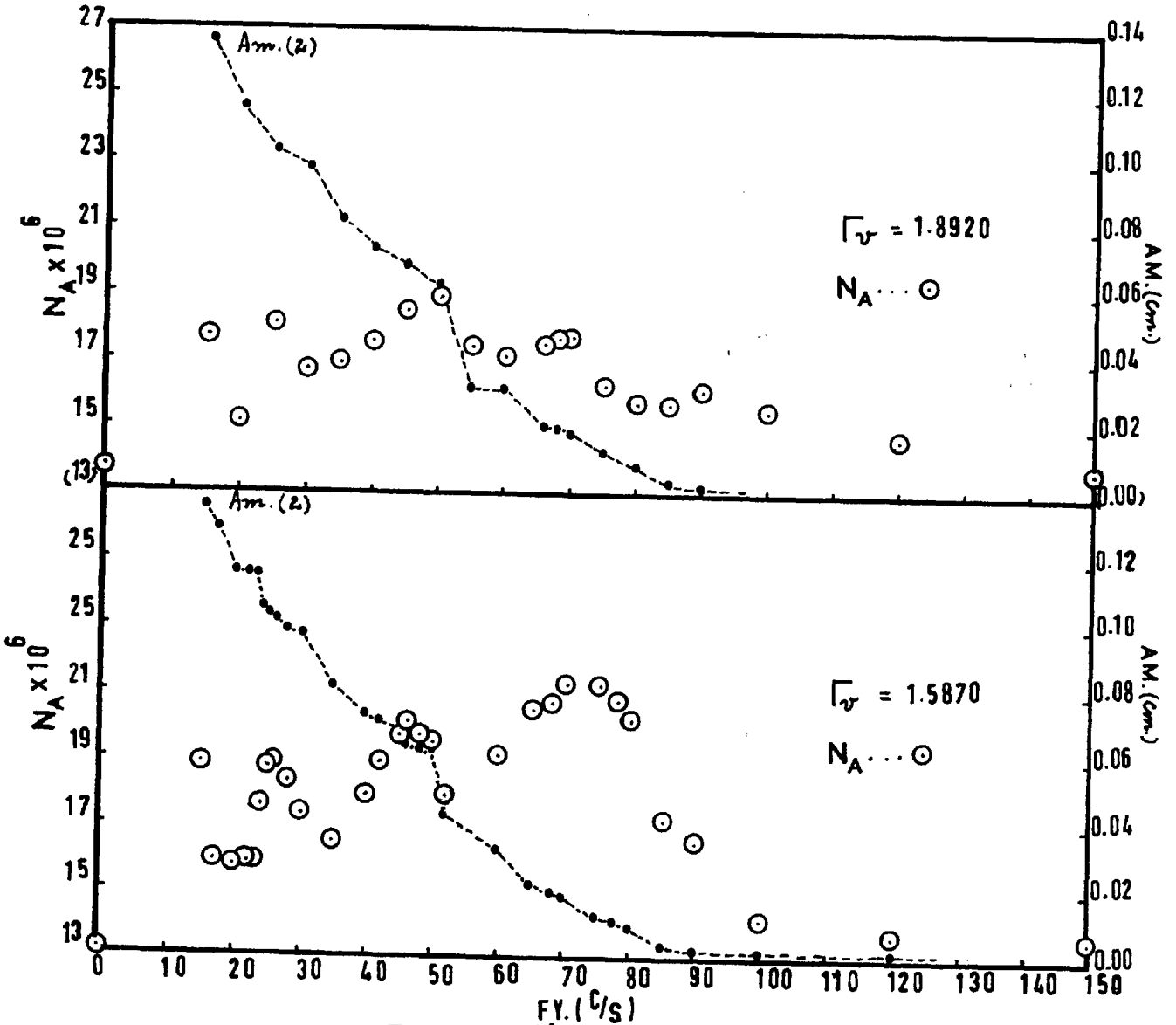
Am.(z)
Γ_v = 1.8920
N_A ··· ⊙
$N_A \times 10^6$
AM.(cm.)
Am.(z)
Γ_v = 1.5870
N_A ··· ⊙
$N_A \times 10^6$
AM.(cm.)
FY.(C/S)

FIG. 8.21(b)

that the liquid film has a different hydro-dynamic stability at each flow rate of liquid. The thickness of the film as well as the height of the region of rippling varies with the flow rate, therefore, the same amount of vibrational disturbance is expected to cause varying degree of interfacial turbulence. Another reason for the unsystematic nature of these results can be their poor reproducibility. It has been pointed out in Section 1 that the absorption results obtained on rippling films are not very reproducible. The variation was found to be as high as 7%.

The following conclusions can be drawn from the above investigation.

1. Absorption can be greatly intensified by applying vibrations to the wall for rippling falling liquid films.
2. The peaks in absorption are independent of the peaks in amplitude.
3. The most suitable frequencies, for intensifying absorption, range from 40 to 80 c/s.

Varying liquid flow: The above investigation was concerned with varying vibration at a constant liquid flow rate. The studies to be described now investigate the behaviour of absorption with a varying liquid flow rate at constant vibration. In the previous study it was found that frequencies of 40-80 c/s were the most suitable for intensifying absorption. Therefore absorption rates were obtained at frequencies of 40, 50, 60, 70 and 80 c/s by varying the liquid flow rates

between 0.3162 and 2.8460 $cm.^2/sec.$ at each. The results are given in Table-8.23. Absorption rates without vibration are also given alongside for comparison. The height of the wetted wall tube used in this case was 15.0 cm.

Table-8.23

Temperature, ^oC = 25
Height of the wetted tube, cm. = 15.0
Diameter " " " " " = 1.270
Liquid used = Pure water.

	Fy.=0 Am.=0	Fy.=40 Am.=0.0290	Fy.=50 Am.=0.0225	Fy.=60 Am.=0.0095	Fy.=70 Am.=0.0041	Fy.=80 Am.=0.0015
Γ_v	$N_A x10^6$	$N_A x10^6$	$N_A x10^6$	$N_A x10^6$	$N_A x10^6$	$N_A x10^6$
0.3200	10.66	15.58	15.52	14.43	13.17	12.42
0.6390	12.86	21.60	20.71	22.32	21.80	20.78
0.9570	13.78	24.16	23.92	25.31	25.07	25.20
1.2370	14.42	25.46	24.64	25.22	26.18	26.48
1.5870	14.81	25.62	26.16	25.75	25.80	27.53
1.8920	15.18	25.95	26.21	26.37	26.00	26.70
2.2200	15.74	26.96	27.20	27.97	26.40	27.06
2.5300	16.50	26.84	26.90	27.30	27.05	27.30
2.8460	16.98	27.98	27.32	27.50	27.62	27.85

From Fig.3.23, where the absorption results without vibration are plotted, it is seen that there is no agreement of the experimental points with the theoretical Eq.(3.210). It is, therefore, pointless to compare the results of vibrations with the theory. The results in Table 8.23 have been plotted in Fig.8.22. The scatter of points for vibrations is so small that a single curve can be drawn through them.

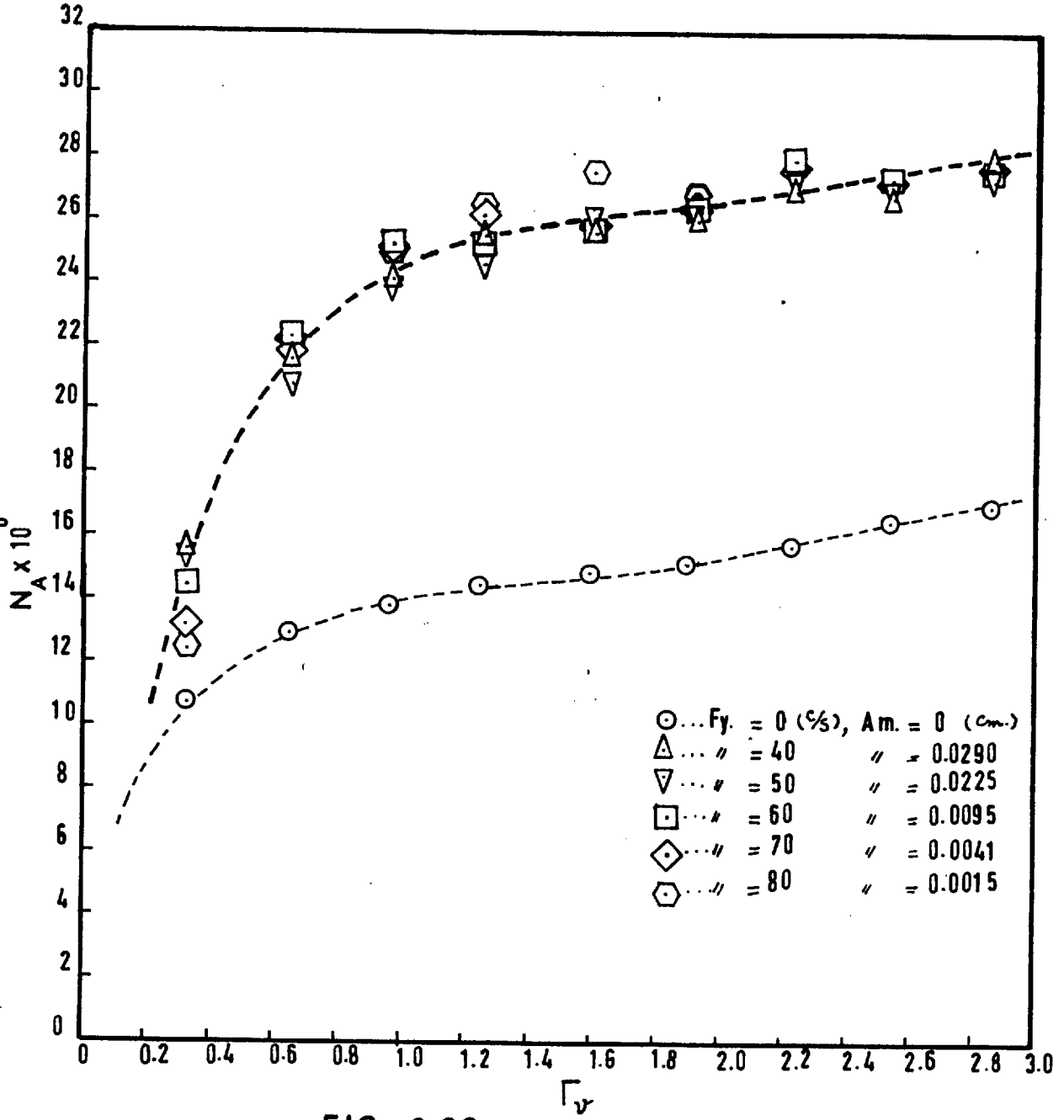
$N_A \times 10^6$
32
30
28
26
24
22
20
18
16
14
12
10
8
6
4
2
0
0
0.2
0.4
0.6
0.8
1.0
1.2
1.4
1.6
1.8
2.0
2.2
2.4
2.6
2.8
3.0
Γ_v
⊙... Fy. = 0 (%), Am. = 0 (cm.)
△... // = 40 // = 0.0290
▽... // = 50 // = 0.0225
□... // = 60 // = 0.0095
◇... // = 70 // = 0.0041
⬡... // = 80 // = 0.0015

FIG. 8.22

Dotted curves have been drawn through both the results, with and without vibration. It is seen that at small liquid flow rates ($\Gamma_v \ll 1.000$), the curve for vibrations tends to converge towards the curve for no vibrations. This is just to be expected because when the film is very thin its hydro-dynamic stability is high due to the influence of the wall. The thinner it becomes, the less prone it is to vibrational disturbance until at a certain limiting thickness the effect of vibrations becomes negligible. The point where the two curves seem to meet each other is a very small flow rate where the liquid film is reported to become ripple-free and truly laminar in nature.

When the flow rate of liquid is more than 1.0 $cm.^2/sec.$, the two curves in Fig.8.22 become almost parallel to each other. This indicates that the degree of intensification of absorption with vibration is almost constant. In other words it means that $\frac{N_A(\text{Vibration})}{N_A}$ is a constant, being independent of the flow rate ($\Gamma_v > 1.00$) for the intensities of vibrations studied. The average value of this constant is estimated from the curves as 1.73. Therefore, '$N_A(\text{Vib})/N_A = 1.73$' can be used to predict absorption rates approximately for rippling falling liquid films for liquid flow rates, such that, $450 \leqslant Re \leqslant 1200$.

(ii) Water Containing SAM.

The absorption results for a stationary surface, with water containing surface active material, have been discussed in Chapter III.

Fig.3.23 contains the results for a wetted wall height of 15.0 cm., which agree very satisfactorily with the theoretical line for Eq.(3.210). For the studies of absorption with vibration, which are to be described now, the same wetted wall height was used. It was found that the application of vibrations to the film, when surface active material was present in water to eliminate rippling, affected the rates of absorption very little.

Table 8.24 contains the absorption results obtained with the use of SAM. The results without vibration are also given alongside. As these results follow the line of the theoretical equation mentioned above, the results for vibration have also been plotted in Fig.8.23 for a comparison with this theoretical line. Table 8.24, therefore, contains both 'N_A' and its reciprocal. The values of '$1/[\nu]^{1/3} \cdot (h_e)^{-1/2}$' were taken from Table-3.23. The plots show that the absorption results for frequencies 40 and 50, which have relatively large amplitudes, seem to lie around line 'A'. The results for frequencies 60, 70, and 80, which have small amplitudes, lie around line 'B'. Both lines 'A' and 'B' are parallel to the theoretical line. As seen from Eq.(3.27), both lines 'A' and 'B' can be represented by the theoretical equation if suitable values for the term '$1/k_i$' are assumed.

Table-8.24

Temperature, ^{o}C = 25

Height of the wetted tube, cm. = 15.0
Diameter " " " " " = 1.270

Liquid used = water containing SAM, (0.01% Lissapol).

Γ_v	Fy.= 0 Am.= 0		Fy. = 40 Am. = 0.0290		Fy. = 50 Am. = 0.0225	
	$N_A x10^6$	$1/N_A x10^{-4}$	$N_A x10^6$	$1/N_A x10^{-4}$	$N_A x10^6$	$1/N_A x10^{-4}$
0.3200	9.09	11.00	9.96	10.04	10.09	9.91
0.6390	10.90	9.17	11.39	8.78	11.41	8.76
0.9570	12.40	8.07	12.96	7.72	13.00	7.69
1.2370	13.55	7.38	14.26	7.01	14.31	6.99
1.5870	14.33	6.97	14.99	6.67	14.79	6.76
1.8920	14.92	6.70	16.12	6.21	15.72	6.36
2.2200	15.53	6.44	17.16	5.83	16.80	5.95
2.5300	16.30	6.13	17.80	5.62	17.46	5.73
2.8460	16.98	5.89	18.90	5.29	18.56	5.39

(Table 8.24 - contd.).

Fy. = 60 Am. = 0.0095		Fy. = 70 Am. = 0.0041		Fy. = 80 Am. = 0.0015	
$N_A x10^6$	$1/N_A x10^{-4}$	$N_A x10^6$	$1/N_A x10^{-4}$	$N_A x10^6$	$1/N_A x10^{-4}$
9.31	10.74	9.36	10.68	9.32	10.73
11.24	8.90	11.12	8.99	11.14	8.98
12.72	7.86	12.58	7.95	12.63	7.92
13.92	7.18	13.93	7.18	13.96	7.16
14.59	6.85	14.49	6.90	14.54	6.88
15.16	6.60	15.25	6.560	15.13	6.61
15.92	6.28	15.86	6.30	15.74	6.36
16.78	5.96	16.65	6.01	16.62	6.01
17.48	5.72	17.20	5.81	17.18	5.82

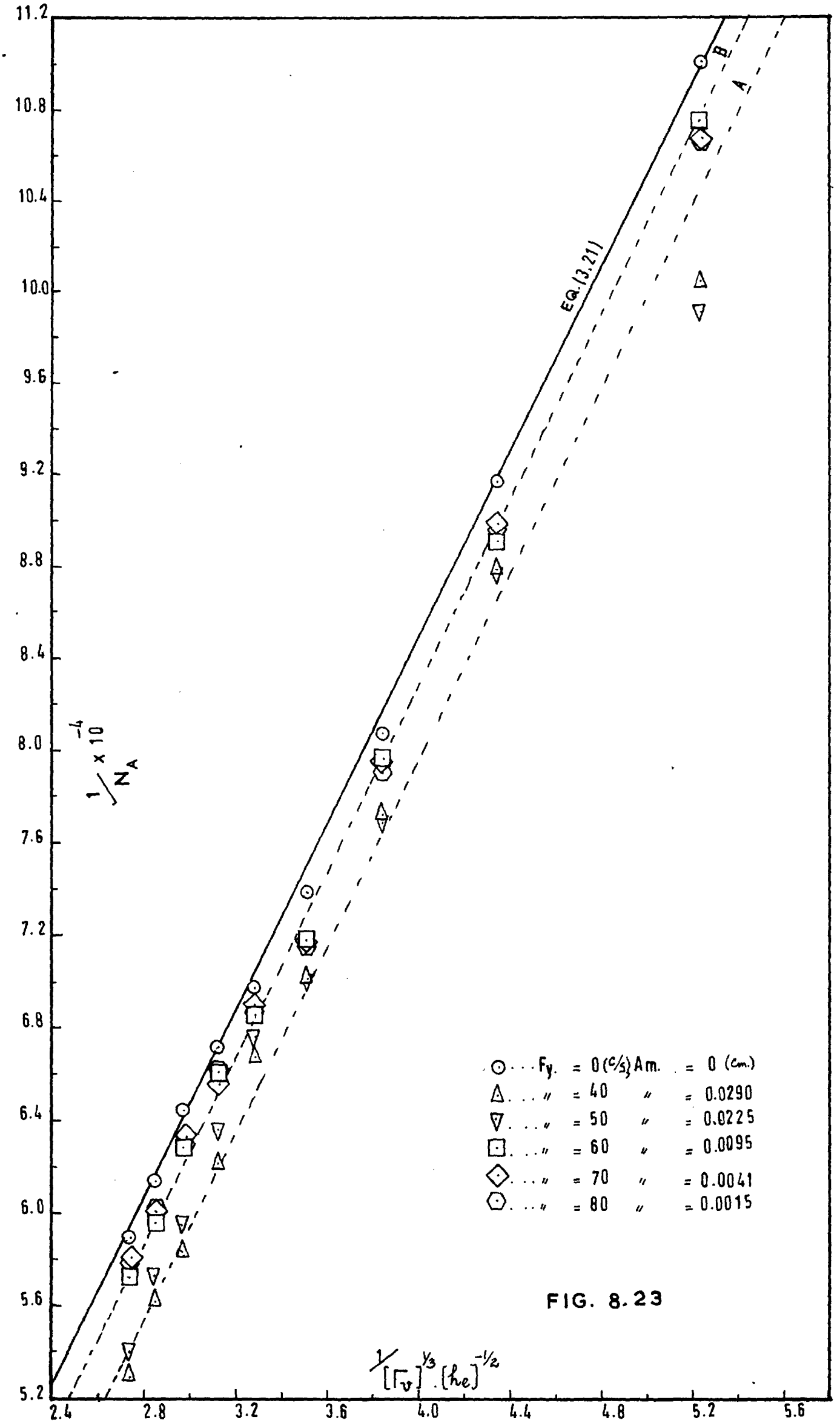
11.2
10.8
10.4
10.0
9.6
9.2
8.8
8.4
8.0
7.6
7.2
6.8
6.4
6.0
5.6
5.2
$\frac{1}{N_A} \times 10^{-4}$
2.4
2.8
3.2
3.6
4.0
4.4
4.8
5.2
5.6
$\frac{1}{[\Gamma_v]^{1/3}.[he]^{-1/2}}$
EQ.(3.21)
B
A
⊙ . . . Fy. = 0 (c/s) Am. = 0 (cm.)
△ . . . " = 40 " = 0.0290
▽ . . . " = 50 " = 0.0225
□ . . . " = 60 " = 0.0095
◇ . . . " = 70 " = 0.0041
⬡ . . . " = 80 " = 0.0015

FIG. 8.23

Thus, the equation of line 'A' can be given as,

$$1/N_A = \frac{1}{C^*} \left\{ 1/k_L + 0 \right\}$$

$$= 1/C^* k_L \qquad \ldots (8.21)$$

and for line 'B',

$$1/N_A = \frac{1}{C^*} \left\{ 1/k_L + \frac{1}{2.1} \right\}$$

$$= \frac{1}{C^*} \left\{ 1/k_L + 0.476 \right\} \qquad \ldots (8.22)$$

It should not be understood from the derivation of the above equations that the application of vibrations affects the magnitude of interfacial resistance. The value of the interfacial resistance has been chosen arbitrarily to fit the results. The two sets of results obtained at the two vibration intensities indicate that there is a critical amplitude above and below which the two respective Eqs.8.21 and 8.22 hold, and that the frequency has no influence. The critical amplitude should lie between 0.0225-0.0095 cm.

Results at Turbulent Liquid Flows (Re $\geq$ 1200).

When turbulent liquid flow rates were used, the gas was seen to be trapped in the liquid receiver as vibrations were applied. This was similar to the entrainment of gas observed in studies on rough surfaces. Blank experiments were performed to estimate the error due to trapping on air-water system, with the water saturated with air. Corrections were found to be a maximum of 3.5%, and were applied at corresponding flow rates and vibrations.

The absorption results discussed in the previous sections indicate no influence of the presence of surface active material on absorption in the turbulent region of liquid flow. In the application of vibrations, however, it was observed that the absorption results were considerably lowered when the surface active material was present. The presence of SAM seemed to make the film more tenacious so that the vibrational mixing was considerably reduced. This observation is similar to those reported in literature on the influence of surface active materials on the hydro-dynamics of liquid systems. Thus the presence of SAM has been found to suppress the internal circulation in drops such that they behave like solid spheres.

The increase in absorption with the application of vibrations was found to be as high as 99%. The higher was the flow rate of liquid, the higher was the percentage increase. This is because when the film becomes thicker with the increase in flow rate, its hydrodynamic stability decreases resulting in greater vibrational mixing. The results were obtained by varying the flow rate at a constant vibration. The vibrations used were the same as were used at laminar flows (40-80 c/s). The absorption results, for both pure water and water containing SAM, are given in Table-8.25. It is seen from the table that the percentage intensification of absorption increases with the increase in flow rate. The results without vibration are also given alongside for comparison. In calculating the absorption rates the interfacial surface has been assumed as smooth. This assumption has been justified previously. The increase in absorption due to vibrations is attributed only to intensified turbulence.

Table 8.25

Temperature, ^{o}C = 25

Height of the wetted wall tube, cm. = 15.0
Diameter " " " " " " = 1.270

f_v	Fy.=0 Am.=0	Fy. = 40 Am. = 0.0290		Fy. = 50 Am. = 0.0290		Fy. = 60 Am. = 0.0095	
	*P.W.	P.W.	SAM	P.W.	SAM	P.W.	SAM
	$N_A' \times 10^6$	$N_A' \times 10^6$	$N_A' \times 10^6$	$N_A' \times 10^6$	$N_A' \times 10^6$	$N_A' \times 10^6$	$N_A' \times 10^6$
3.240	17.52	28.60	19.95	28.70	18.56	27.66	17.90
4.420	18.87	29.64	26.80	29.50	24.63	29.36	22.45
5.570	20.24	31.30	29.42	32.10	27.52	32.44	24.16
6.824	21.47	37.60	34.00	35.90	32.64	34.96	29.64
8.058	22.35	41.50	41.08	38.35	38.24	37.20	33.95
9.600	24.11	48.20	48.20	47.67	47.65	47.28	44.55

* P.W. = Pure water.

SAM = Water containing surface active material (Lissapol 0.01%).

(Table 8.25 - contd.).

Fy. = 70 Am. = 0.0041		Fy. = 80 Am. = 0.0015	
P.W. $N_A \times 10^6$	SAM $N'_A \times 10^6$	P.W. $N'_A \times 10^6$	SAM $N'_A \times 10^6$
28.80	17.80	27.67	17.78
29.23	19.87	29.70	19.40
32.10	22.82	32.19	21.70
33.80	24.48	33.36	23.98
37.24	29.40	35.80	28.20
44.25	38.10	42.60	31.90

The results were first compared with Eq.(4.33). This was done similarly as for rough surfaces (discussed in the last section). $10\left[1/\Gamma_v\right]^{1/3}$ has been plotted against $1/N_A' \times 10^{-4}$ in Fig.8.24 for pure water as well as water containing SAM at two representative vibrations. The parameters of these plots are given in Table 8.26. It appears from the curves obtained that the experimental results bear no semblance to the line of Eq.(4.33). The value of 'M' is therefore not constant and may be a complicated function of many variables. The dotted curves have been drawn through the experimental points for vibration to show the trend of results.

Table-8.26

$10\left[1/\Gamma_v\right]^{1/3}$	Fy. = 40 Am. = 0.0290		Fy. = 60 Am. = 0.0095	
	P.W. $1/N_A' \times 10^{-4}$	SAM $1/N_A' \times 10^{-4}$	P.W. $1/N_A' \times 10^{-4}$	SAM $1/N_A' \times 10^{-4}$
6.75	3.496	5.015	3.615	5.590
6.09	3.374	3.730	3.405	4.450
5.64	3.195	3.400	3.084	4.140
5.27	2.660	2.940	2.860	3.375
4.99	2.410	2.435	2.690	2.945
4.71	2.075	2.075	2.115	2.244

In order to discuss the results for vibration, the absorption rates in Table-8.25 have been plotted against the liquid flow rate. These are plotted separately for each vibration in Fig.8.25a, b, c, d, and e, to avoid confusion due to overlapping of results.

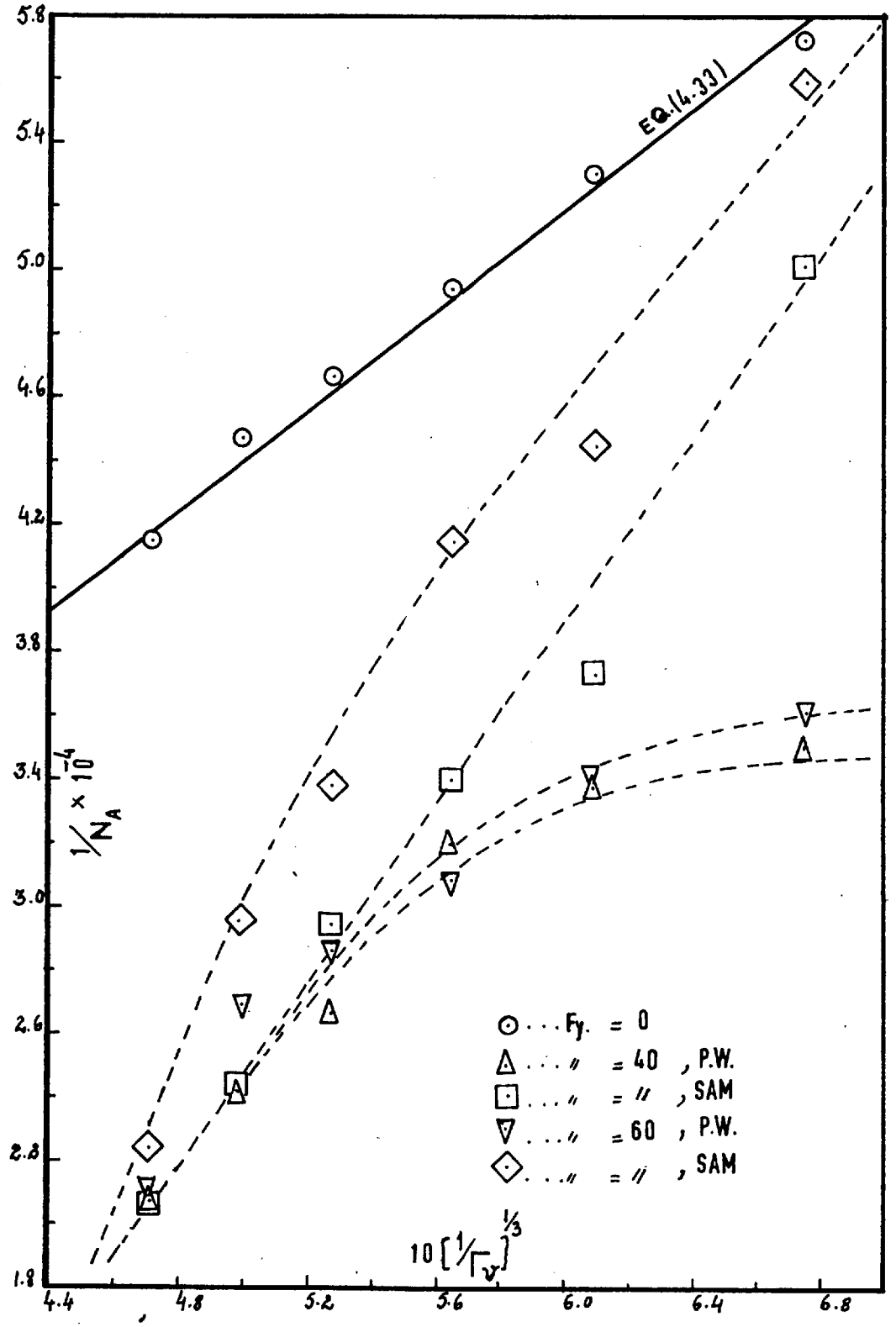
EQ.(4.33)
$10^{4} \times 1/N_A$
$10\left[1/\Gamma_v\right]^{1/3}$
5.8
5.4
5.0
4.6
4.2
3.8
3.4
3.0
2.6
2.8
1.8
4.4
4.8
5.2
5.6
6.0
6.4
6.8
⊙ . . . Fy. = 0
△ . . . // = 40 , P.W.
□ . . . // = // , SAM
▽ . . . // = 60 , P.W.
◇ . . . // = // , SAM

FIG. 8.24

The results without vibration are also plotted alongside. Dotted lines indicate the pattern of variation. The following points are illustrated from these plots:

1. When these results are compared with the results of vibration in the laminar region (see Figs.8.22 and 8.23 for pure water and SAH respectively) it is seen that the absorption curves start becoming steeper as soon as they enter the turbulent region. The critical value of liquid flow rate has been taken as Re = 1200. This indicates that the rate of intensification of absorption in the turbulent region is much higher than it is in the laminar region.

2. The curves for pure water are almost similar in slopes and positions for all the vibrations. These curves start in these graphs at values of abscissa where the curve in Fig.8.22 has left off. Therefore these can be regarded as extensions of the curve from the laminar region. The fact that these curves are identical, is in agreement with the observations in the laminar region. However the value of $\frac{N_A\ (Vib.)}{N_A}$ is not constant but increases with the flow rate.

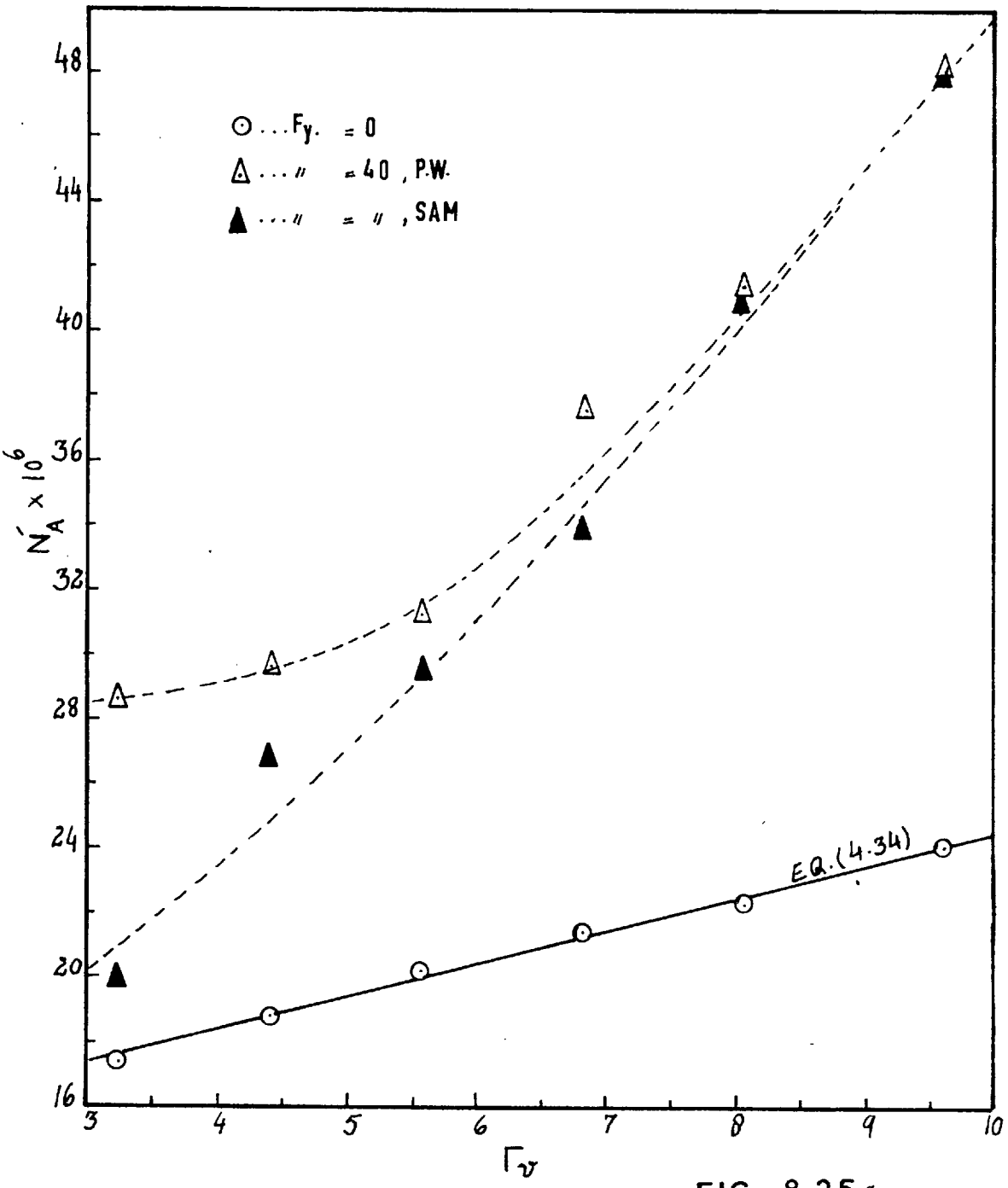
48
44
40
36
32
28
24
20
16
3
4
5
6
7
8
9
10
$N_A' \times 10^6$
Γ_v
⊙ ... F_y. = 0
△ ... // = 40 , P.W.
▲ ... // = // , SAM
EQ.(4.34)

FIG. 8.25 a

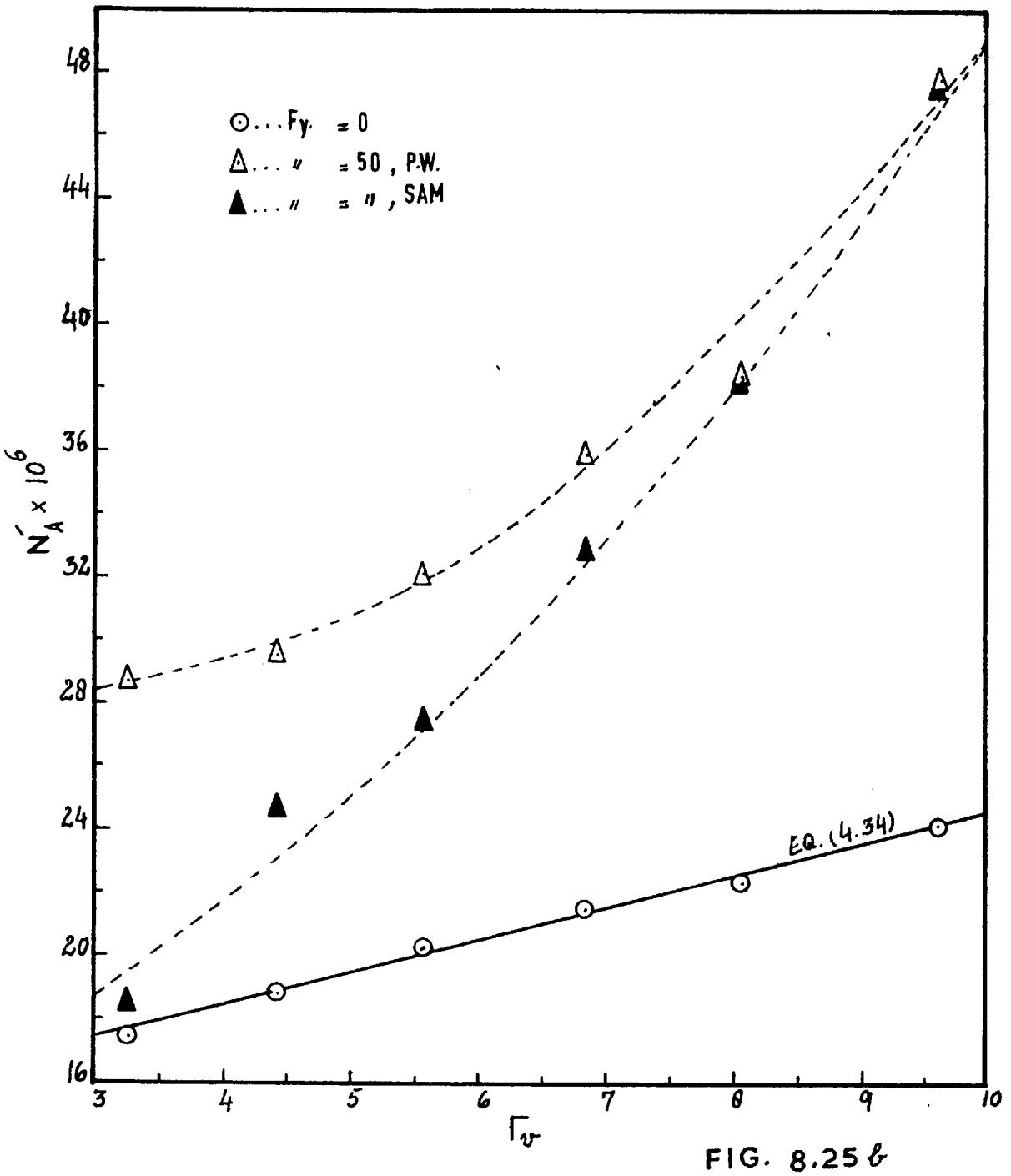
⊙... Fy = 0
△... " = 50 , P.W.
▲... " = " , SAM
EQ. (4.34)
$N_A' \times 10^6$
Γ_v
48
44
40
36
32
28
24
20
16
3
4
5
6
7
8
9
10

FIG. 8.25 b

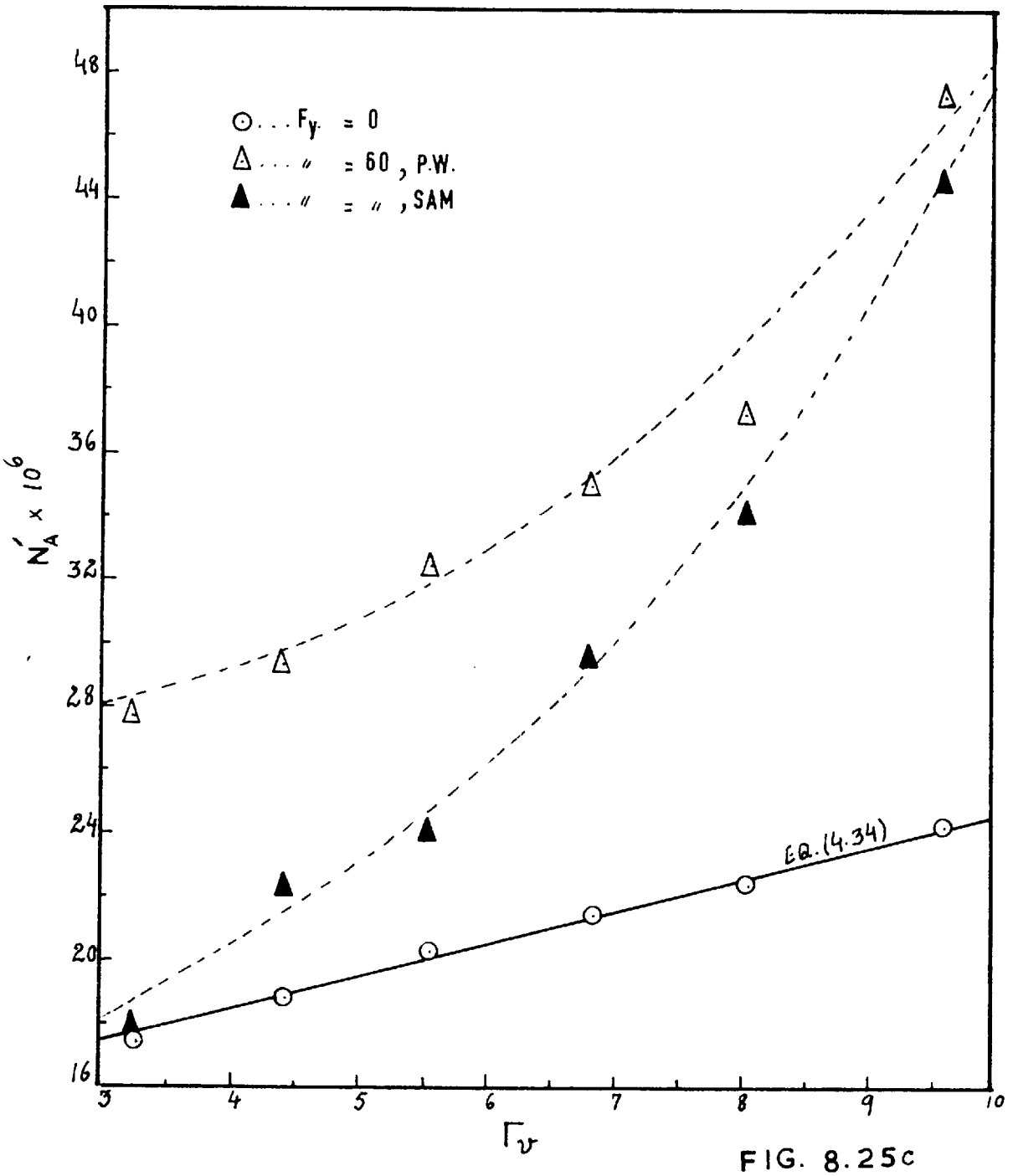
⊙ . . . F_y = 0
△ . . . " = 60 , P.W.
▲ . . . " = " , SAM
$N'_A \times 10^6$
48
44
40
36
32
28
24
20
16
3
4
5
6
7
8
9
10
Γ_v
EQ.(4.34)

FIG. 8.25c

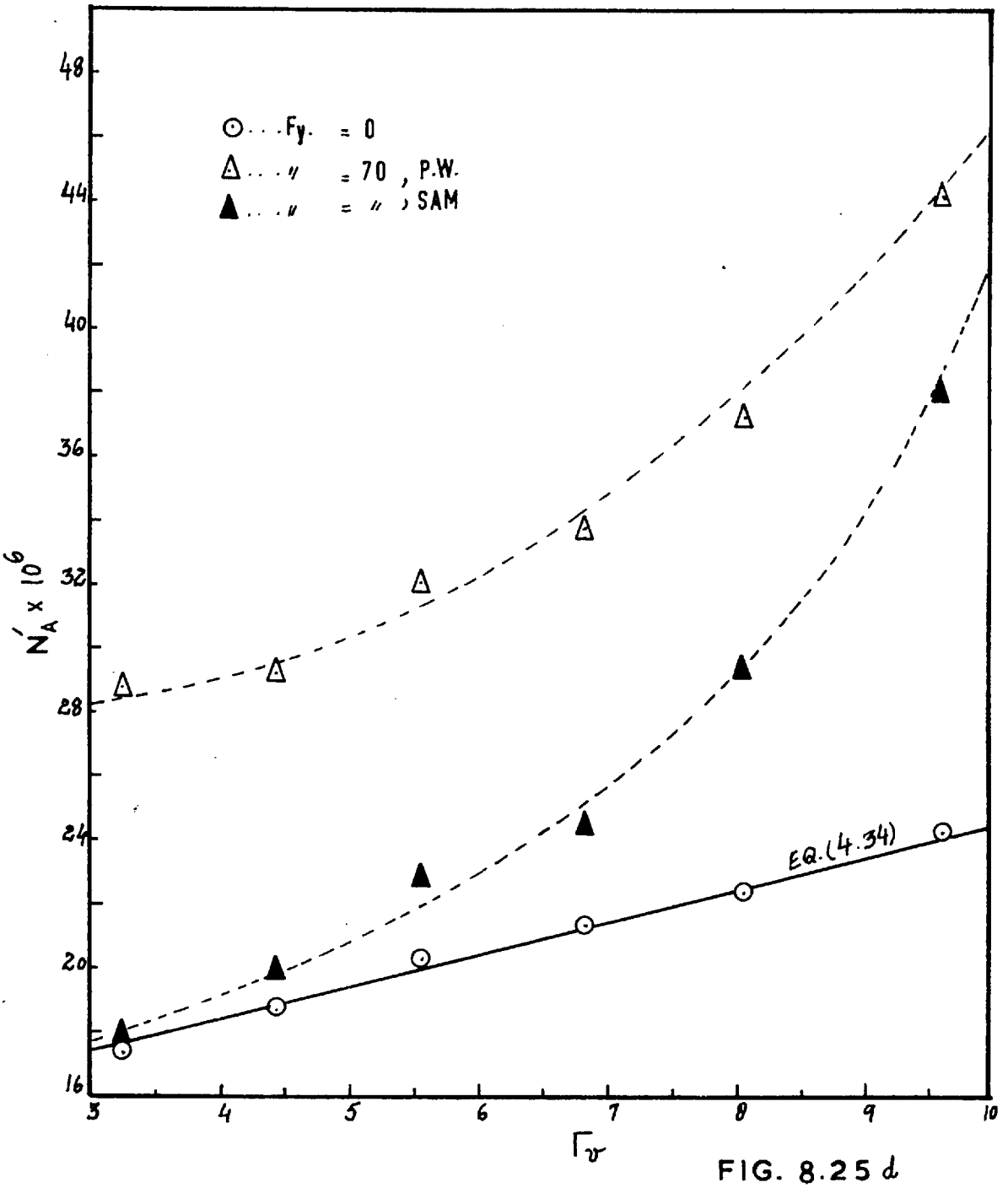
⊙ . . . Fy. = 0
△ . . . " = 70 , P.W.
▲ . . . " = " , SAM
EQ.(4.34)
$N'_A \times 10^6$
Γ_v
48
44
40
36
32
28
24
20
16
3
4
5
6
7
8
9
10

FIG. 8.25 d

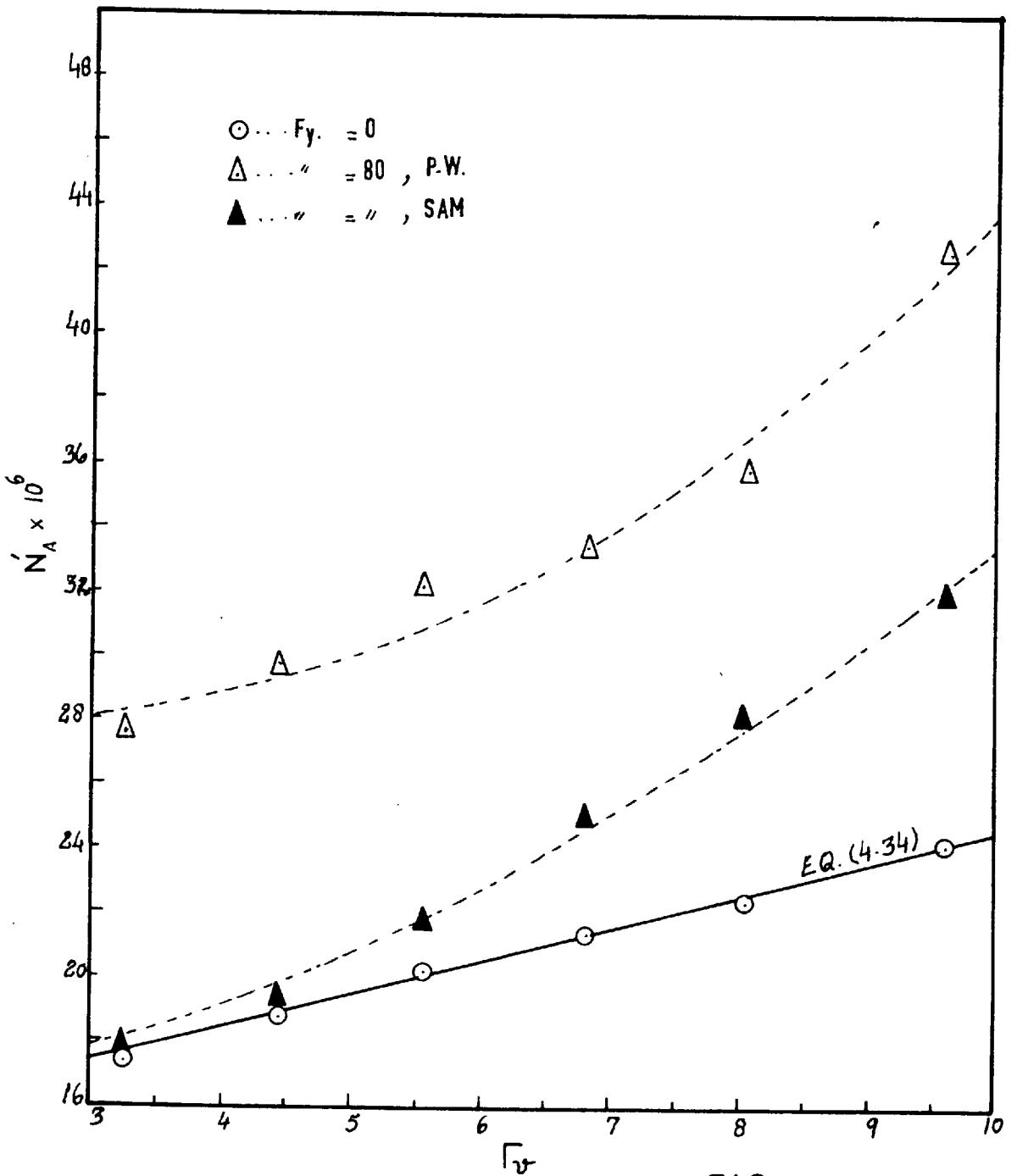
⊙ . . . Fy. = 0
△ . . . " = 80 , P.W.
▲ . . . " = " , SAM
EQ. (4.34)
$N'_A \times 10^6$
Γ_v
48
44
40
36
32
28
24
20
16
3
4
5
6
7
8
9
10

FIG. 8.25e

3. The curves for the surface active material can similarly be regarded as extensions of the curves from the laminar region. The slope of the curves in this case also increases very steeply in this region of flow. At high liquid flow rates in the turbulent region the curves for SAM tend to converge towards the curves for pure water. This is because the film becomes so thick that its hydrodynamic stability is little affected by the presence of SAM. The intensity of vibrational turbulence, therefore, approaches that of pure water.

SYMBOLS AND NOTATIONS

A, Area of the liquid surface, $cm.^2$

Am., Amplitude of vibration, cm.

A_{xy}, Area under the curves in Fig.4.22, $cm.^2$

C, Local concentration of the solute in the liquid, $gm/cm.^3$

c, Constant in Eq.(7.23).

C*, Concentration of the solute in the liquid in equillibrium with the gas, $gm/cm.^3$

C_o, Initial concentration of the solute in the liquid, $gm/cm.^3$

C_i, Concentration of the solute in the liquid at the interface, $gm/cm.^3$

C_p, Heat capacity, (B.T.U.)/(lb.)(F^o).

D, Coefficient of diffusion in the liquid phase, $cm.^2/sec.$

D, Hydraulic diameter of the pipe (Art.5.1), cm.

e, Height of the roughness elements, cm.

f, Fanning friction factor (dimensionless).

f_o, Eddy renewal rate without pulsation, $sec.^{-1}$

$f_{av.}$, Average frequency of surface renewal, $sec.^{-1}$

f_p, Pulse frequency, $sec.^{-1}$

Fy., Frequency of vibration, $sec.^{-1}$

g, Acceleration due to gravity, 981 $cm/sec.^2$

h, Height of the wetted wall column, cm.

h_e, Height of the wetted wall column effective in absorption, cm.

h_o, h_p, Heat transfer coefficients with/without pulsation respectively, (B.T.U.)/(Hr.)(Ft.)^2(F^o).

h_r, Height of the stagnant-end effect in a wetted wall column, cm.

H, Height of the wetted tube on the photographs (h x magnification ratio), cm.

I, Comparison factor (dimensionless).

J, Dimensionless factor.

k, Thermal conductivity, (B.T.U.)/(Hr.)(Ft.)(F^o).

k_G, Gas film mass transfer coefficient, cm/sec.

k_G^*(vib), Mass transfer coefficient with vibrations, cm/sec.

k_i, k_s, Mass transfer coefficients lost due to interfacial resistance, cm/sec.

k_L, Liquid film mass transfer coefficient, cm/sec.

$(k_L)_{l.m.}$, Liquid phase mass transfer coefficient based on a log-mean concentration driving force, cm/sec.

K_F, Film number defined in Eq.(1.31).

K_G, Overall mass transfer coefficient based on a partial pressure driving force, cm/sec.

K_L, Overall mass transfer coefficient based on a concentration driving force, cm/sec.

M, Mixing coefficient, $cm.^2$/sec.

N, Local rate of mass transfer, gm/sec.

N_A, Rate of mass transfer per unit area, gm/$cm.^2$sec.

N_A', Mass transfer rate per unit area at turbulent flow of the liquid film given by Eq.(4.33), gm/$cm.^2$sec.

N_{Ac}, Mass transfer rate at the critical point of transition to turbulence (Re = 1200), gm/$cm.^2$sec.

p, Partial pressure of the solute gas in the gas phase, atmos.

p^*, Partial pressure of the solute gas in equillibrium with the liquid, atmos.

p_i, Partial pressure of the solute gas at the interface, atmos.

Pr, Prandtl number (dimensionless).

Re, Reynolds number (dimensionless).

Re_i, Re_w, Re_c, Re_l, Reynolds numbers at break points in the slope of the curve of Re vs. Resistance number, for film flow as observed by Brauer (27).

Re_v, Vibrational Reynolds number (Art.7.2).

S, Fraction of area renewed per unit time as used in Eqs.(1.414-1.418).

Sc, Schmidt number.

t, t_c, Time of contact with the gas, sec.

$t_{abs.}$, Time required for absorption of a volume 'V' of a gas,sec.

T, Absolute temperature of the system, ^oA.

T_o, Absolute temperature at 0^oC , 273 ^oA.

u^*, Friction velocity as defined in Art.5.1, cm/sec.

$\bar{u}$, Root-mean-square velocity of the gas molecules,cm/sec.

$v_{av.}$, Average velocity of the falling liquid film, cm/sec.

v_i, Interfacial velocity of the falling liquid film, cm/sec.

V, Volume of gas absorbed, cm^3.

x, Distance from the interface inside the liquid film (Eq.(1.419)), cm.

x, Magnification ratio on the photographs (Chapter IV).

x_L, Thickness of the hypothetical liquid film, cm.

(Symbols & Notations - contd.)

y, Specific gravity of the liquid in Eq.(1.31).

z, Factor defined in Eq.(1.420).

α, Accommodation Coefficient (Eq.(1.424)).

δ, Thickness of the falling liquid film, cm.

δ_i, Thickness of the falling liquid film in the turbulent region of flow as given by Eq.(4.22), cm.

δ_l, δ_t, Thickness of the falling liquid films in the laminar and turbulent region respectively (Eq.(1.13,1.14)), cm.

ϵ, Coefficient of eddy diffusion, $cm.^2/sec.$

η, Factor defined in Eq.(1.11).

μ, Viscosity, gm/cm.sec.

μ_d, Dynamic viscosity of the falling liquid as used in Eq.(1.31), gm/cm.sec.

ν, Kinematic viscosity ($= \mu/\rho$) of the liquid, $cm.^2/sec.$

ρ, Density, $gm/cm.^3$

ρ_o, Density at N.T.P., $gm/cm.^3$

τ_{oe}, Frictional stress, $gm/cm.sec.^2$

θ, Time (as used in Eq.(1.414-1.416)), sec.

σ, Surface tension of the liquid (Eq.(1.31)), $dynes/cm.^2$

Γ_v, Volumetric flow rate of liquid per unit periphery, $cm.^3/cm.sec.$

REFERENCES.

(1) Hopf, L., Ann. Physik., 32, 777 (1910).

(2) Nusselt, W., Z.Ver.Dent. Ing., 60, 541, 569 (1916).

(3) Claassen, H., Zentr. Zukerind., 26, 497 (1918).

(4) Schoklitch, A., Akad. Wien., Math.-Nature, Abt.IIa, 129 (1920).

(5) Chwang, C.T., S.M. Thesis, M.I.T. (1926).

(6) Fallah, R., Hunter, T.G., Nash, A.W., J.Soc. Chem. Ind., London, 50, 369-T (1934).

(7) Cooper, C.M., Drew, T.B., McAdams, W.H., Ind. Eng. Chem., 26, 428 (1934).

(8) Friedman, S.J., Miller, C.O., Ibid, 33, 885 (1941).

(9) Kirkbride, C.G. Ibid, 26, 425 (1934).

(10) Duckler, A.E., Bergelin, O.P., Chem.Eng.Prog., 48, 557 (1952).

(11) Grimley, S.S. Trans. Inst.Chem.Engrs., 23, 228 (1945).

(12) Jackson, M.L.,A.I.Ch.E. Journal, 1, 231 (1955).

(13) Von Karman, T.,Trans. Am.Soc.Mech.Engrs., 61, 705 (1939).

(14) Nikuradse, J., Forschungsheft, No.361 (1933).

(15) Kramers, H., et.al., Chem.Eng.Sci., 4, 49 (1955).

(16) Brauer, H., VDI-Forschungsheft, 457 (1956).

(17) Thomas, W.J., Portalski, S., Ind.Eng.Chem., 50, 1081 (1958).

(18) Asbjornsen, O.A.,Chem.Eng.Sci., 14, 211-227 (1961).

(19) Wilkes, J.O., Neddermann, R.M., Ibid, 17, 177 (1962, I).

(20) Brauer, H., Kältetechnik, 9, No.9 (1957).

(21) Zhivaikin, L.Y., Khimichesoe Mashinostroen, No.6 (1961) Translation: Int.Chem.Engng., 2, 337 (1962).

(22) Vivian, J.E., Peaceman, D.W., A.I.Ch.E. Journal, 2, 437 (1956).

(23) Duckler, A.E., Chem.Eng.Progress, 55, 62-7, October,(1959).

(24) Tailby, S.R., Portalski, S., Trans.Inst.Chem.Engrs., 38,324 (1960).

(25) Kapitsa, P.L., J.Expt.Theoret.Phys.(U.S.S.R.), 19, 105 (1949).

(26) Lamb, H.,Sir, "Hydrodynamics", Cambridge Univ.Press (1945).

(27) Brauer, H., Chem.Ing.Tech., 30, 75-84 (1958).

(28) Whitman, W.G.,Chem. Met. Eng., 29, 146 (1923).

(References - contd.)

(29) Higbie, R., Trans. Am.Inst.Chem.Engrs., 31, 365 (1935).

(30) Danckwerts, P.V., Research, 2, 494 (1949).

(31) Danckwerts, P.V., Ind. Eng.Chem., 43, 1460 (1951).

(32) Emmert, R.E., Pigford, R.L., Chem.Eng.Progress, 50, 87 (1954).

(33) Kishinevski, M.K., Zh.Prikl.Khim., 27, 382 (1954).

(34) Toor, H.L., Marcello, J.M., A.I.Ch.E. Journal, 4, 97 (1958).

(35) Davidson, J.F., Cullen, E.J., Hanson, D., Roberts, D., Trans. Inst.Chem.Engrs., 37, 131 (1959).

(36) Scharge, R.W., A Theoret. Study of Interphase Mass Transfer, Columbia Univ. Press (1953).

(37) Cullen, E.J., Davidson, J.F., Trans. Faraday Soc., 53, 113 (1957).

(38) Cullen, E.J., Davidson, J.F., Trans. Inst. Chem.Engrs., 35, 51 (1957).

(39) Goodgame, T.H., Sherwood, T.K., Chem.Eng.Sci., 3, 37 (1954).

(40) Kuznetzow, M.D., Zhur. Prikl.Khim., 21, 48 (1947).

(41) Scriven, L.E., Pigford, R.L., A.I.Ch.E. Journal, 4, 439 (1958).

(42) Harvey, E.A., Smith, W., Chem.Eng.Sci., 10, 274 (1959).

(43) Goodridge, D.J., Bricknel, F., Trans.Inst.Chem.Engrs., 40, 54(1962).

(44) Chiang, S.H., Toor, H.L., A.I.Ch.E. Journal, 5, 165 (1959).

(45) Raimondi, P., Toor, H.L., Ibid, 5, 86 (1959).

(46) Danckwerts, P.V., Kennedy, A.M., Trans.Inst.Chem.Engrs., 32, S53 (1954).

(47) Blank, M., Ph.D. Thesis, Univ. of Cambridge (1959).

(48) Anon., Ind. Eng. Chem., 45, 640 (1953).

(49) Cullen, E.J., Davidson, J.F., Chem.Eng.Sci., 6, 49 (1956).

(50) Kennedy, A.M., Ph.D. Dissertation, Univ.of Cambridge (1954).

(51) Ternovskaya, A.N., Belopolski, A.P., Zhur. Fiz.Khim. (U.S.S.R.), 24, 43 (1950).

(52) Tailby, S.R., Portalski, S., Trans.Inst.Chem.Engrs., 39,328 (1961).

(53) Blokker, P.C., "Second Inter. Cong.of Surface Activity" 1, 503 (1957), Academic Press, N.Y.

(54) Roberts, D., Ph.D. Thesis, Univ. of London (1961).

(References - contd.)

(55) Nedderman, R.M., Ph.D. Thesis, Cambridge Univ. (1960).

(56) Inter. Critical Tables, McGraw-Hill.

(57) Vielstich, W., Chem.Ing.Tech., 28, 543 (1956).

(58) Colebrook, C.F., J.Inst.Civil Engrs., 11, 133 (1938-39).

(59) Chisholm, D., Laird, A.D.K., Trans.Am.Soc.Mech.Engrs., 80, 276 (1958).

(60) Moody, L.F., Ibid, 66, 671 (1944).

(61) Pohl, W., Forsch.Gebiet.Ing., 4A, 230 (1933).

(62) Cope, W.F., Proc.Inst.Mech.Engrs., 145, 99 (1941).

(63) Colburn, A.P., Purdue Univ.Eng.Bull.Research,Series 84, 52 (1942).

(64) Pratt, H.R.C., Trans.Inst.Chem.Engrs., 28, 177 (1950).

(65) Smith, T.W., Epstein, N., A.I.Ch.E. Journal, 3, 242 (1957).

(66) Nunner, W., VDI-Forsch. No.455 (1956).

(67) Kays, W.M., Trans.Am.Soc.Mech.Engrs., 77, 471 (1955).

(68) Stephens, E.J., Morris, G.A., Chem.Eng.Progress, 47, 232 (1951).

(69) Taylor, R.F., Roberts, F., Chem.Eng.Sci., 5, 168 (1956).

(70) Martinelli, R.C., Boelter, L.M.K., Proc.5th Intern. Congr. Appl. Mechanics, 758 (1938).

(71) Andreas, Arno, German Patent No.717, 766 (Feb.5, 1942).

(72) Marchant, J.H., Trans.Am.Soc.Mech.Engrs., 65, 796 (1943).

(73) West, F.B., Taylor, A.T., Chem.Eng.Progress, 48, 39 (1952).

(74) Lemlich, R., Ind.Eng.Chem., 47, 1175 (1955).

(75) Lemlich, R., Chemical Engineering, 68, 171 (May, 1961).

(76) Thompson, W.E., Chem.Eng.News, p.92, May 30, 1960; p.41, Dec. 26, 1960.

(77) Mathewson, W.F., Smith, J.C., CEP Symposium Series 41, 59 (1963). Heat Transfer – Houston.

(78) Lemlich, R, Levy, M.R., A.I.Ch.E. Journal, 7, 240 (1961).

(79) Fand, R.M., Kaye, J., Trans. Am.Soc.Mech.Engrs., Series 'c', 83, 133 (1961).

(80) Zhavaronkov, N.M., Orlov, V.Y., Dokl.Akad. Nauk. (S.S.S.R.), 129, 161-164 (1959).

(References - contd.)

(81) Shirotuska, T., Honda, N., Bull.Sci.Engng.Res., Waseda Univ., No.8, 58 (1958).

(82) Bretsznajder, S., Pasiuk, W., Bull.Acad.Polon.Sci.Chim., 10, 153 (1962).

(83) Mirev, D., Boyadzhief, L., Balarev, K., Izv.Inst.Obsht.Negrg. Khim.Org.Khim., Bulgar.Akad.Nauk., 8, 67-60 and 83-101 (1961).

(84) Harbaum, K.L., Houghton, G., J.App.Chem., 12, 234-40 (1962).

(85) Gibbons, J.H., Houghton, G., Chem.Eng.Sci., 15, 146 (1961).